ADDIS ABABA UNIVERSITY

ADDIS ABABA INSTITUTE OF TECHNOLOGY

SCHOOL OF ELECTRICAL AND COMPUTER ENGINEERING

Investigating of SU-MIMO techniques for LTE-Release 8 in highly scattering environment

By

Nebiyu Suleyman

Advisor

Dr. Murad Ridwan

A thesis submitted to the School of Electrical and Computer Engineering in Partial Fulfillment of the requirements for the Degree of Masters of Science in Communication Engineering

July, 2017

Addis Ababa, Ethiopia

ADDIS ABABA UNIVERSITY

ADDIS ABABA INSTITUTE OF TECHNOLOGY

SCHOOL OF ELECTRICAL AND COMPUTER ENGINEERING

Investigating of SU-MIMO techniques for LTE-Release 8 in highly scattering environment

By: Nebiyu Suleyman

Approved by Board of Examiners

_______________	_____________
Chair Person	Signature
Dr.Murad Ridwan	_____________
Advisor	Signature
_______________	_____________
Internal Examiner	Signature
_______________	_____________
External Examiner	Signature

Dedicated to My Mother

Worknesh W/Michael

Declaration

I, the undersigned, declare that the thesis comprises my own work in compliance with internationally accepted practices; I have fully acknowledged and refereed all materials used in this thesis work.

Nebiyu Suleyman ____________________

Name Signature

Place: **Addis Ababa University, Ethiopia**

Date of Submission: ________________

This thesis has been submitted for examination with my approval as a university advisor.

Dr. Murad Ridwan ____________________

Advisor's Name Signature

Abstract

LTE systems promise of delivering large data rate to users which is substantially larger than what the previous third generation (3G) systems offered. However, as user traffic grows it will put greater demands on network capacity. More importantly, in urban environment the construction of buildings, which are taller than base station's height, create highly scattering environment for radio signal which leads to multipath fading. Small antenna height has in turn negative effect on both coverage and capacity.

Multiple Input Multiple Output (MIMO) antenna systems are one of the most efficient leading innovations to accommodate high data traffic and eliminate the effect of multipath scattering environment. MIMO systems can turn multipath propagation, traditionally a pitfall of wireless transmission, into a benefit for the user. It can also be used to achieve improved system performance, including improved system capacity and improved coverage, as well as improved service with higher per-user data rates. The operator can achieve all these without increasing average transmit power or frequency bandwidth.

This thesis investigates the performance evaluation of different schemes of Single User MIMO (SU-MIMO) for the downlink of LTE. This evaluation will be based on performance metrics such as ergodic capacity and average Bit Error Rates (BER) for different MIMO antenna transmission schemes and their tradeoff. For this case study, the ideal MIMO radio channel models assume a Rayleigh fading environment which is used as a reasonable model for the effect of heavily built-up urban. It will be shown analytically and with MATLAB simulation the impressive improvements in capacity and BER brought about by the use of SU-MIMO techniques. Finally suggestion will be given to which modes of MIMO to use for different kind of highly scattering environment depending upon the speed (fast and slow moving) and location (cell-centered and cell-edge) of the user equipment (UE). The developed techniques can be applied to fast and accurate performance evaluation for future network planning, deployment and optimization of LTE-MIMO systems.

Keywords: *SU-MIMO, LTE Release 8, OFDM, Rayleigh fading. Spatial diversity, Spatial multiplexing, Ergodic capacity, BER*

Acknowledgement

I seize this opportunity to acknowledge all those who have contributed in one way or the other towards the success of our work. The greatest thanks go to Almighty God.

I would like to thank to my Advisor Dr: Murad Ridwan for his invaluable help and encouragement. This thesis cannot be accomplished without his genuine and consistence guidance.

Special word of thanks goes to my mother Worknesh W/Michael, my brother Noah Suleyman and Kalkidan Mesfin for their unconditional love and support. I would like to thank to my parents for their eternal support during my education life.

I am also very grateful for all the instructors who thought and guided me and reach at this stage. I would like to thank department stuffs especially Kebira. I am also so grateful to my classmates, who always motivate and support me to complete this thesis.

Table of Contents

List of Figures

List of Tables

List of Acronyms

3GPP	Third Generation Partnership Project
4G	Fourth Generation
AWGN	Additive white Gaussian noise
BER	Bit-error rate
BPSK	Binary Phase Shift Keying
CCI	Channel covariance information
CDF	Cumulative distribution function
CDI	Channel distribution information
CDIR	Receiver channel distribution information
CDIT	Transmitter channel distribution information
CFO	carrier frequency offset
CL-SM	Closed loop Spatial multiplexing
CP	Cyclic prefix
CSI	Channel state information
CSIR	Receiver channel state information
CSIT	Transmitter channel state information
DFT	Discrete Fourier transform
eNodeB	evolved Node
FDD	Frequency-division duplex
FFT	Fast Fourier transform
HSPA	high-speed packet access
ICI	inter-carrier-interference
IEEE	Institute of Electrical and Electronics Engineers
iid	independent, identically distributed
IFFT	Inverse FFT
IP	Internet Protocol
ISI	Intersymbol interference

LMMSE	Linear Minimum Mean Square Error
LTE	Long Term Evolution
LTE Rel-8	Long Term Evolution Release-8
MIMO	Multiple-input multiple-output
MISO	Multiple-input single-output
ML	Maximum likelihood
MRC	Maximum ratio combining
MU-MIMO	Multi-User Multiple Input Multiple Output
nFFT	Number of Fast Fourier Transform
nDSC	Number of used subcarriers
OFDMA	Orthogonal frequency-division multiple access
OL-SM	Open Loop Spatial Multiplexing
pdf	probability distribution function
QAM	Quadrature amplitude modulation
QoS	Quality of Services
QPSK	Quadrature phase-shift keying
RF	Radio frequency
RMS	Root Mean Square
SC	Single carrier
SC-FDM	Single Carrier Frequency Division Multiplexing
SISO	Single-input, single-output
SIMO	Single-input, multiple-output
SNR	Signal-to-noise ratio
STBC	Space–time block code
SU-MIMO	Single user multiple input multiple output
SVD	Singular-value decomposition
TDD	Time-division duplex
UE	User Equipment
UMTS	Universal Mobile Telecommunications System
VoIP	Voice over IP
ZMSW	Zero mean spatially white

CHAPTER 1

1 INTRODUCTION

In this Chapter, a brief introduction to the concept and application of LTE- MIMO system and what this thesis is all about will be presented. Following the Basics of SU-MIMO performance and capacity in Subsection 1.1.3, then why SU-MIMO for LTE Release 8 in Subsection 1.1.2 will proceed. The coming studies also include the motivation and contribution of this thesis in Section 1.3 and objectives in 1.4 respectively. Then we will discuss about the methodology in Section 1.5 and then scopes and limitations in 1.6. Finally, literature review will follow in 1.7 before the outline of the thesis is described.

1.1 Background

LTE was introduced in 3GPP (Third Generation Partnership Project) Release 8. The objective is a high data rate, low latency and packet optimized radio access technology. The main goals of LTE include improving spectral efficiency in 4G networks, allowing operators to provide more data and future voice services (VoIP) over a given bandwidth. It can also be used by lowering costs, improving services, making use of new spectrum and better integration with other open standards of the operator [1].

LTE has introduced a number of new standards to allow IP based wireless mobile broadband. One of the most important standards is MIMO technology. The hybridization of MIMO technologies with LTE has generated features such as spatial multiplexing, transmit diversity and receive diversity for better speed and efficiency to support future broadband data service.

MIMO is going to be a viable alternative for future generation broadband services in order to meet the striving requirements for throughput and system robustness. In LTE, MIMO technologies have been broadly used to get better downlink peak rate, cell coverage, as well as average cell throughput. MIMO can better utilize the spatial resource and increase spectral efficiency [2]. Two use cases exemplify the potential of LTE MIMO to meet increasing capacity demands:

- A user close to the cell center, limited by cell capacity and peak throughput.
- A user close to the cell edge, limited by network coverage.

The basic concept for LTE in downlink is OFDM (Orthogonal Frequency Division Multiplexing) and Uplink with Single Carrier Frequency Division Multiplexing (SC-FDM). LTE is designed to be optimized for low speeds of about 15km/hr, provide high performance at speeds up to 120km/hr and to maintain the link at speeds up to 350km/hr [3]. Modulation modes are QPSK, 16QAM, and 64QAM. Spatial multiplexing gains can provide doubled, quadrupled, or more data rates. In a cell with a downlink bandwidth of 20 MHz, the theoretical target peak rates for individual UEs in 1×2, 2×2, and 4×4 MIMO systems are 75 Mbit/s, 150 Mbit/s, and approximately 300 Mbit/s, respectively

Multiple antenna systems are classified according to the number of antennas at the transmitter (RF channel inputs) and receiver (RF channel outputs) .The input (MI) defines how many signals are sent through the air, while the output (MO) defines how many signals are received from the air. According to the number of transmit antennas and the number of receive antennas, wireless systems can be classified as single-input single-output (SISO), single-input multiple-output (SIMO), multiple-input single-output (MISO), and multiple-input multiple output (MIMO) systems, where the input and output are with respect to the channel between the transmitter and the receiver. Most of the time SIMO is receive diversity, MISO is transmit diversity and MIMO is spatial multiplexing [5].

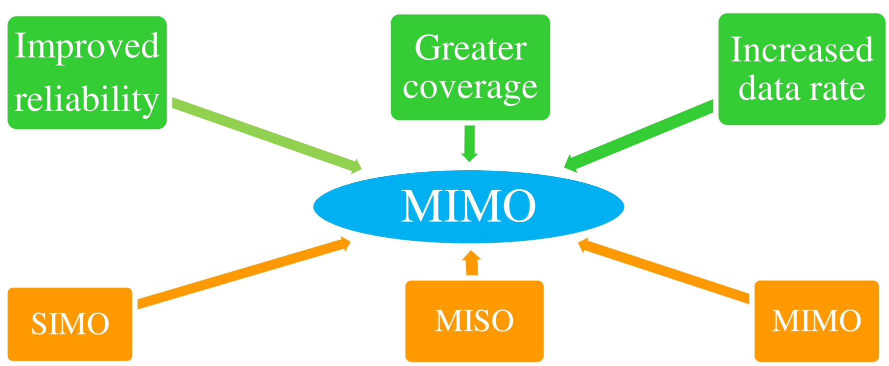

Figure 1-1 Features of MIMO

The quality of a wireless link can be described by three basic parameters. They are the transmission rate, the transmission range and the transmission reliability. Conventionally, the transmission rate may be increased by reducing the transmission range and reliability.

By contrast, the transmission range may be extended at the cost of a lower transmission rate and reliability, while the transmission reliability may be improved by reducing the transmission rate and range [6]. However, with the advent of MIMO assisted OFDM systems, the above- mentioned three parameters may be simultaneously improved.

MISO (Transmit diversity) increases the robustness of the signal to poor channel conditions. It does not increase data rates but increases coverage and therefore cell capacity. SIMO (Receive diversity) improves the received SNR by combining multiple copies of the same signal. Like MISO it does not increase data rates but extends coverage and hence cell capacity. However, MIMO (spatial multiplexing) increases data rate [7].

1.1.1 Basics of SU-MIMO Capacity and BER Performance

From a technical standpoint, the most important consideration in the specification of mobile data transmission systems is the optimum utilization of the following two transmission characteristics for the mobile radio channel [8]:

1. **Channel Capacity**- the maximum transmittable error free data rate in (Bit/s or (Bit/s)/ Hz).
2. **BER Performance**- minimizing the probability of transmission errors (bit error rate).

In LTE, due to system constraints or regulations, the transmit power is limited in general. Theoretically, the best way to increase data rates over a wireless link is to increase the overall received signal power for a given transmit power. An effective way of increasing the received power is to use additional antennas at the transmitter and/or the receiver [9]. For fixed bandwidth of B, the maximum capacity (spectral efficiency) that a time and frequency communication system can achieve as follows:

$$C/B = \log_2 (1 + |h|^2 \, SNR) \text{ bits/sec/Hz} \tag{1.1}$$

where h is the normalized complex gain of a Rayleigh fading channel.

The capacity is increasing as a log function of the SNR, which is a slow increase. Clearly increasing the capacity by any significant factor takes an enormous amount of power in a SISO channel. A one-hundred-time increase in power will increase the channel capacity by additional value of 6.3 b/s/Hz only. Wouldn't it be nice if we can increase the capacity instead by a linear function with MIMO? But, there is no violation because the diversity and signal processing employed with MIMO transforms a point-to-point single channel into multiple parallel or matrix channels, hence in effect multiplying the capacity.

If multiple antennas are used, Shannon equation will be modified as the capacity is increased by a multiplication of the minimum number of antennas i.e. min(M,N) used, where M and N are the number of transmit and receive antennas respectively . Then the spectral efficiency is:

$$C / B = \min(M,N) * \log_2 (1 + |h|^2 \, SNR) \text{ bits/sec/Hz} \qquad (1.2)$$

Along with capacity requirements, the Quality of Service (QoS) requirements need to be determined to achieve high efficient performance. A channel may be affected by fading and this will impact the SNR. In turn this will impact the error rate. Increasing the quality or reducing the effective error rate in a multipath fading channel is extremely difficult. In Rayleigh fading, using space diversity MIMO gain d=M*N implies that, the probability of bit error ber decays at a rate of $1/SNR^d$ as opposed to 1/SNR for a SISO system [10] .

1.1.2 Why SU-MIMO over MU-MIMO for LTE Release 8

In 3GPP, the MIMO systems can be configured as Single User MIMO (SU-MIMO) or Multi-User MIMO (MU-MIMO). In LTE SU-MIMO, the data of a single user is transmitted simultaneously on several parallel data streams, using the available transmission resources, both in time and frequency dimensions [4]. In MU-MIMO multiple users share a single time-frequency resource to exploit multi-user diversity resulting in a significant gain over SU-MIMO. In LTE Release 8 (LTE Rel-8), MU-MIMO has lower expected performance than SU-MIMO.As a result, MU-MIMO is not expected to be widely deployed at this stage. This thesis focuses on SU-MIMO mode in 3GPP LTE downlink network because of the limitations and additional capital expenditures associated with LTE Release 8

Advantages of using SU-MIMO over MU-MIMO are the followings:

- SU- MIMO techniques dominated the algorithms selected for the first version of LTE, but with MU-MIMO becoming more established in Releases 9 and 10 [11].
- There is very limited support for downlink MU-MIMO in Release 8.Basic MU-MIMO for Release 8 is not widely used.
- SU-MIMO capacity results are known for many cases where the corresponding MU-MIMO problems remain unsolved. Very little is known about multi-user capacity.

- In general, MU- MIMO is beneficial for improving average user spectral efficiency. However, cell edge user spectral efficiency may be reduced if MU-MIMO is used exclusively; due to residual inter-user interference arising from practical multi-user and reduced transmit power allocated to each user. One of the challenges in LTE is how to achieve better throughput at the cell edge where the user is at a position where it receives two or more signals that are roughly at the same power level [11].
- MU-MIMO does not increase an individual user's data rate.
- MU-MIMO can be best understood as extensions of the SU-MIMO cases of transmit diversity and spatial multiplexing.
- MU-MIMO always requires the Channel State Information (CSI) at the transmitter to properly serve the spatially multiplexed user.

1.2 Thesis Motivation and Contribution

SU-MIMO is a key component of next-generation wireless technologies 4G and provides the bulk of LTE's peak throughput gains when compared with older technologies. Operators can maximize the performance of LTE networks by using SU-MIMO and will be able to provide quality service to its users with the smallest amount of infrastructure investment. The contribution of this thesis is to explore how to achieve high service quality, high data rate, network coverage and lesser processing time using SU-MIMO for LTE Release 8. Motivations of implementing SU-MIMO for LTE are the followings:

- MIMO effectively takes advantage of random multipath fading in urban environment. Radio propagation heavily depends on the base station antenna height with respect to the average height of the surrounding objects. This leads to deep fading and channel impairments.
- Implementation of MIMO will solve issues related to data rate, quality and coverage due to the customers' demand for higher speed internet connection for business district sites.
- Antenna solutions that are introduced in LTE can also used by evolved High Speed Packet Access (eHSPA).
- Adding new sites is extremely expensive and time consuming and geographically difficult. Optical fiber backhaul is needed for each added cell which is very expensive.

- No cost of extra spectrum is largely responsible for the success of MIMO. Low to medium cost to improve transmission performance.

1.3 Objectives

The major goal of this thesis is to model SU-MIMO and analyze the performance of it for highly faded channel environments. Then we evaluated the capacity and BER performance of SU-MIMO depending upon the speed and location of the UE. We both used theoretical approach. We then plot the capacity and BER performance for different modes of SU-MIMO. We then introduce the different kinds of SU-MIMO modes for increasing the capacity and BER performance of the system.

1.3.1 General Objectives

The general objective of this thesis is to study and introduce SU-MIMO for LTE. The followings are also under study:

- To analyze linear detection methods for estimated signals of MIMO systems.
- To evaluate the ergodic capacity for both open loop (fast moving UE) and closed MIMO (slow moving UE) system of receive diversity, transmit diversity and spatial multiplexing.
- To further mathematically approximate the ergodic capacity for low SNR regime (cell-edge UE) and high SNR regime (cell-centered UE) for both open and closed MIMO systems.
- To evaluate the average BER performance of receive and transmit diversity and combined receive-transmit diversity for a deep fade channel conditions.
- To reduce the BER performance equations to approximate for high SNR regime (cell-centered UE).

1.3.2 Specific Objectives

Particularly, the thesis focuses on the evaluation of SU-MIMO that encountered in highly scattering non-line of sight of sites. The followings are the specific objectives:

- To simulate the detected signals using Linear detection methods and also compare the detection methods' efficiencies with each other.
- To demonstrate the transmitted signal at the stages when it's faded by the channel, when it's received and mixed with noise. Then compare the signals at different stages with the transmitted signal.
- To simulate and demonstrate spatial multiplexing using Singular Value Decomposition (SVD) decoupling of SU-MIMO system.
- To simulate and then compare and contrast the ergodic capacity of different modes of SU-MIMO.
- To simulate and then compare the different average BER performance for SISO, SIMO, MISO and MIMO.
- To simulate the tradeoff between spatial multiplexing (which increase capacity) and diversity (which decrease BER performance).

1.4 Methodology

The methodology used in doing this thesis comprises of three major phases. The first phase encompasses the reviews and study of various literatures on LTE MIMO systems. The other two phases clarify how such major tasks as modeling, performance analysis, evaluation, and simulating are carried out.

The methods used to achieve the desired objectives of this thesis were as follows:

1) Literature reviews – focuses on gaining all the necessary background information required to understand the broader picture of SU-MIMO systems.
2) System modeling – involves how to characterize and model highly scattering environment analytically with Rayleigh modeling .Then select appropriate algorithm to derive the performances for different modes of SU-MIMO system.
3) Simulation – involves Outline simulation workflows and programming the system in Matlab R2014a. The results will be interpreted and conclusion will be drawn based on the results obtained. Finally suggestions will be given to which modes of SU-MIMO to use for specific types of channel condition.

1.5 Limitations and Scope of the Thesis

Most of the researchers are focusing on investigation of MIMO systems under the important assumption that fading is Rayleigh. Such results provide good limiting estimates for capacity, BER performance for real world scenarios. However, it often provides over optimistic results. Using SU-MIMO in LTE Release 8 has the following limitations:

- Uplink SU-MIMO for LTE Release 8 has not been fully specified because of cost, size, battery and asymmetrical traffic distribution. [4] In the uplink of LTE Rel-8, although multiple receive antennas are present at the UEs, only one transmit antenna is available. This is because only one power amplifier and transmitter chain is used in order to minimize cost and simplify the hardware design.
- LTE Rel-8 supports a maximum of four-layer spatial multiplexing in SU-MIMO. 2×2 and 2×1 antenna configuration are widely deployed in LTE. [9] Recent advancements are making 2×4 and 4×4 MIMO a reality for LTE devices. Harnessing advanced pattern diversity technology, antenna designers can position multiple antennas in close proximity to one another and still achieve high isolation and low correlation.
- Beamforming or Beamsteering mode of SU-MIMO is not used in commonly used Frequency Division Duplex (FDD). This is due to channel reciprocity in TDD (Time Division Duplex) between the uplink and downlink paths and not in FDD mode [11]. In LTE TDD, both transmitter and the receiver are on the same frequency, the channel condition is readily available to the transmitter. In LTE FDD, since the forward and reverse links are at different frequencies, this requires a special feedback link from the receiver to the transmitter.
- The complexity of a SU-MIMO technique is usually in proportion to the number of antennas used. On the network side, increasing the number of antenna elements involved in a MIMO implementation generally requires visits to each base station, to modify the physical antenna configuration and wiring. It also needs extra processing on one or both sides of the RF channel. Fortunately, the feasibility of implementing the necessary signal processing algorithms is enabled by the corresponding increase of computational power of integrated circuits.

1.5.1 Scope of the Thesis

. In this thesis we made the following assumptions and simplifications:

- Non physical channel model is chosen but only statistical model is used.
- There are many scattering objects in the environment and there are many propagation paths between transmit and receive antennas. Therefore we modeled the channel environment as Rayleigh fading. This model captures the long term average distribution of the channel coefficients averaged over multiple propagation environments.
- Typically, we will assume that the channel to be spatially rich but also independent and identically distributed (i.i.d.) complex circularly symmetric Gaussian random variables with zero mean and unit variance. This is because we concentrate on non-line of sight highly fading environment in Addis Ababa which leads to uncorrelated channel paths.
- The thermal noise at any receiver antenna is a Zero mean i.i.d., temporally and spatially white Gaussian random variable with variance $\sigma^2=1/2$. This is commonly used to simulate background noise of the channel.

1.6 Literature Review

Multiple-antenna technology is a rich area of research. Many researches in this area have been very active during recent years. The literature review outlines previous work by other researchers, which forms the foundation of this thesis. Much of the initial work about MIMO systems was due to pioneering work by Foschini and Telatar (1996), predicting remarkable capacity growth for wireless systems with multiple antennas when the channel exhibits rich scattering and its variations can be accurately tracked. However, these predictions are based on somewhat unrealistic assumptions about the underlying time-varying channel model and how well it can be tracked at the receiver as well as at the transmitter. This work resulted in an explosion of research and commercial activity to characterize the theoretical and practical issues associated with MIMO systems [11].

The following theses were studied and took their future works for the basis of this thesis:

1) In [12] Performance Evaluation of LTE Downlink with MIMO Techniques by Gessese Mengistu Kebede ,Oladele Olayinka. They showed that the performance of MIMO is better than SISO in both channel models particularly when Soft Sphere Decoding (SSD) is employed. When high order modulation is utilized, performance in the flat-fading channel model is better than ITU pedestrian B channel at low SNR regions.
2) In [13] performance analysis of space time coding on MIMO and cooperative diversity system" by Dereje Girma advised by Dr.–Ing Dereje Hailemariam. This thesis discusses the application of a technique called Almouti space time block coding (STBC) on a system based on the joint use of cooperative diversity and MIMO schemes, which the system performance can be increased further. They studied MIMO schemes and simulate Rayleigh fading channel and Rician fading channel.

1.7 Outline of the Thesis

In the first Chapter, we aim to introduce the basic structure of LTE and MIMO, Basic building block of LTE MIMO and Basics of Capacity and performance of MIMO in LTE are also introduced. The basic idea why and how SU-MIMO was chosen over MU-MIMO for LTE Rel-8 is explained. We also discussed about the motivation and contribution of this thesis. The objectives of this thesis and thesis organization are dealt briefly. Then we cover the methodology, limitation and also literature review.

The remainder of this thesis is organized as follows: In Chapter 2 channel impairment mechanisms such as multi-path effect and Doppler fading and how MIMO deal with this problems are explained .Here in this Chapter, a strong attention is given on the problem arrived because of small-scale fading. We dealt with frequency and flat fading in case of multipath and fast and slow fading of Doppler spread. The i.i.d Rayleigh 'channel model are described in detail. The system model for MIMO systems is illustrated. Moreover we take the features of OFDM as a very important simplification to flat fading channel analysis. Then we discuss about the relationships between the transmit signal vector with receive vector .We formulate the general matrix for this relationship using the channel gain matrix H. We then characterize the channel matrix. Finally we discuss about the linear detection methods.

In Chapter 3, Modes of SU-MIMO used in LTE Rel-8 are receive, transmit diversity and Spatial multiplexing and their Algorithms for Transmit diversity and Spatial diversity are presented. While Maximal ratio combining for receive diversity, Space Frequency Block Coding and Alamouti space-Space coding scheme will be used for transmit diversity. The sub groups opened spatial multiplexing; closed spatial multiplexing will be covered in detail.

In Chapter 4, we introduce the notions about ergodic capacity and how it changes with different channel conditions depending up on the availability of Channel State Information at the transmit antenna. Depending on the channel state information at the receiver we broadly categorize the channel as closed (slow fading) and open loop (fast fading) SU-MIMO system. Then we derive the ergodic capacity of MISO, SIMO and MIMO transmission techniques.

In the 5th Chapter we will analyze and simulate the BER for receive and transmit diversity. We deal with maximum ratio combing for the two antennas receive diversity case. We also investigate the effect of antenna diversity for a double transmit and multiple receive antenna supported LTE that employs Alamouti's space time block coding (STBC) and with one and two receivers using maximal ratio combining (MRC) scheme . For a fixed number of transmit antennas, the performances of different STBC codes are analyzed in terms of BER

Then, Chapter 6 will give the plot using MATLAB R2014a and interprets the results found. Simulation results, observations and interpretations on the capacity and BER performance of SU-MIMO receivers under fading channels are presented. The first plot is to show how data is recovered after the signal is faded and mixed with noise for spatial multiplexing .Then ergodic capacity of SU- MIMO for different modes and different types of channel environments will be presented. Then we will see the simulations for open loop and closed loop SU-MIMO system and compare them with each other. Moreover we will consider the BER performances of Receive diversity using MRC, Transmit diversity using Almouti STBC algorithms, and their combination will be simulated and compared. In conclusion we will see the diversity-spatial multiplexing trade-off.

In Chapter 7, we will briefly explain how operators can greatly benefit from SU-MIMO. We will suggest which kinds of modes are useful for which kind of channel conditions and how switching will be made from one mode of SU-MIMO to other. Finally we will suggest about the future work to be done.

CHAPTER 2

2 SU-MIMO SYSTEMS FOR LTE

Some of the desired attributes of a wireless communication system are high spectral efficiency (capacity), high data rates, low bit error rate, wide coverage range, and low deployment, maintenance, and operation costs. All these requirements need to be guaranteed, sometimes simultaneously, over a wireless channel, which by nature is very hostile, especially in non–line-of-sight (NLOS) scenarios [14].

This Chapter summarizes some of the problems and challenges encountered by wireless transmission process. It's because the performance of wireless communication systems is mainly governed by the wireless channel environment. As MIMO operation requires low channel to- channel correlation, it is important to understand how these spatial characteristics may influence system performance. 4G LTE should provide high data rate and performance over very challenging channels that is time-selective and frequency-selective.

In the next few Sections of this Chapter there is a review of the basic characteristics found in any wireless channel, such as delay spread and Doppler spread. The essential feature of wireless transmission is the randomness of the communication channel which leads to random fluctuations in the received signal commonly known as fading. It has a significant impact on the received signal strength which can be severely degrade the signal as will be shown. The remaining part of the Chapter will provide an overview of channels encountered during mobile radio propagation and their effects on signal quality. Then after, we will focus on SU-MIMO under these fading channels.

We consider an approximate realistic channel models that take into account the dynamic channel responses and fading conditions. The combination of MIMO and OFDM has the potential of meeting this stringent requirement since MIMO can boost the capacity and the diversity and OFDM can mitigate the detrimental effects due to multipath fading. To simplify matters, we will chose a very basic MIMO transmission model, which is not always satisfied in practice, but is strong enough to provide basic insights into MIMO communications while being sufficiently simple in its analytical representation. This Chapter explains the chosen MIMO transmission model, its analogies to a real communications environment, and the necessary assumptions to verify the choice of this representation.

2.1 Introduction to Faded Wireless Channels

In LTE, the performance of a link is fundamentally determined by the Signal-to-Noise Ratio (SNR), which measures the received signal strength of a transmission relative to the thermal noise in the receiver hardware that distorts the received signal. The random fluctuation in signal level, known as fading, can severely affect the quality and reliability of wireless communication. Additionally, the constraints posed by limited power and scarce frequency bandwidth make the task of designing high data rate, high reliability LTE systems extremely challenging. Improvements in spectral efficiency by LTE MIMO can translate into other metrics including higher data rates to the user, improved coverage, improved service reliability, and lower network cost to the operator [9].

Proper modeling of the characteristics of a wireless channel is an important requirement for the design of mobile systems. Channel propagation usually results in a reduced power in received signals relative to the transmitted signal. In general; the power reductions are treated in two categories:

(i) Large-scale fading or signal attenuations

(ii) Small-scale fading or signal fading

Path loss and shadowing are macro effects that cause slow fading in which the signal strength varies slowly over time as the receiver moves or the environment changes. Small-scale fading includes multipath fading and time dispersion due to mobility.

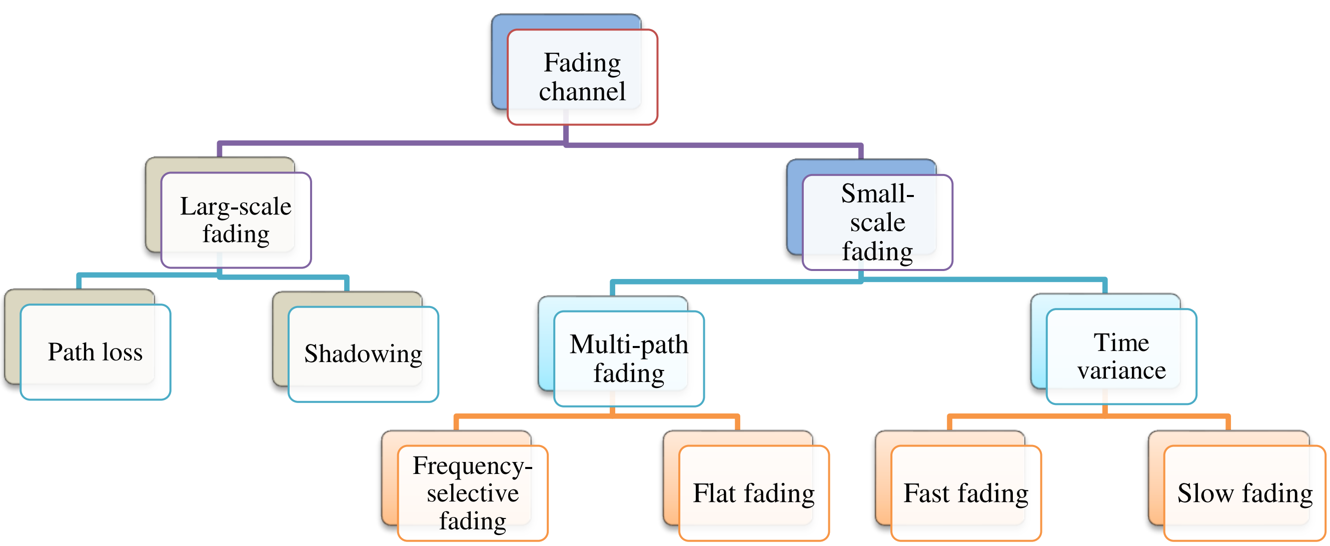

Figure 2-1 Classification of fading channels with Small-scaling considered

2.2 MIMO Fading Channels

Diversity techniques that mitigate multipath fading, both slow and fast are called **Micro-diversity**, whereas those resulting from path loss, from shadowing are an order of magnitude slower than multipath, are called **Macro-diversity** techniques. MIMO design issues are limited only to micro-diversity**.** Macro-diversity is usually handled by providing and overlapping EnodeB coverage and handover algorithms and is a separate independent operational issue [15].

Path loss and fading are the two most important factors to consider in link budget Moreover, a number of large scale models have been developed, and their application is identical for both single- and multi-antenna systems. Link budget is an important tool in the design of wireless communication systems. Accounting for all the gains and losses through the wireless channel to the receiver, it allows for predicting the received signal strength along with the required power margin. Operators uses the model called Cost231-Hata for large scale fading for urban and dense urban environments [4].

These large-scale features are taken into account in design and cellular topography. Variations of the received power due to shadowing and path loss can be efficiently counteracted by power control. In a deeply fading environment, the path-loss and shadowing are usually identical on all links. Conceptually, moving around in a shadow behind a tall building will not greatly change the amount of sunlight, nor will movements much less than the distance from the transmitter affect the path loss [16].

Therefore the predominant channel degradation in LTE is a result of short-term fading caused by multipath propagation and Doppler fading. These features are of short duration and must be adaptively dealt with. The design of the PHY (Physical Layer) should include techniques that effectively deal with these types of channel impairment [17]. We need to account for the effects of a fading channel in order to provide an accurate evaluation of the LTE system performance. This thesis concentrates on small-scale fading and neglects the effects of large- scale loss.

2.2.1 Multipath Fading Effects

The most problematic kind of fading for LTE is due to multi-path. Multipath is the virtually infinite number of ways that a signal can take from sender to receiver, reflecting off smooth objects, scattering off rough objects, and diffracting around sharp corners. This scattering leads to a situation in which many copies of the signal arrive at the receiver having traveled along many different paths. When these copies combine they may add constructively, giving a good overall signal, or destructively, mostly canceling the overall signal, all depending on the relative phases of the portions. In microcellular environments in most sites in Addis Ababa, in which antenna heights are relatively low, and hence, multipath scattering near the base station and the mobile is just as likely [9].

The net effect of multi-path fading is that the received wireless signal can vary significantly over time, frequency and space. This is a problem for good performance because at any given time there is a significant probability of a deep fade that will reduce the SNR of the channel below the level threshold. Even when the line of sight (LOS) path signal is present, the multipath components are usually also present. [16] For small scale fading depending on the relative extent of a multipath, a channel is characterized as:

(i) Flat fading- If all the spectral components of the transmitted signals are affected by the same amplitude gains and phase shifts, the channel is called flat fading channel. In this case, the transmitted signal bandwidth is much smaller than the channel's coherent bandwidth. Flat fading occurs when the symbol period of the signal is more than the root mean square (rms) delay spread of the channel. The amplitude distribution of flat fading is either Rayleigh distribution or Ricean distribution.

(ii) Frequency selective fading -If the spectral components of the transmitted signals are affected by different amplitude gains and phase shifts, the fading is said to be frequency selective. In this case the transmitted bandwidth is larger than the channel's coherence bandwidth. Due to the short symbol duration as compared to the multipath delay spread, multiple-delayed copies of the transmit signal is significantly overlapped with the subsequent symbol, incurring inter-symbol interference (ISI). Frequency selective fading will induce inter-symbol interference, which can be undone by OFDM [1].

2.2.2 Doppler Fading

The Doppler effect is the change in frequency or wavelength of a wave as perceived by an observer moving relative to the source of the waves. This effect occurs due to the relative speed between the elements in the channel. Thus the fades are due to movements of the transmitter or receiver as well as movements of objects along the propagation paths [18]. The effect of the Doppler is directly proportional to the magnitude of the relative speed and is modeled here as a contribution to the carrier frequency f_c. As a result of mobile terminal movement, the profile of channel impulse response can vary. The maximum Doppler frequency, $f_{d,max}$, is related to the relative velocity v by the following equation

$$f_{d,max} = f_c \frac{V}{C} \qquad (2.1)$$

where v is the velocity of the UE, f_c is the carrier frequency (Hz) and c is the constant for the speed of electromagnetic wave. The spectral spreading of the pure tone would cover the range of $f_c \pm f_{d,max}$. Assuming the average maximum speed attained by a UE in urban environment road is v=100km/hr=27.77 m/s, f_c =1800 MHz the maximum Doppler frequency is calculated

$$f_{d,max} = f_c(\frac{V}{C}) = 1800MHz\,(\frac{27.77\,m/s}{((3*(10^8))m/s}) = 166.67\,Hz \qquad (2.2)$$

Fading due to Doppler spread includes both slow fading and fast fading [8].

(i) Fast fading occurs when the channel changes significantly during the duration of a symbol. When the channel varies rapidly, it distorts the symbol's amplitude and phase erratically over its interval.

(ii) Slow fading occurs when the channel changes much slower than one symbol duration. This does not imply that the effects of the channel can be neglected, but it is possible to track the changes in the channel to appropriately compensate for channel dynamics.

We define coherence time T_C of the channel as the period of time over which the fading process is correlated. T_C is closely related to Doppler spread $f_{d,max}$ as:

$$T_C \approx 1/f_{d,max} = 1/\,(166.67Hz) = 0.006s = 6ms \qquad (2.3)$$

If the symbol time duration T_S is smaller than T_C, the fading is slow fading; otherwise, the fading is fast fading. As the UE moves , typically a drop in SNR of 20-30 dB is observed.

2.2.3 Rayleigh Fading

Rayleigh fading is viewed as a reasonable model for the effect of heavily built-up urban environments. Rayleigh fading is most applicable and utmost representative when there is no dominant propagation along a line of sight between the transmitter and receiver. If there were more scatterers present and more antennas at each end, this would mean there is more multipath available to exploit and also more separate channels could be created to enhance the separation of the signals. This is quantified by what is known as scattering richness, which will be of great benefit to MIMO.

If there is no line-of-sight between the transmitter and the receiver, the attenuation coefficients corresponding to different paths are often assumed to be independent and identically distributed (iid). Due to the central-limits, if the occurrence of scatter is adequate, the channel impulse response (h) will be well-modeled as a Gaussian process (complex random variable) irrespective of the distribution of the individual components but if there's no dominant component to the scatter, then such a process will have a zero mean and phase evenly distributed between 0 and 2Π radians. The channel response h will therefore have random amplitude whose envelope will follow a Rayleigh distribution. [1] Rayleigh channel is modeled with a circularly symmetric complex Gaussian random variable of h_{re} and h_{im} having the following form:

$$h = h_{re} + jh_{im} \tag{2.4}$$

$$|h|^2 = |h_{re}|^2 + |h_{im}|^2 \tag{2.5}$$

where h is a random variable taken here as the received amplitude .The probability density function of the magnitude h of complex has been defined which is expressed:

$$f(h) = \frac{h}{\sigma^2}\ e^{\frac{-h^2}{2\sigma^2}} \tag{2.6}$$

whose first two moments respectively are:

$$E\{h\} = \sigma\sqrt{\frac{\Pi}{2}} \tag{2.7}$$

$$E\{h^2\} = 2\,\sigma^2 \tag{2.8}$$

A similar response would also be found for a stationary subscriber as a function of time due to the relative motion of scatterers in the local vicinity of the subscriber. Because the noise variance is usually constant, the instantaneous received SNR fluctuates similarly to the channel energy $E\{x^2\}$ and drop dramatically during certain periods.

Generally LTE provide the best service under line-of-sight conditions. However MIMO thrives under rich scattering conditions. This is normally present within typical indoor and most urban environments. In order to achieve promised throughputs in LTE systems, operators must optimize its networks' multipath conditions for MIMO, targeting rich scattering conditions for each multipath signal. MIMO work in propagation medium is rich scattering or Rayleigh fading and fades are independent and identically distributed. The ideal MIMO radio channel models assume a Rayleigh fading environment, which assume that the fades for each transmitting-receiving antenna pair are independent [7].

2.3 Multipath LTE-Specific Channel Profiles

Multipath fading is characterized by a power-delay profile comprising two components: a vector of relative delays and a vector of average power parameters mean excess delay or the root mean square (rms) delay spread. For urban micro cell (R=0.59), the typical delay spread at cell edge can be calculated easily as follows.

The time a signal takes to travel from the transmitter to the receiver depends on its path length. Conceptually, we can divide the channel into a continuum of paths of equal length. These paths necessarily trace out ovals, with the transmitter and receiver at the foci. For a given oval, all paths from the transmitter to any point on the oval, then to the receiver, have equal length, and thus equal propagation delay [19]. The maximum distance the signal travel is approximately the difference between non-line of sight with maximum distance of 2R and line of sight with distance of R. Thus, for UE at cell edge the propagation delay distance is equal to 3R-R=2R. Then the approximate typical delay spread for 120^0 sectored microcell is:

$$\tau_{max} = \frac{2R}{C} = \frac{2*(590m)}{(3*10^8 m/s)} = 3.26\ \mu s \qquad (2.9)$$

Therefore, the RMS delay is in the range between 1μs and 2μs. For Rayleigh distribution, $\tau_{rms} = \tau_{max}/ 4 = 0.98$μs . The Coherence Bandwidth is calculated as:

$$B_c = \frac{1}{\tau_{rms}} \qquad (2.10)$$

Therefore $B_c=1/\tau_{rms}=$ 1/0.98μs = 1.02 MHz .But for moving users, it can be calculated from table 2.1 using the equation (2.13). The delay power density spectrum ρ(τ) that characterizes the frequency selectivity of the mobile radio channel gives the average power of the channel output as a function of the delay τ .

The mean delay τ, the root mean square (RMS) delay spread $\tau_{rms}$and the maximum delay τ_{max} are characteristic parameters of the delay power density spectrum. RMS delay spread is an important measure which characterizes the time dispersive of the channel and it is defined as follows [20]:

$$\tau_{1m} = \frac{\sum_{i=1}^{n} p_i \, \tau_i}{\sum_{i=1}^{n} p_i} \qquad \textit{(First moment)} \qquad (2.11)$$

$$\tau_{2m} = \frac{\sum_{i=1}^{n} p_i^2 \, \tau_i}{\sum_{i=1}^{n} p_i^2} \qquad \textit{(Second moment)} \qquad (2.12)$$

Thus the rms delay spread is

$$\tau_{rms} = \sqrt{(\tau_{1m} - \tau_{2m}{}^2)} \qquad (2.13)$$

The 3GPP Technical Recommendation (TR) 36.104 specifies three different multipath fading channel models: the Extended Pedestrian A (EPA), Extended Vehicular A (EVA), and Extended Typical Urban (ETU). [9] The channel profile quantifies the delays and relative powers of the multipath components. It can be observed that the EPA model has seven multipath components whereas the EVA and ETU models have nine multipath components each.

The delay profiles of these channel models correspond to a low, medium, and high delay spread environment, respectively and a value of 5, 70, or 300 Hz will be used as the maximum Doppler shift. From the tap delay and relative power we can calculate the RMS delay using (2.13) and then find the important parameters of Coherence Bandwidth for each channel profile. Given the maximum Doppler frequency for each profile, we can use (2.1) to get the maximum speed of the user.

Table 2-1 LTE channel models (EPA, EVA, ETU) for Cost231-Hata: delay profiles [9]

Channel model	Excess tap delay (ns)	Relative power (dB)	RMS delay value(ns)	Doppler frequency (Hz)	Coherence Bandwidth (MHz)	Maximum speed (km/hr)
Extended Pedestrian	[0 30 70 90 110 190 410]	[0 −1 −2 −3 −8 −17.2 −20.8]	45	5	22.22	3.0
Extended Vehicular	[0 30 150 310 370 710 1090 1730 2510]	[0 −1.5 −1.4 −3.6 −0.6 −9.1−7 −12 −16.9]	357	70	2.8	42
Extended Typical Urban	[0 50 120 200 230 500 1600 2300 5000]	[−1 −1 −1 0 0 0 −3 −5 −7]	991	300	1.0	180

2.4 Basic Building Blocks of LTE-MIMO

Wireless systems are designed to convey information from a transmitter, across a channel, to a receiver. The components of an LTE- MIMO system are [5]:

i) Transmitters at eNodeB with a space-time modulator that maps bits to space-time codewords. Codeword: represents user data before it is formatted for transmission.

ii) A matrix propagation channel **H** that is a function of the wireless environment, and

iii) Space-time receivers at the UE that uses an estimate of the propagation channel to decide on the transmitted bit stream.

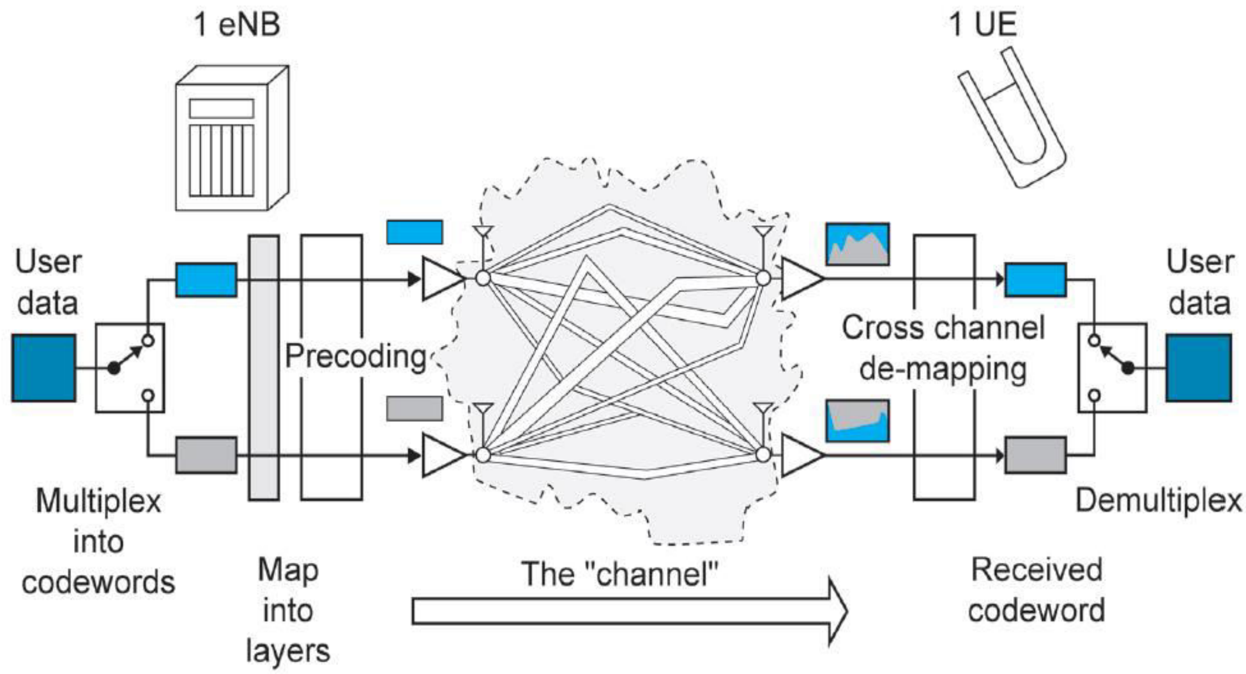

Figure 2-2 SU-MIMO in the downlink with two antennas; Codebook 0 shown [5]

The baseband signal generation for the data channel uses the following steps [21]:

1. Scrambling of coded bits in each of the codewords to be transmitted on a channel.
2. Modulation of scrambled bits to generate complex-valued modulation symbols.
3. Mapping of the modulation symbols onto one or several transmission layers. A maximum of four layers is supported in LTE Rel-8.
4. Precoding of the modulation symbols on each layer for transmission on the antennas
5. Mapping of the modulation symbols for each antenna port to resource elements.
6. Generation of a time-domain OFDM signal for each antenna port.

The receiver collects the signals at the output of each receive antenna element and reverses the transmitter operations in order to decode the data: receive space–time processing, followed by space–time decoding, symbol demapping, deinterleaving and decoding.

The Algorithms of the thesis topics considered will depend on the following network area categories:

• **Radio** –characterize the channel, derive models of its behavior and deal with how it impacts the performance. Another important factor is the analytical model using stochastic property of Rayleigh fading. So the channel gain Matrix H is very important parameter.

- **Signal processing** – The MIMO signals will need to be processed such that they have algorithms to detect the incoming MIMO signals and successfully decode them. Algorithms include Maximal ratio combining, Zero Forcing (ZF) , Linear Minimum Mean Square Error (LMMSE). We also use algorithm called waterfilling for power allocation,
- **Coding** – Techniques such as space–time codes (Almouti coding), Singular value decomposition for precoding and postcoding and eigenforming aim at achieving a balance between increasing the data rate and introducing redundancy.

2.5 Multi-Antenna Configurations

It is very important to model the exact location of antennas before deploying them just adding antennas does not guarantee signal improvement and may have a contrary effect. The physical relationship called correlation between the antennas becomes a new variable to deal with, affecting the relationship between the paths that the signals take [22].

In case of eNodeB antennas in typical micro-cell environments an antenna distance in the order of ten wavelengths (10λ) is typically needed to ensure a low mutual fading correlation. An antenna distance in the order of only half a wavelength (0.5λ) is often sufficient to achieve relatively low mutual correlation and an angular shift of at least 1/8 of the antenna beamwidth may optimize signal diversity.

This is because the multi-path reflections that cause the fading mainly occurs in the near-zone around the mobile terminal. Thus, as seen from the mobile terminal, the different paths will typically arrive from the different paths will typically arrive from a wide angle. A four-branch antenna is quite practical at f_c =1.8GHz. For an operator with a frequency carrier of f_c =1.8 GHz (λ=C/ f_c=16.66 cm), Antenna spacing or distance D for UE and eNodeB respectively must be [23]:

$$D(UE)=\lambda/2=8.33cm \qquad (2.14)$$

$$D(eNodeB)= 10\,\lambda = 1.66\,m \qquad (2.15)$$

The reason for the difference between the eNodeB and the mobile terminal is that the multi-path reflections that cause the fading mainly occurs in the near-zone around the mobile terminal. Thus, as seen from the mobile terminal, the different paths will typically arrive from the different paths will typically arrive from a wide angle.

2.6 Overview of OFDM

OFDM is a multicarrier transmission scheme. In conventional single-carrier systems, a single fade or interferer can cause the entire link to fail, but in multi-carrier systems, only a small percentage of the subcarriers will be affected. The beauty of OFDM is that it divides the channel in a way that is both computationally and spectrally efficient. High aggregate data rates can be achieved, while the encoding and decoding on different subcarriers can use shared hardware components. [5] The basic OFDM signal comprises a large number of closely spaced continuous wave (CW) tones in the frequency domain. The most basic form of modulation applied to the subcarriers is square wave phase modulation, which produces a frequency spectrum represented by a sinc (=sin(x) / x) function that is convolved around the subcarrier frequency.

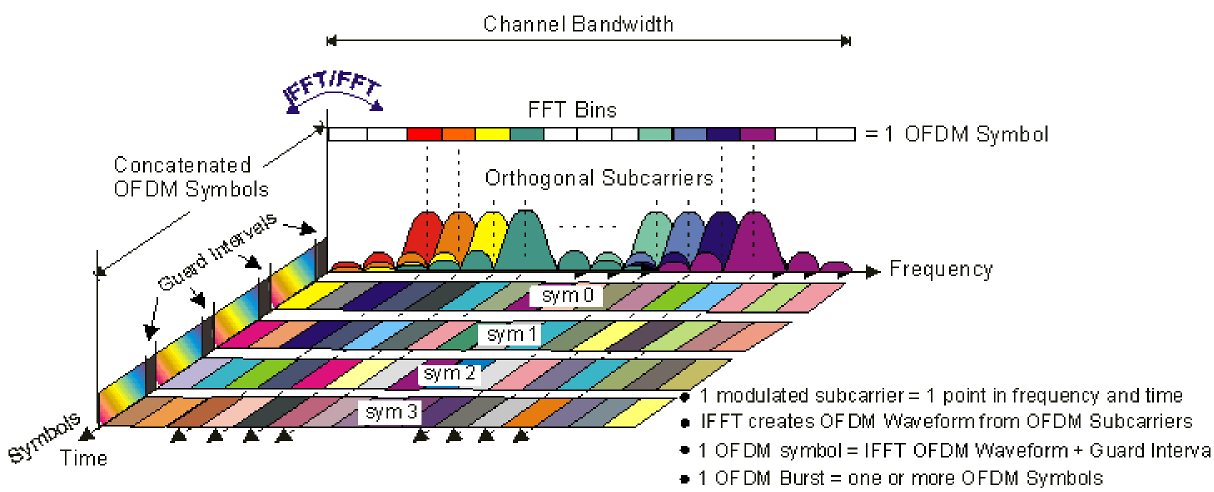

Figure 2-3 Frequency-Time Representative of an OFDM signal [24]

The main idea behind it is to subdivide the information transmitted on a wideband channel in the frequency domain and to align data symbols with multiple narrowband orthogonal subchannels known as subcarriers. Since the subcarriers can be individually demodulated, OFDM provides a higher robustness to the transmitted signals [9]. For standard LTE each modulating symbol lasts 66.7 μs. By setting the subcarrier spacing to be 15 kHz (=1/ (66.7μs)) the peaks and nulls line up perfectly such that at any subcarrier frequency, the subcarriers are orthogonal; i.e., there is no interference between them. As shown in (Table 2.1), the 15 kHz sub-carrier spacing, whose bandwidth is much less than coherence bandwidth C_{BW} =1.01MHz of the typical urban environment.

2.7 MIMO-OFDM

OFDM-based systems are sensitive to the inter-carrier interference (ICI) generated by a carrier frequency offset (CFO), which degrades the error probability performance for both single-antenna OFDM systems. [1] Moreover, in a multipath fading environment, performances of OFDM system in LTE are severely degraded by random variations in the amplitude of the received signals as well as by the presence of inter-symbol interference (ISI) and inter-carrier-interference (ICI) which also limit the OFDM system performance. This is because the orthogonality between the subcarriers will be partially lost due to the overlap of the demodulator correlation interval for one path with the symbol boundary of another.

To address these challenges, a promising combination has been exploited, namely, MIMO with OFDM which has already been adopted for present and future of LTE. MIMO OFDM is a technology that combines MIMO and OFDM together to transmit data in order to deal with frequency selective channel effect. OFDM transmission scheme in each antenna constructs the resource grid, generates the OFDM symbols, and transmits. In a MIMO-OFDM system, this process is repeated for multiple transmit antennas [25].

Following transmission of OFDM symbols associated with multiple resource grids on multiple transmit antennas, at each receive antenna the OFDM symbols of all transmitted antennas are combined. But this MIMO cannot achieve zero ISI and hence cannot be used alone [14]. The MIMO signaling can easily be overlaid on an OFDM based system. The MIMO signaling treats each subcarrier in OFDM as an independent narrowband flat channel.

2.7.1 MIMO-OFDM Modeling

The modeling of MIMO channels is a multistep procedure. If realistic modeling is wanted, it must be based on measurements from which the relevant features are extracted. It is impossible to know all of the channel information, much less have the ability to solve for all possible boundary conditions in a real-life channel. We have to make some assumptions to make the problem mathematically tractable. Assuming more general randomness, a simulation model may be required to satisfy the experimental conditions only approximately in order to simplify matters. It is a common approximation to assume random phases from scatterers, in which case summation from a few scatterers leads to the well-known complex Gaussian distributions with Rayleigh distributions for the amplitudes [18].

In contrast to physical models, analytical channel models characterize the impulse response of the channel between the individual transmitting and receiving antennas in analytical way without explicitly accounting for wave propagation. The effect of a linear channel on the transmitted energy is characterized by the channel impulse response. A channel's impulse response completely characterizes its input–output relationship. The implicit assumption is that all energy from all paths in the physical channel combines to form a single response. The individual impulse responses are subsumed in a MIMO channel matrix. Analytical models are very popular for synthesizing MIMO matrices in the context of system and algorithm development and verification [26].

2.7.2 Analytical MIMO-OFDM Channel Models

Essentially, in LTE relationships between multiple transmit and receive antennas are best explained at each individual subcarrier rather than across the entire bandwidth. A successful implementation of a MIMO system hinges on solving systems of linear equations at the receiver in order to correctly recover the transmitted data. This means that the relationship between multiple transmitters and receivers can be expressed with a MIMO system of linear equations, which are solved at the receiver for each and every subcarrier of the full spectrum in order to recover the transmitted signal. A matrix **H** is then assembled to relate each transmit signal to each receive antenna [9]. For MIMO system with M transmit antennas and N receive antennas .The linear equation is as follows:

$$y_n(t) = \sum_{i=1}^{M} h_{nm}(t,\tau) * x_m(t) + n_n(t) \qquad (2.16)$$

$$y_n(t) = \sum_{i=1}^{M} \left(\int_{-\infty}^{\infty} h_{nm}(t,\tau)\, x_m(t-\tau)\, d\tau \right) + n_n(t) \qquad (2.17)$$

where * denotes convolution and $h_{nm}(t)$ is a weight or attenuation coefficient that represents the impact of the mth transmitting signal $x_m(t)$ on the nth receiver signal strength. Noise at receiver $n_n(t)$ is zero mean complex circularly symmetric (ZMCCS). Note that. In this thesis *boldface* uppercase and lowercase letters will represent *matrices and column vectors* respectively.

We start with a general channel which has both multipath fading and Doppler spread. Each path coefficient is a function of not only time t because the mobile is moving but also a time delay relative to other paths. The variable τ indicates relative delays between each component caused by frequency shifts. The time variable t represents the time-varying nature of the channel such as one that has Doppler or other time variations. In this case, the **H** (t, τ) matrix changes randomly with time [23]. The channel matrix H(t, τ) for this channel takes this form :

$$\mathbf{H}\,(\mathrm{t},\tau) = \begin{bmatrix} h_{11}(\mathrm{t},\tau) & \cdots & h_{1M}(\mathrm{t},\tau) \\ \vdots & \ddots & \vdots \\ h_{N1}(\mathrm{t},\tau) & \cdots & h_{NM}(\mathrm{t},\tau) \end{bmatrix} \qquad (2.18)$$

The rank of the channel matrix defines the number of linearly independent rows or columns in H. It indicates how many independent data streams can be transmitted simultaneously. If **H** is full rank, which is referred to as a *rich scattering environment*, then

$$r = \min(M,N) \qquad (2.19)$$

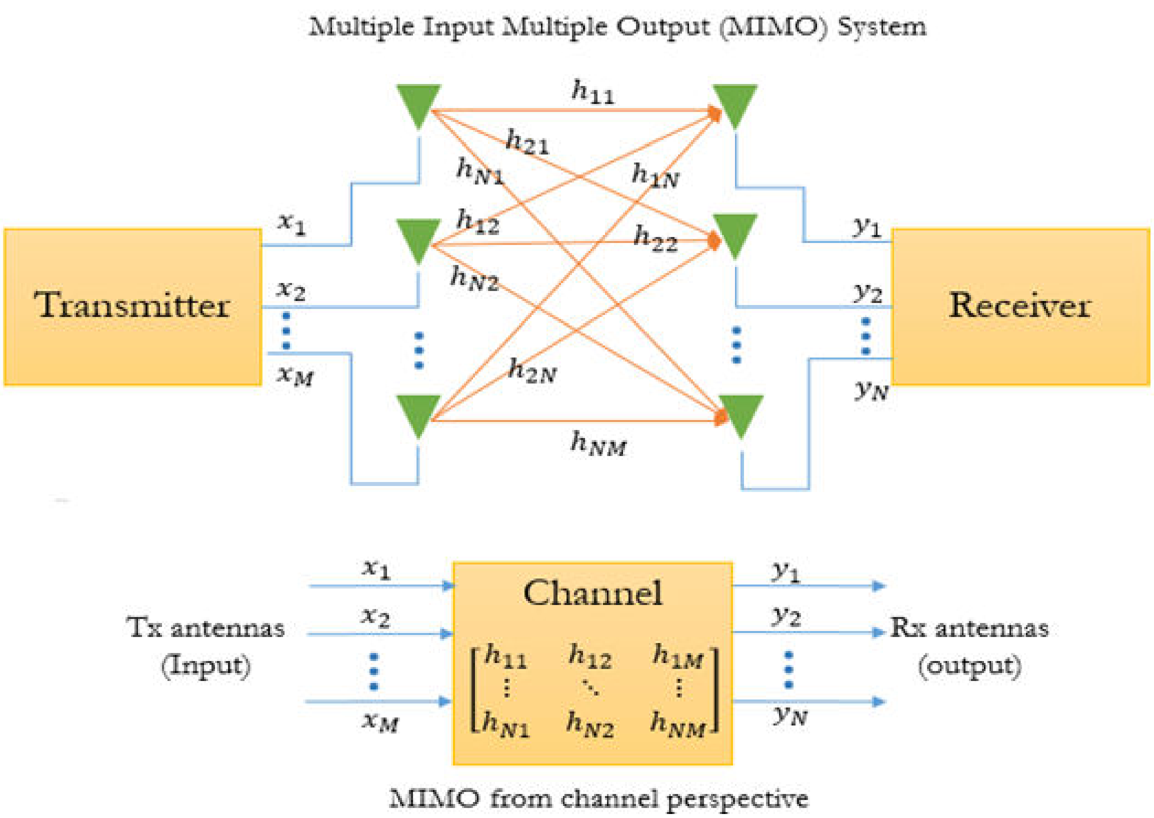

Figure 2-4 LTE-MIMO system for M × N antennas [27]

In order for MIMO to work, there must be a reasonable degree of difference between each of the transmission paths ($h_{nm}(t,\tau)$). If they are all identical then each of the signals received at the subscriber unit antennas will also be identical and it will not be possible to invert the matrix and hence extract the different transmitted signals.

Differences across paths tend to occur in mobile environments where there is rarely a line of sight to the eNodeB and multiple reflections take place. **H** will characterize how the performance of the SU-MIMO system. In this thesis, each channel coefficient elements of the matrix are Rayleigh i.i.d. So they are full rank and uncorrelated [18]. Many MIMO algorithms are based on the analysis of transmission matrix **H** characteristics. It is this channel state matrix **H** that is useful in assessing the MIMO channel, and therefore is described further here afterwards.

2.8 Narrowband MIMO System Model

The MIMO channel models can be divided into wideband and narrowband by considering the system bandwidth. In the wideband channel models, the channel is assumed to have different channel responses for different frequencies, so that the channel is a frequency selective fading channel [14]. On the contrary, the narrowband channel model is assumed to have an equal response over the system bandwidth. Since OFDM transforms the wideband channel into narrowband flat fading, we will only deal with Narrowband channel in this thesis.

For narrowband MIMO with symbol period T > τ_{max}, the convolutions in (2.11) cause h (t, τ) to be modeled by a single dependence on t: written as h(t). In the sampled domain, h(k) =h(kT) is simply the sampled channel representation of h(t). The channel coefficient at time k between transmit antenna m and receive antenna n is denoted h_{nm}(k). At time k, the signal x_m(k) is transmitted from antenna m.

At receive antenna n, the received signal is denoted as y_n(k)and the additive noise as n_n (k). x_m (k), y_n (k) and n_n (k) are all assumed to be complex quantities. However it is time-varying, i.e. has Doppler, we would write this relationship without the convolution as h(k).M signals are transmitted forming the vector input signal x(k) and N signals are received forming the vector output signal y(k).

$$y_n(t) = \sum_{m=1}^{M} h_{nm}(t)\, x_m(t) + n_n(t) \tag{2.20}$$

$$y_n(k) = \sum_{m=1}^{M} h_{nm}(k)\, x_m(k) + n_n(k) \tag{2.21}$$

Since OFDM is used to decompose a possibly frequency-selective channel into parallel, noninterfering tones. This means that the relationship between multiple transmitters and receivers can be expressed with a MIMO system of linear equations, which are solved at the receiver for each and every subcarrier of the full spectrum in order to recover the transmitted signal [28]. Thus the received signal on the any one of the tone (OFDM subcarrier) is:

$$\boldsymbol{y}(t) = \boldsymbol{H}(t)\boldsymbol{x}(t) + \boldsymbol{n}(t) \tag{2.22}$$

$$\boldsymbol{y}(k) = \boldsymbol{H}(k)\boldsymbol{x}(k) + \boldsymbol{n}(k) \tag{2.23}$$

where $\mathbf{x}(k) = \begin{bmatrix} x_1(k) \\ \vdots \\ x_M(k) \end{bmatrix}$, $\mathbf{y}(k) = \begin{bmatrix} y_1(k) \\ \vdots \\ y_N(k) \end{bmatrix}$, $\mathbf{n}(k) = \begin{bmatrix} n_1(k) \\ \vdots \\ n_N(k) \end{bmatrix}$

N additive noise signals are grouped in the vector n(k). n(k) is the sampled noise vector, containing the noise contribution at each receive antenna, such that the noise is white in both time and spatial dimensions, the energy of the noise is :

$$E\{n_i(k) * n_j(k)\} = \sigma^2 \delta(k - l). \tag{2.24}$$

$$E\{\boldsymbol{n}(k)\} = \sigma^2 \boldsymbol{I}_{\boldsymbol{N}} \tag{2.25}$$

Transmission matrix **H** contains the channel impulse responses h_{nm} which reference the channel between the transmit antenna m and the receive antenna n. The nth column of **H** is often referred to as the spatial signature of the nth transmit antenna across the receive antenna array. We define a channel matrix **H** for narrowband channel as:

$$\mathbf{H}(\mathrm{k}) = \begin{bmatrix} h_{11}(\mathrm{k}) & \cdots & h_{1M}(\mathrm{k}) \\ \vdots & \ddots & \vdots \\ h_{N1}(\mathrm{k}) & \cdots & h_{NM}(\mathrm{k}) \end{bmatrix} \tag{2.26}$$

Finally, it is important to emphasize about normalization used in the following Chapters of this thesis to characterize the channel matrix on a given link. Normalization matters, we assume that the channel remains constant over symbol duration, and drop the time index *k* for better legibility. It must be clear from the context that *M* and *N* designate antennas and not sampled time instants.

As a general rule, if an equation that involves **H** also explicitly contains the SNR, then the channel matrix can be assumed to be normalized [28]. We usually normalize the average squared channel Frobenius norm of channels as follows:

$$E\{||\boldsymbol{H}||^2\} = E\{\sum_{m=1}^{M}\sum_{n=1}^{N}|h_{nm}^2|\ \} = MN \tag{2.27}$$

This normalization has no impact on the channel model itself, as it represents only a scaling factor of the whole matrix. It is nevertheless highly relevant when considering transmit power constraints and path-loss effects, especially when estimating the mutual information. The key message, however, is always to make sure that the transmit power remains constant (and not necessarily the average receive SNR). While Input symbols are independent temporally and spatially:

$$E\{X\boldsymbol{X^H}\} = P_x\ \boldsymbol{I_M} \tag{2.28}$$

2.9 MIMO Detection Techniques

The techniques which are used to recover the original signal are referred to as MIMO detection techniques. In Linear signal detection methods, like Zero Forcing (ZF), Linear estimation (LE) and Linear Minimum Mean Square Error (LMMSE), it treats all the transmitted signals as interference except for the desired stream from the target transmit antenna.

On the other hand, non-linear detection technique, like Maximum Likelihood (ML), it optimally takes into account the properties of noise and interference. However the complexity of the ML detector grows quadratically with the size of the signal constellation. A QPSK with a single symbol results in 2^2=4 complex operations. Therefore, we were motivated to use simpler practically realizable suboptimum receivers [26].

In the previous Sections, MIMO is represented with the model of **y=Hx + n**. The optimal detection problem in multi-antenna wireless communication systems often reduces to the problem of finding the least-squares solution to a system of linear equations. In each stage, we do partial differentiating J(X) with respect to the *vector* **x** and then setting it to zero to get the optimum value $\hat{x}$. The transmitter vector x is estimated using the following techniques:

1. *Zero forcing detectors* invert the channel matrix and have small complexity but perform badly at low SNR (cell-edge users). It does not depend on the modulation. By using a zero-forcing error, we estimate $\boldsymbol{x}$ by minimizing J($\mathbf{X}$) = $||\mathbf{y} - \mathbf{Hx}||^{2}$

The estimated transmitted signal $\hat{\mathbf{x}}$ after faded by the channel is:

$$\hat{\boldsymbol{x}} = [(\boldsymbol{H}^{H}\boldsymbol{H})^{-1}\ \boldsymbol{H}^{H}]\boldsymbol{y} \tag{2.28}$$

Zero forcing corresponds to bringing down the Inter Symbol Interference (ISI) to zero in a noise free case.

2. *Linear estimation* for MIMO, we follow Bayesian approach for a transmitted vector and receive vector with J($\mathbf{X}$) =E{ $||\hat{\mathbf{x}} - \mathbf{x}||^{2}$},

Since the noise and transmitted signal being uncorrelated, we have:

$$\mathrm{E}\{\mathbf{n}\mathbf{x}^{H}\} = \mathrm{E}\{\mathbf{n}^{H}\mathbf{x}\} = \mathbf{0} \tag{2.29}$$

Using the above uncorrelation property, the estimated received signal is:

$$\hat{\boldsymbol{x}} = \boldsymbol{G}^{H}\ \boldsymbol{y} \tag{2.30}$$

E{.}denotes the expectation operator and the optimal value of **G** is obtained as :

$$\boldsymbol{G} = ([\boldsymbol{E}\{(\boldsymbol{y}\boldsymbol{y}^{H})\}]^{-1})\ (\boldsymbol{E}\{(\boldsymbol{y}\boldsymbol{x}^{H})\}) \tag{2.31}$$

3. *Linear Minimum Mean Square Error (LMSSE) detectors* reduce the combined effect of interference between the channels and noise, but require knowledge of the SNR. The LMMSE detector is the optimal detection that seeks to balance between cancelation of the interference and reduction of noise enhancement. With J($\mathbf{X}$) = $||\mathbf{Y} - (\mathbf{HX} + \mathbf{n})||^{2}$, the solution is obtained as the covariance matrix of the signal vector is $p_d\boldsymbol{I}$. Then the estimated detected signal vector is obtained as [6] :

$$\hat{\boldsymbol{x}} = p_d(\ (p_d\ \boldsymbol{H}^{H}\ \boldsymbol{H} +\ \sigma^{2}\boldsymbol{I})^{-1})\ \boldsymbol{H}^{H} \tag{2.32}$$

This is the LMMSE computed using the average signal power $\mathrm{p_d}$ .We used Bay's identity. We will simulate these stages in the 6th Chapter and compare their efficiencies with each other. We will show how the estimated signal compared with the transmitted signal in each method.

CHAPTER 3

3 DOWNLINK MODES OF SU-MIMO

One of the tools in the LTE toolbox of radio features is MIMO antennas. In MIMO the performance will depend on many factors and it is clear that there is no single mode that universally provides superior performance in all usage scenarios. However, it is possible for a subset of modes to be implemented and the system configured to intelligently switch among them to optimize performance [28].

In LTE, different UEs in a cell are allowed to have different transmission modes. Operators can compare scanning receiver measurements to UE-reported data logged by the network to determine if the eNodeB is effectively adapting transmissions to the RF environment. Selection of the correct SU-MIMO mode depends on factors such as mobility, SNR. Depending on reported channel conditions and the UE's ability to quickly send detailed updates on these conditions, the eNodeB selects between SU-MIMO modes.

This Chapter discusses the basic MIMO techniques available in LTE downlink operations. Because network conditions and UE capabilities can vary greatly, MIMO systems must be highly flexible in order to maximize gains in throughput. Since each eNodeB can be configured differently in terms of how it adapts transmissions in real time, it is important to understand the key transmission modes available in LTE, as well as the conditions under which they are most useful. These modes are designed to take the best advantage of different channel and multipath conditions and eNodeB antenna configurations, as well as differences in UE capabilities and mobility.

However, these throughput gains depend on three factors: maximizing rich scattering conditions within a cell, configuring the eNodeB to properly match MIMO settings to real-world conditions, and ensuring that UEs can take full advantage of the multipath conditions that are present. Scanning receivers that can provide accurate real-world measurements of multipath conditions and potential throughput are essential tools for evaluating the performance of all three of these factors [3]. With these measurements, operators will be able to maximize the data rates and reliability of LTE networks, resulting in a premium return on their LTE equipment investments while improving customer satisfaction.

3.1 Spatial Diversity and Spatial Multiplexing

Generally, there are two categories of multiple antenna techniques in LTE Release 8 of FDD mode. The first one aims to improve the power efficiency by maximizing **spatial diversity**. Such techniques SIMO, also called receive diversity, as well as MISO, also called transmit diversity. The second type uses **spatial multiplexing** where under rich scattering environments, independent data streams are simultaneously transmitted over different antennas to increase the effective data rate [17].

These systems may be implemented in a number of different ways to obtain either a diversity gain to combat signal fading or to obtain a capacity improvement to achieve throughput gains. In addition to good multipath conditions, spatial multiplexing depends on high SNR to produce large throughput gains. In spatial multiplexing, even though multiple data streams are transmitted, the total power of the transmission remains the same [5].

3.1.1 Space Diversity

Diversity techniques have several benefits: the link quality is more stable, the average performance is improved. They are transmit and receive diversity. These MIMO technologies improve performance in particular with respect to the radio cell boundaries, in other words they effectively increase the size of the radio cell. This is very important for Operators since if one eNodeB is down because of electric power shortage the other eNodeBs will widen their coverage and cover the place where the network signal can’t be found [29].

Assume that the receiver is provided with multiple replicas of the same information bearing signal, and denote by p the probability that the instantaneous SNR is below the receiver threshold on a single diversity branch p_{out} denotes the probability of outage for that specific threshold in this case. If the receiver is provided with L replicas that fade independently, then the probability that all the branches are at, or below the threshold at the same time is equal to $(p_{out})^{L}$. That’s how diversity is one of the most effective ways to combat deep fades. The principle of diversity is to provide the receiver with multiple versions of the same signal. If these can be made to be affected in different ways by the signal path, the probability that they will all be affected at the same time is considerably reduced [7].

3.1.1.1 Receiver Diversity (SIMO)

In a cellular environment, the signal from a single receive antenna will suffer level fluctuations due to various types of fading. Receiver-combining methods combine multiple versions of the transmitted signal at the receiver to improve performance. This aids received data integrity, where SNR is poor due to multipath fading. Two types of combining method can be used at the receiver: Maximum Ratio Combining (MRC) and Selection Combining (SC) in LTE [30].

In MRC, we combine the multiple received signals by averaging them to find the most likely estimate of the transmitted signal. [3] In SC, we use only the received signal with the highest SNR to estimate the transmitted signal. Recently, in the advanced mobile systems, MRC scheme shows the best performance and it tends to be the mostly employed among other diversity schemes.

MRC would not simply add the two signals, after aligning their phases so that they add coherently, but it would scale them suitably so that stronger signals have more weight. In this method, the phase and gain of each branch is optimally adjusted prior to combining the signals. This processing is information lossless. The received signals are aligned in phase so that they can add constructively and a larger weight (scaling coefficient) is assigned to stronger channels. It signifies that branches with strong signal are further boost up, while weak signals are attenuated [22].

The MRC diversity technique provides the best performance to mitigate the wireless channel impact. This allows the recovery of the best possible signal, although the noise can be a major impairment, as it is also amplified with the faded signal. The method performs well when the signals are quite above noise level. Note that in frequency-selective fading, this process is performed differently for each subcarrier according to its specific channel gains. In systems with OFDM, MRC is performed separately for each subcarrier. This requires a good knowledge of each channel, which is derived from pilot analysis. This method estimates each channel independently and then multiplies the signal by the convoluted channel [16].

3.1.1.2 Transmit Diversity (MISO)

In transmit diversity, redundant information is transmitted on different antennas at each subcarrier. It increases the robustness of the signal to poor channel conditions. In LTE, transmit diversity is used as a fallback option when spatial multiplexing (SM) cannot be used. [30]. The advantage of using MISO is that the multiple antennas and the redundancy coding processing is moved from the receiver to the transmitter. In instances such as Smartphone UE, this can be a significant advantage in terms of space for the antennas and reducing the level of processing required in the receiver for the redundancy coding. This has a positive impact on size, cost and battery life as the lower level of processing requires less battery consumption. It is therefore more economical to add equipment to eNodeB rather than UE.

When using two transmit antennas, transmit diversity in LTE is based on Space–frequency Block Coding (SFBC). SFBC is closely related to the more familiar Space Time Block Coding (STBC). The encoding in SFBC is carried out in the antenna/frequency domains (tones) rather than in the antenna/time domains. STBC sends the same user data to both transmit antennas, but at different times, for improving the probability of successfully recovering the desired data [11]. The physical separation of the antenna ports provides the space diversity, and the time difference derived from the bit-reversing process provides the time diversity. These features together make the decoding process in the receiver more reliable.

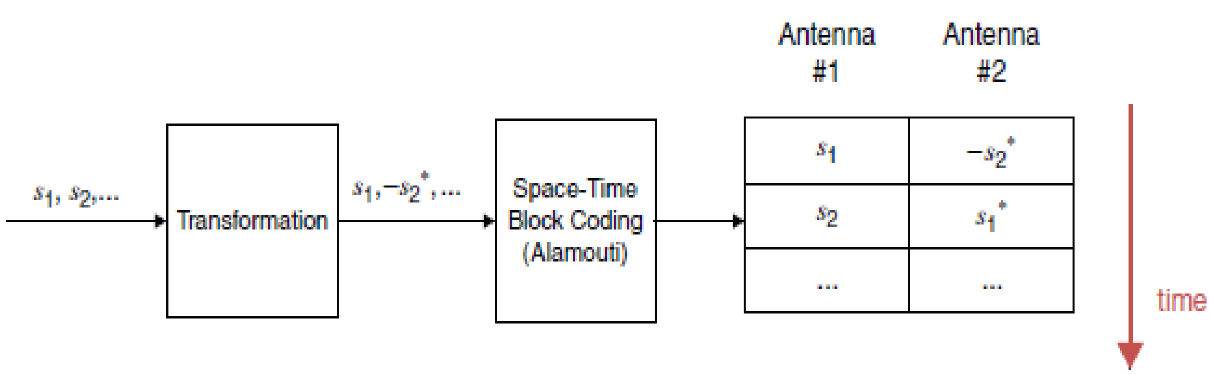

Figure 3-1 SFBC as a combination of a transformation and STBC [9]

One of the simplest forms of STBC is an Alamouti code defined for a two-antenna transmission. In STBC with Alamouti code, as illustrated in Figure 3.2, pairs of modulated symbols (s_1, s_2) are mapped on the first and second antenna ports in the initial sample time.

In the following sample time, the symbols are swapped and conjugated ($-s_2^*$, s_1^*) and mapped to the first and second antenna ports. Note that the two consecutive vectors in time are orthogonal.In this technique, even though different information is sent by each antenna on one symbol, the same information is repeated over the next symbol, thus this is still considered a diversity scheme [29].

SFBC can be considered as frequency domain adaptation of space-time block coding. We can produce the SFBC output symbols through a simple transformation followed by STBC using the Alamouti code. This approach leverages the availability of efficient implementations for STBC and the Alamouti code and is considered advantageous as an example of software reuse [9]. In this thesis we will see the BER performance of STBC for SFBC that's used in LTE since they are similar.

3.1.2 Spatial Multiplexing (SM)

The use of spatial diversity increases the robustness of the channel, the use of spatial multiplexing trades this robustness by capacity when the channel is robust enough.SM is used to achieve higher data rates instead of signal quality. So, it works well when SNR of the channel is high. In other words, the data carrying capacity of the channel is high. When the SNR reaches the saturation point, additional improvements of SNR have little effect on Throughput.

The use of spatial multiplexing enables multiple streams to be used .These parallel streams, can share the SNR and therefore avoid the saturation point issue. The result is that each data stream contains a lower SNR than would be possible with a single data stream. However, because there are *diminishing returns* for additional SNR when SNR is already high, each of the multiple data streams may be capable of transmitting nearly as much data as a single stream [29].

Therefore, multiple data streams can be sent over spatially separate radio beams but over the same RF bandwidth. So, SDM doesn't exhaust the frequency resource, but uses space as a resource by exploiting different directional beams that can be sent from an antenna array. In SDM, the eNodeB divides the data to be sent to a given UE on a given sub-channel into data streams, called layers. Transmission rank is determined according to channel conditions at the UE, as well as other considerations such as available resources at the eNodeB [31].

3.2 Closed Versus Open Loop MIMO Operations

LTE's four SU-MIMO modes include two open loop modes (Open-Transmit Diversity and Open-Loop Spatial Multiplexing) and two closed loop modes (Closed-Loop Spatial Multiplexing and Closed-Loop Spatial Multiplexing). Open loop and closed loop modes differ in the level of detail and frequency with which channel conditions are reported by the UE [32]. The eNodeB relies on detailed and timely information from the UE in order to apply the best antenna and data-processing techniques for the existing channel conditions.

Depending on the UE's data-processing speed as well as the quality of its connection to the eNodeB in both uplink and downlink, LTE will operate in either closed loop or open loop mode. Other factors, such as UE processing speed or uplink data capacity (affected by UE specifications), may result in open loop operations even when the UE is moving relatively slowly [33]. The UE's capabilities are therefore crucial for achieving the best results from particular multipath conditions.

The three most important channel indicators are as follows.

- Precoding Matrix Indicator (PMI) determines the optimum precoding matrix for the current channel conditions.
- Rank Indicator (RI) is the number of layers that can be supported under the current channel conditions and modulation scheme.
- Channel Quality Indicator (CQI) is a summary of the channel conditions under the current transmission mode, roughly corresponding to SNR.

The eNodeB adjusts its transmission mode and the amount of resources devoted to the UE based on whether the CQI and RI reported by the UE matches the expected values.

Open loop and closed loop MIMO can be explained using PM, RI and CQI as follows:

- In **open loop** -the eNodeB receives minimal information from the UE: an RI and CQI. The eNodeB then uses the CQI to select the correct coding scheme for the channel conditions. The eNodeB communicates with a UE in open loop when the UE is moving too fast to provide a detailed report on channel conditions in time for the eNodeB to select the precoding matrix.
- In **closed loop-** the UE provides an RI as well as a PMI. Finally, the UE provides a CQI given the RI and PMI, rather than basing CQI on the current operation mode. This allows the eNodeB to quickly and effectively adapt the transmission to channel conditions [3].

3.3 Channel Conditions for Transmission Modes

In LTE, different UEs in a cell are allowed to have different transmission modes, with the ability to do mode switching. As an example, a UE moving at slow speed starts with a default transmission mode 4 but, when it moves to the cell edge, the eNodeB scheduler has the ability to switch it to transmission mode 3 if the PMI feedback becomes unreliable. The LTE standard allows dynamic switching between these modes to suit the prevailing circumstances [21].

Table 3-1 Summary of various downlink transmission modes for LTE Release 8 [21]

MIMO Modes	Purpose	Precoding	Multipath/ Scattering	Preferred UE speed (km/h)	Channel information	Dynamic Adaptation
1-Receive diversity	combat fading	None	Low	All	CQI	None
2-Open-loop transmit diversity	combat fading	SFBC/ STBC	Low(cell-edge, rural)	>30	CQI, RI	None
3-Open-loop spatial multiplexing	Exploit fading	None	High (urban)	>30	CQI, RI,	Transmit Diversity
4-Closed-loop Spatial multiplexing	Exploit fading	Precoding V of SVD	High (urban)	<30	CQI, RI, PMI	Transmit Diversity

There may be applications where a higher order of diversity is needed. The Transmit and Receive diversity methods can be combined in a so called MISO-SIMO.A combination of spatial diversity with spatial multiplexing is also possible. [7] Spatial Multiplexing can work as a combination of SIMO and MISO techniques, resulting in even greater SNR gains, further boosting coverage and data rates. However, when SNR is high, additional throughput gains are minimal, and there is little benefit from further boosting SNR. Suitable channel conditions are needed to make this practicable. Applications requiring extremely high reliability seem well suited for transmit diversity techniques whereas applications that can smoothly handle loss appear better suited for spatial multiplexing.

CHAPTER 4

4 ERGODIC CAPACITY OF SU-MIMO

The two major limitations in wireless channels are due to multipath interference, and the data throughput limitations as a result of Shannon's Law. SU-MIMO provides a way of utilizing the multiple signal paths that exist between a transmitter and receiver to significantly improve the data throughput available on a given channel with its defined bandwidth and transmit power. The capacity of a wireless system is the maximum transmission rate for which the decoding error probability can be brought arbitrarily close to zero. Capacity is the primary tool to characterize the performance of MIMO systems and it also serves in practical system as a guide to properly design the transmitted signals as well as the processing of the received signals [26].

The bandwidth has a close relationship with data-rates in turn has a dependency with channel capacity. In the late 1990's Foschini and Telatar predicted remarkable spectral efficiencies for wireless systems with multiple antennas when the channel exhibits rich scattering and its variations can be accurately tracked. The large spectral efficiencies associated with MIMO channels are due to the fact that a rich scattering environment provides independent transmission paths from each transmit antenna to each receive antennas [34].

In this Chapter, we use analytical method to calculate MIMO system ergodic capacity. The information-theoretic bound on the spectral efficiency is a function of the total transmit power and the channel phenomenology. In implementing SU-MIMO systems, we must decide whether channel estimation information will be fed back to the transmitter so that the transmitter can adapt.

The performance of transmission modes varies with the variation of multipath channel, UE speed and UE location within a cell. So, it is necessary to analyze their performance by considering the above facts. In this Chapter due path loss fading that low SNR regimes are found at the cell edge and high SNR regime are found at the cell centered. We first derive the ergodic capacity depending on UE speed and finally we will reduce the equations obtained for high SNR (for cell-centered UE) and low SNR (cell-edge user). For each scenario, we build on the SISO, SIMO, MISO and channels to present the MIMO channel to calculate their respective ergodic capacities

4.1 Effective Bit Energy-to-Noise Density Ratio of OFDM

For LTE system simulations, in general, the SNR at the receive antenna is used as input parameter for both capacity and BER performance evaluations. Let E_s/N_o be the SNR per sample at the input of the receiver baseband processing. It is the actual SNR of the data payload. Then, clearly, there is a relation between E_b/N_o and E_s/N_o [35].

Normally for a simple QPSK system, bit energy and symbol energy are the same. So E_b/N_o and E_s/N_o are the same for a QPSK system. But for an OFDM QPSK system, they are not the same. This is because; each OFDM symbol contains additional overhead in both time domain and frequency domain. The baseband processing of a MIMO transmission system consists of a number of subsequent blocks that have an influence on the relation between E_b/N_o and E_s/N_o. Thus we will take the SNR (ρ) as:

$$\rho = E_b/N_o \qquad (4.1)$$

In this Section, we will discuss a simple OFDM transmitter and receiver, find the relation between E_b/N_o and E_s/N_o. Since OFDM system has total number of nFFT subcarriers, number of used subcarriers (nDSC) of which are active. The remaining nFFT- nDSC are *virtual* subcarriers are used as frequency guard bands. And also the fact that the cyclic prefix will share the energy of the signal energy.

Table 4-1 Important parameters for BER for typical LTE Release 8 performance [4]

Parameter	**Value**
FFT size. nFFT	64
Number of used subcarriers. nDSC	52
FFT Sampling frequency	20MHz
Cylcic prefix duration, T_{cp}	0.8us
Data symbol duration, T_d	3.2us
Total Symbol duration, T_s	4us

Therefore we will see the effects of the ratio of the number of data subcarriers to number of FFT symbols and the ratio of Data symbol duration to total symbol duration. So the actual bit energy depends on as due to cyclic prefix and frequency spreads [36].

(i) For Cyclic prefix: -each OFDM symbol contains both useful data and overhead (in the form of cyclic prefix). The bit energy represents the energy contained in the useful bits. In this case, the bit energy is spread over N bits (where N is the FFT size).In an OFDM transmission, we know that the transmission of cyclic prefix does not carry 'extra' information. The signal energy is spread over time T_d+T_{cp} whereas the bit energy is spread over the time T_d i.e.

$$E_{s1}\ (T_d+T_{cp}) = E_b\ T_d \tag{4.2}$$

$$E_{s1} = \frac{T_d}{(T_d+T_{cp})} E_b \tag{4.3}$$

(ii) Frequency spread :- Again, in the frequency domain, the useful bit energy is spread across nDSC subcarriers, whereas the symbol energy is spread across $nFFT$ subcarriers**.**In OFDM transmission, all the available subcarriers from the DFT is not used for data transmission.

Typically some subcarriers at the edge are left unused to ensure spectrum roll off. For the 20MHz bandwidth , out of the available bandwidth from -10MHz to +10MHz, only subcarriers from -8.1250MHz (-26/64*20MHz) to +8.1250MHz (+26/64*20MHz) are used. This means that the signal energy is spread over a bandwidth of 16.250MHz, whereas noise is spread over bandwidth of 20MHz (-10MHz to +10MHz), i.e.

$$\frac{E_{s2}}{E_b} = \frac{nDSC}{nFFT} = \frac{16.25MHz}{20\ MHz} \tag{4.4}$$

Then the cumulative actual value E_s is equal to

$$E_s = \left(\frac{T_d}{(T_d+T_{cp})}\right)\left(\frac{nDSC}{nFFT}\right)\quad E_b \tag{4.5}$$

From (i) and (ii), the overall effect of both cyclic prefix and unused subcarriers on E_s/N0 or the relation between the actual bit energy and the bit energy is as follows:

$$\frac{E_s}{N_o} = \left(\frac{T_d}{(T_d+T_{cp})}\right)\left(\frac{nDSC}{nFFT}\right)\frac{E_b}{No} \tag{4.6}$$

Finally, we get

$$\frac{E_s}{N_o} = \varepsilon \frac{E_b}{N_o} \qquad (4.7)$$

Using the data from Table 5.1, we will calculate **ε**=0.65 for LTE Release 8. Therefore the actual or effective OFDM SNR ρ_s is equal to:

$$\rho_s = \frac{E_s}{N_o} = \varepsilon\rho \qquad (4.8)$$

where ρ is the energy of a bit per noise.

4.2 Characteristics of Capacity in Fading Environment

LTE exhibit different characteristics and performance according to the propagation environment. Those characteristics have to be carefully taken into account when defining capacity. In this Chapter, capacity is described according to two conditions:

1. *The knowledge of the channel at the transmitter and receiver*. A common assumption, adopted throughout this Chapter, is that the channel is perfectly known at the receiver. At the transmitter, two different types of channel knowledge are considered: either the instantaneous value of the channel is known or only its distribution is known.

2. *The nature of the wireless channel*. We treat three kinds of channels: the time invariant channel, the fast fading channel (the codewords spread over many channel variations) and the slow fading channel (the channel is constant across a given codeword).

[26] Note that CSI contains the information of **H** as well as the statistical properties of **n** in (2.22). However, by CSI, we often mean the knowledge of **H** (under the assumption that the statistical properties of **n** are available). Different assumptions can be made about the knowledge of the channel gain matrix **H** at the transmitter and receiver, referred to as channel side information at the transmitter (CSIT) and channel side information at the receiver (CSIR), respectively. The channel state information at the transmitter (CSIT) is the information about the channel available at the transmitter while the channel state information at the receiver (CSIR) is the information about the channel available at the receiver.

4.3 Singular Value Decomposition (SVD) of a Channel Matrix H

The SVD decomposition of the channel matrix is fundamental in understanding MIMO:

i. It extracts the equivalent independent AWGN channel structure,

ii. It gives the maximum number of streams that can be multiplexed simultaneously,

iii. It provides a very simple way to compute the capacity which becomes the sum of AWGN channel capacity [37].

In MIMO with M × N, the capacity achieving scheme consists of sending multiple symbols per transmission period. The transmission and reception of each symbol relies on pre- and post-processing that is matched to the underlying structure of the channel based on its SVD. This pre- and post-processing allows for the extraction of a *spatial route* for a SISO channel for each transmitted symbol. Multiple pairs of pre- and post-processing create multiple spatial routes. Those multiple spatial routes are *independent* and the MIMO system becomes equivalent to a set of independent M SISO channels [38]. From now on, we assume that the channel remains constant over symbol duration, and drop the time index *k* for better legibility. For any matrix **H**, we can obtain its singular value decomposition as:

$$\boldsymbol{H} = \boldsymbol{U\Sigma}\,\boldsymbol{V}^H \tag{4.9}$$

where the $N\times N$ matrix **U** and the $M\times M$ matrix **V** are unitary matrices with:

$$\boldsymbol{U}^H\boldsymbol{U} = \boldsymbol{U}\,\boldsymbol{U}^H = \boldsymbol{I_N} \tag{4.10}$$

$$\boldsymbol{V}^H\boldsymbol{V} = \boldsymbol{V}\,\boldsymbol{V}^H = \boldsymbol{I_M} \tag{4.11}$$

The operator $(\cdot)^{\boldsymbol{H}}$ represents the Hermitian a matrix, i.e. the conjugate transpose of complex matrix .Therefore by letting $\Lambda = \boldsymbol{\Sigma\Sigma}^{\mathrm{H}}$, we can calculate $\boldsymbol{HH}^H$ and $\boldsymbol{H}^H\boldsymbol{H}$ as follows:

$$\boldsymbol{HH}^H = (\boldsymbol{U\Sigma V}^H)(\,\boldsymbol{U\Sigma V}^H)^H = \boldsymbol{U\Sigma}\,\boldsymbol{V}^H\boldsymbol{V\Sigma U}^H$$

$$\boldsymbol{HH}^H = \boldsymbol{U\Sigma}(\boldsymbol{V}^H\boldsymbol{V})\boldsymbol{\Sigma U}^H = \boldsymbol{U}(\boldsymbol{\Sigma}\,\boldsymbol{\Sigma}^H)\boldsymbol{U}^H$$

$$\boldsymbol{HH}^H = \,\boldsymbol{U}\Lambda\boldsymbol{U}^H \tag{4.12}$$

$$\boldsymbol{H}^H\boldsymbol{H} = (\,\boldsymbol{U\Sigma V}^H)^H(\boldsymbol{U\Sigma V}^H) = \boldsymbol{V\Sigma U}^H\boldsymbol{U\Sigma V}^H$$

$$\boldsymbol{H}^H\boldsymbol{H} = \boldsymbol{V\Sigma}(\boldsymbol{U}^H\boldsymbol{U})\boldsymbol{\Sigma V}^H = \boldsymbol{V}(\,\boldsymbol{\Sigma}\,\boldsymbol{\Sigma}^H)\boldsymbol{V}^H$$

$$\boldsymbol{H}^H\boldsymbol{H} = \boldsymbol{V}\Lambda\boldsymbol{V}^H \tag{4.13}$$

Also note that **V** is the matrix of Eigenvectors of $\boldsymbol{H}^H\boldsymbol{H}$, while **U** is the matrix of eigenvectors of $\boldsymbol{H}\boldsymbol{H}^H$ and $\boldsymbol{\Sigma}$ is an $M \times N$ diagonal matrix of singular values $\{ \lambda_i \}$ of **H**. The singular values of **H** provide a measure of the strength and separation of the MIMO data streams. These singular values have the property that $\lambda^2{}_i$, the *i*th eigenvalue of either $\boldsymbol{H}\boldsymbol{H}^H$ (if M>N) or $\boldsymbol{H}^H\boldsymbol{H}$ (if M< N)., with $r \leq \min(M,N)$. If **H** is full rank, which is sometimes referred to as a rich scattering environment, then $r = \min(M,N)$ [26].

4.3.1 Independent AWGN Channels: Equivalent MIMO System

The parallel decomposition of the channel is obtained by defining a transformation on the channel input and output **x** and **y** through transmit *precoding* and *receiver shaping*. In transmit precoding the input to the antennas **x** is generated through a linear transformation on input vector $\bar{\mathbf{x}}$ as:

$$\bar{\boldsymbol{x}} = \boldsymbol{V}^H \boldsymbol{x} \qquad (4.14)$$

So $\boldsymbol{x}=\boldsymbol{V}\,\bar{\boldsymbol{x}}$ receiver shaping performs a similar operation at the receiver by multiplying the channel output **y** with $\boldsymbol{U}^H$ i.e. $\tilde{\boldsymbol{y}} = \boldsymbol{U}^H\boldsymbol{y}$. The columns in matrix $\boldsymbol{U}$ and $\boldsymbol{V}$ are defined by the eigenvectors of $\boldsymbol{H}\boldsymbol{H}^H$ i.e. they can be calculated purely from the channel matrix. Matrix $\boldsymbol{V}$ is then used for the reverse transformation to the original signal vector space [11]. Since from the SVD (4.1) and using (4.9), (4.10), (4.11) and (4.12) , we will have:

$$\bar{\boldsymbol{y}} = \boldsymbol{U}^H \boldsymbol{y}$$

$$\bar{\boldsymbol{y}} = \boldsymbol{U}^H (\boldsymbol{Hx}+\boldsymbol{n}) \qquad (4.15)$$

$$\bar{\boldsymbol{y}} = \boldsymbol{U}^H (\boldsymbol{U\Sigma V}^H \boldsymbol{x} + \boldsymbol{n})$$

$$\bar{\boldsymbol{y}} = \boldsymbol{U}^H (\boldsymbol{U\Sigma V}^H \boldsymbol{V}\bar{\boldsymbol{x}} + \boldsymbol{n})$$

$$\bar{\boldsymbol{y}} = (\boldsymbol{U}^H \boldsymbol{U})\,\boldsymbol{\Sigma}\,(\boldsymbol{V}^H \boldsymbol{V})\,\bar{\boldsymbol{x}} + \boldsymbol{U}^H$$

$$\bar{\boldsymbol{y}} = \boldsymbol{\Sigma}\,\bar{\boldsymbol{x}} + \bar{\boldsymbol{n}}, \qquad (4.16)$$

$$\bar{\boldsymbol{n}} = \boldsymbol{U}^H \boldsymbol{n} \qquad (4.17)$$

This implies that $\boldsymbol{U}^H\mathbf{HV}=\boldsymbol{\Sigma}$ is a diagonal matrix. Note also that the signal terms of (4.17) are uncoupled, due to the diagonal structure of $\boldsymbol{\Sigma}$. Therefore if we pre-process the signals by $\mathbf{V}$ at the transmitter and then post-process them with $\boldsymbol{U}^H$, we will produce an equivalent diagonal matrix as shown in figure 4.1. As $\mathbf{U}$ and $\mathbf{V}$ are invertible, $\mathbf{x}$ and $\mathbf{y}$ can be recovered uniquely from $\bar{\mathbf{x}}$ and $\bar{\mathbf{y}}$. Hence, the new system with input $\bar{\mathbf{x}}$ and outputs $\bar{\mathbf{y}}$ is an equivalent representation of the original system. This equivalent system is the result of a linear pre-processing at the transmitter and a linear post-processing at the receiver [39].

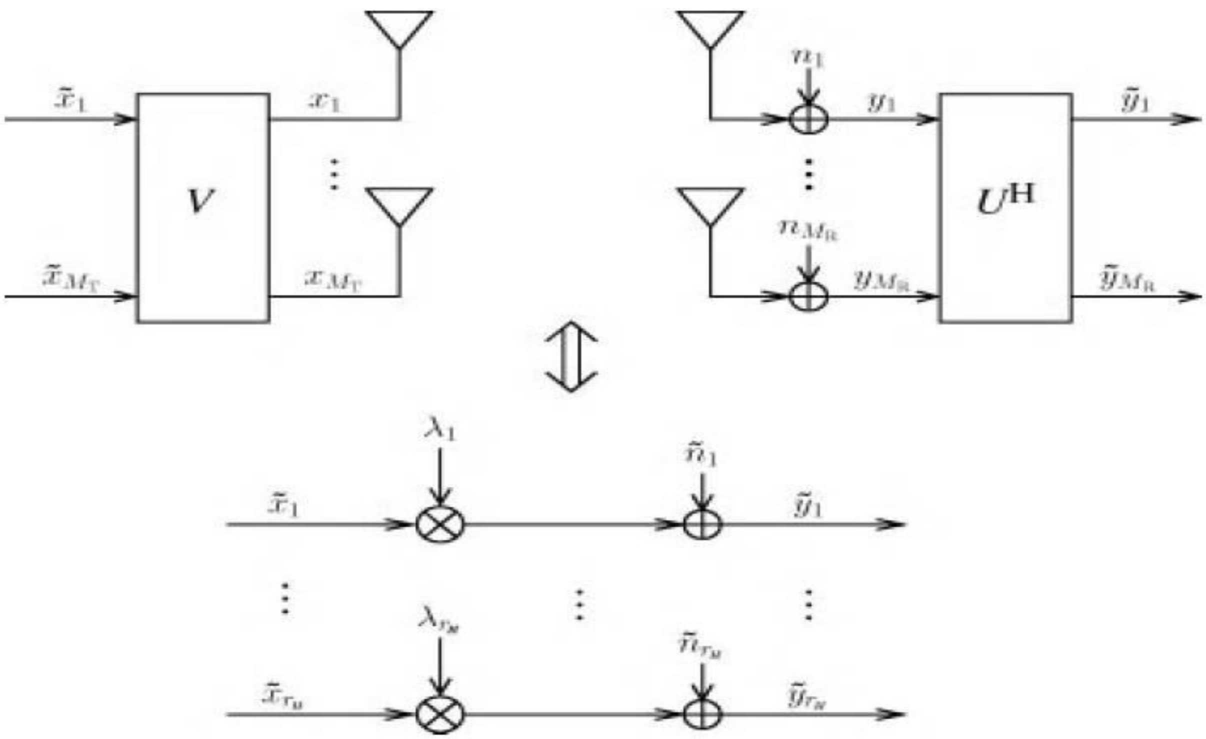

Figure 4-1Equivalent MIMO model of r AWGN independent channels with ($\boldsymbol{M_t}$=M ,$\boldsymbol{M_r}$=N) [26]

Physically, $\bar{\boldsymbol{x}}$ and $\tilde{\boldsymbol{y}}$ are still the actual signals transmitted and received. However, when viewed in terms of $\bar{\boldsymbol{x}}$ and $\bar{\boldsymbol{y}}$, the effective channel between them is simply $\boldsymbol{\Sigma}$. Thus, the transmit precoding and receiver shaping transform the MIMO channel into *r* parallel independent channels where the *i*th channel has input $\bar{x}_i$, output $\bar{y}_i$, noise $\bar{n}_i$, and channel gain λ_i . Note that the λ_is are related since they are all functions of $\mathbf{H}$ .But since the resulting parallel channels do not interfere with each other, we say that the channels with these gains are independent, linked only through the total power constraint. Each independent channel is also called an *eigenchannel or subchannel* as the associated channel coefficients an eigenvalue of the channel matrix [25].

Note, however, that the performance on each of the channels will depend on its gain λ_i .Each output i, i = 1, . . ., r of the equivalent system ($\lambda_1 \geq \lambda_2 \geq \cdot \cdot \cdot \geq \lambda_r$) can be written as:

$$\tilde{y}_i = \lambda_i \bar{x}_i + \bar{n}_i \tag{4.18}$$

4.3.2 Singular Values and Channel Energy

The transmit power from antenna m is $\mathrm{E}\{|x_m|^2\}$. The sum of transmit powers is constrained to be smaller than p. To maximize the transmission rate, the transmit power is set constant to its maximal value p which is the total average energy available at the transmitter over a symbol period having removed *losses due to propagation* and *shadowing* as discussed in Section (2.2). The transmit power constraint can be written as:

$$\sum_{m=1}^{M} E\{|x_m|^2\} = tr(\boldsymbol{R_{xx}}) \leq p \tag{4.19}$$

The autocorrelation of transmitted signal vector is defined as:

$$\boldsymbol{R_{xx}} = E\{\boldsymbol{x}\,\boldsymbol{x}^H\} \tag{4.20}$$

U and **V** being unitary, the total power of the original signals, received signals or noise remains unchanged during precoding or shaping. Note that multiplication by a unitary matrix does not change the distribution of the noise, i.e. $\boldsymbol{n}$ and $\bar{\boldsymbol{n}}$ are identically distributed [16]. For unitary Matrix **U** and **V**, we have $E\{\boldsymbol{U}\} = E\{\boldsymbol{U}^H\} = \mathbf{I_N}$ and $E\{\boldsymbol{V}\}=E\{\boldsymbol{V}^H\} = \mathbf{I_M}$. Furthermore using (4.6) and (4.9), we can prove that the autocorrelation of the transmitted and precoded transmitted signals are equal to each other as follows:

$$E\{\bar{\boldsymbol{x}}\bar{\boldsymbol{x}}^H\} = E\{\boldsymbol{V}^H\boldsymbol{x}\,(\boldsymbol{V}^H\boldsymbol{x})^H\} = E\{\boldsymbol{V}^H\boldsymbol{x}\,\boldsymbol{x}^H\boldsymbol{V}\}$$

$$E\{\bar{\boldsymbol{x}}\bar{\boldsymbol{x}}^H\} = E\{\boldsymbol{V}^H\}E\{\boldsymbol{x}\,\boldsymbol{x}^H\}E\{\boldsymbol{V}\} = E\{\boldsymbol{x}\,\boldsymbol{x}^H\} \tag{4.21}$$

$$E\{\bar{\boldsymbol{n}}\bar{\boldsymbol{n}}^H\} = E\{\boldsymbol{U}^H\boldsymbol{n}(\boldsymbol{U}^H\boldsymbol{n})^H\} = E\{\boldsymbol{U}^H\boldsymbol{n}\boldsymbol{n}^H\boldsymbol{U}\}$$

$$E\{\bar{\boldsymbol{n}}\bar{\boldsymbol{n}}^H\} = E\{\boldsymbol{U}^H\}E\{\boldsymbol{n}\boldsymbol{n}^H\}E\{\boldsymbol{U}\} = E\{\boldsymbol{n}\,\boldsymbol{n}^H\} = \sigma^2\,\boldsymbol{I_N} \tag{4.22}$$

(4.21) holds true for $\bar{\mathbf{x}}$, so the original power constraint on $\mathbf{x}$ still applies to $\bar{\mathbf{x}}$. Thus in the coming Sections we can use $\boldsymbol{x}$ and $\bar{\boldsymbol{x}}$ interchangeably for power and capacity calculations. The total transmitted power p, is the sum of all the diagonal elements of the autocorrelation matrix. The following relationship between channel energy and singular values will be useful. Indeed, the energy in the channel is:

$$tr(\boldsymbol{H}\boldsymbol{H}^{\boldsymbol{H}}) = \sum_{m=1}^{M} \sum_{n=1}^{N} | h_{nm}(k)|^2 = \sum_{i=1}^{r} {\lambda_i}^2 \tag{4.23}$$

Let p_i be the transmit power of eigenchannel i (the power in precoded signal $\bar{\mathbf{x}}$) .Using (4.18) ,the instantaneous signal power in each subchannel , which is the power in $\boldsymbol{\Sigma}\,\bar{\mathbf{x}}$, ,is equal to $p_i\,|{\lambda_i}^2|$ The instantaneous power in the noise $\bar{\mathbf{n}}$ is σ^2 . We can get the received power of ith eigenchannel to be:

$$p_{ri} = \left(\frac{{\lambda_i}^2}{\sigma^2}\right)\; p_i \tag{4.24}$$

4.4 Ergodic Capacity of SU-MIMO Channels

The ergodic capacity of a MIMO channel is the ensemble average of the information rate over the distribution of the elements of the channel matrix. In a fading channel, the SNR is constantly changing. As the rate of fade changes, the capacity changes with it. We can use a fixed **H** matrix as our benchmark of performance where the basic assumption is that, for that one realization, the channel is fixed and hence has an ergodic channel capacity. In other words, for just that little time period, the channel is behaving like an AWGN channel [25].

We then break a channel into portions of either time or frequency so that in small segments, even in a frequency-selective channel with Doppler, channel can be treated as having a fixed realization of the **H** matrix, i.e. allowing us to think of it instantaneously as a AWGN channel. A classical assumption when evaluating the capacity of MIMO channels is to consider the fading coefficients between the pairs of transmit-receive antennas as independent and identically Rayleigh distributed (i.i.d.).

We can perform the capacity calculations over several realizations of **H** matrix and then compute average capacity over these. Ergodic capacity is averaged over all channel states (long-term average). [17] For a transmitter with multiple antennas, to get optimal performance, the transmitter should adapt to the spatial distribution of the channel coefficients across antennas. This is done by optimizing the spatial distribution of the transmitted signals to the spatial distribution of the channel. In particular, the covariance matrix of the input signals should fit the channel distribution.

In fast fading (open loop MIMO) the channel varies very fast so that the coding horizon spans many channel fades. In slow fading (closed loop MIMO), the channel varies very slowly and coding spans over a single channel fade. In fast fading Capacity characterizes performance over a time period that includes an infinite number of fading states and represents a long-term average over the channel fades. In slow fading Capacity characterizes the optimal performance of a coding scheme experiencing only one channel fade but where the channel is a random variable [26].

Even if the instantaneous value of the CSIT is not known, a reliable communication can be achieved by coding over an asymptotically large number of channel coherence periods, thus averaging out the channel fades. Based on the CSIT distribution, a maximal rate for reliable communication can be determined. This rate is constant over the channel fades and is the ergodic capacity.

4.5 Ergodic capacity of SISO

There is ever growing demand of wireless services of higher data rates. Unfortunately, a conventional single-input single-output (SISO) system where the transmitter and receiver are equipped with single antenna could have limitations to support higher data services. In comparison with other antenna configurations, the peak data rate of SISO is limited by Shannon's law. Its performance is degraded by Interference and fading than other [27].

Often the transmitter is not able to acquire the instantaneous knowledge of the channel state. Yet it can have partial knowledge, typically the statistical distribution (CSIT). In a SISO channel, the CSI is constant and does not change from bit to bit. Thus the knowledge of CSI in a SISO link is often not needed as it is characterized by steady state SNR. The input–output relationship of a narrowband SISO channel at time k is:

$$y(k) = h(k)\, x(k) + n(k) \tag{4.25}$$

$h(k)$ is the value of the channel coefficient at k th time .

The instantaneous signal power, which is the power in h(k)x(k), is equal to $E\{\|h(k)x(k)\|^2\}= p|h(k)|^2$. The instantaneous power in the noise n(k) is σ^2. To obtain optimal performance, the transmit power is set to its maximal value P. Thus, the instantaneous SNR at time k is equal to [34]:

$$SNR(k) = \frac{p|h(k)|^2}{\sigma^2} \tag{4.26}$$

The ergodic capacity for a fast fading SISO channel with CSIT distribution is calculated as:

$$C_{SISO}^{OL} = E\{log_2\ (1+SNR(k))\} \tag{4.27}$$

$$C_{SISO}^{OL} = \mathrm{E}\{\ log_2\ (1+(\frac{p|h(k)|^2}{\sigma^2}))\} = E\{\ log_2\ (1+(|h(k)|^2\ \rho_s))\} \tag{4.28}$$

The capacity achieving coding scheme has a fixed rate and the codewords spread over an asymptotically large number of coherence periods.

4.6 Ergodic Capacity of SIMO

For the case of a SIMO channel with one transmit antenna and N receive antennas, the input-output relationship of a flat SIMO channel at time *k* is:

$$\boldsymbol{y}(k) = \boldsymbol{h}_{SIMO}(k)\boldsymbol{x}(k) + \boldsymbol{n}(k) \tag{4.29}$$

where $\mathbf{h}(k) = \begin{bmatrix} \mathrm{h}_1(k) \\ \vdots \\ \mathrm{h}_N(k) \end{bmatrix}$

The MRC receiver transforms the SIMO system into an equivalent SISO system. The channel is assumed to be known at the transmitter, the SIMO channel can be made equivalent to the fast fading SISO channel. The input output relationship is:

$$\tilde{\boldsymbol{y}}(k) = (\boldsymbol{h}_{SIMO}(k))^H\boldsymbol{y}(k) = /(\boldsymbol{h}_{SIMO}(k))/^2\boldsymbol{x}(k) + (\boldsymbol{h}_{SIMO}(k))^H\boldsymbol{n}(k) \tag{4.30}$$

The instantaneous signal power, which is the power in $\|(\mathbf{h}_{\mathrm{SIMO}}(\mathrm{k}))\|^2$ x(k) ,is equal to $\mathrm{P}\|(\mathbf{h}_{\mathrm{SIMO}}(\mathrm{k}))|^2|^2$. [1] The instantaneous power in the noise $(\mathbf{h}_{\mathrm{SIMO}}(\mathrm{k}))^{\mathrm{H}}\mathrm{n}(\mathrm{k})$ is $\|(\mathbf{h}_{\mathrm{SIMO}}(\mathrm{k}))\|^2\ \sigma^2$. The capacity results for the SISO fast fading channel can be applied here for an SNR at time k equal to:

$$SNR(k) = \frac{\mathrm{P}||(\mathbf{h}_{SIMO}(k))|^2|^2.}{|(\boldsymbol{h}_{SIMO}(k))|^2\ \sigma^2} = \frac{\mathrm{P}|\mathbf{h}_{SIMO}(k)|^2}{\sigma^2} \tag{4.31}$$

In a SIMO system, the average SNR increases is proportional to the number of receive antennas. Therefore ergodic capacity of a fast fading SIMO channel:

$$C_{SIMO}^{OL}(\boldsymbol{H},p/\sigma^2) = \mathrm{E}\{\ log_2\ (1+(\frac{p|\boldsymbol{h}_{SIMO}(\boldsymbol{k})|^2}{\sigma^2}))\} \tag{4.32}$$

For Rayleigh (with unit mean variance), then the average power gain is $\mathrm{E}\{|(\mathrm{h}_{\mathrm{SIMO}}(\mathrm{k}))|^2\} = \sum_{\mathrm{j}=1}^{\mathrm{M}} |\mathrm{h}_{\mathrm{j}}(\mathrm{k})|^{2} = \mathrm{N}$ is the norm of the vector. Therefore we can see that the ergodic capacity of SIMO is greater than that of SISO. For high SNR, it reduces to:

$$C_{SIMO}^{OL}(\boldsymbol{H},p/\sigma^2) = log_2\ (1+N(\frac{P}{\sigma^2})) = log_2\ (1+N\ \rho_s\ ) \tag{4.33}$$

4.7 Ergodic Capacity for a General MIMO

For an optimal transmission, the covariance of the input signals $\boldsymbol{R}_{\mathbf{xx}}$ should be adapted to the channel distribution. The ergodic capacity is the average of the maximal achievable rate over the channel fades. This leads to the transmitter optimization problem - i.e., finding the optimum input covariance matrix to maximize ergodic capacity subject to the transmit power constraint. The capacity of a deterministic channel is defined as:

$$C_d = max\, I(\boldsymbol{x};\boldsymbol{y}) \tag{4.34}$$

In which $I(\mathbf{x};\mathbf{y})$ is the mutual information of random vectors **x** and **y**. Mutual information is a measure of the amount of information that one random variable contains about another variable. Namely, the channel capacity is the maximum mutual information that can be achieved by varying the probability distribution function of the transmit signal vector.

From the fundamental principle of the information theory, the mutual information of the two continuous random vectors, x and y; is given as:

$$I(\boldsymbol{x};\boldsymbol{y}) = h(\boldsymbol{y}) - h(\boldsymbol{y}\,/\,\boldsymbol{x}) \tag{4.35}$$

Where $h(\cdot)$ in this case denotes the differential entropy of a continuous random variable

In which h(**y**) is the differential entropy of **y** and h(**y**|**x**) is the conditional differential entropy of **y** when **x** is given. Thus mutual information is maximized if the entropy in **y** is maximized. Using the input-output relationship at any given time instant (k):

$$\boldsymbol{y}(k) = \boldsymbol{H}(k)\,\boldsymbol{x}(k) + \boldsymbol{n}(k) \tag{4.36}$$

The definition of entropy yields that h(**y**|**x**) = h(**n**), the entropy in the noise. Since this noise n has fixed entropy independent of the channel input, maximizing mutual information is equivalent to maximizing the entropy in **y** [34]. Then relationship between mutual information and entropy, (4.27) can be expanded as follows:

$$I(\boldsymbol{x};\boldsymbol{y}) = h(\boldsymbol{y}) - h(\boldsymbol{y}|\boldsymbol{x})$$

$$I(\boldsymbol{x};\boldsymbol{y}) = h(\boldsymbol{y}) - h((\boldsymbol{Hx}+\boldsymbol{n})|\boldsymbol{x})$$

$$I(\boldsymbol{x};\boldsymbol{y}) = h(\boldsymbol{y}) - h((\boldsymbol{H}(\boldsymbol{x}|\boldsymbol{x})) - h(\boldsymbol{n}|\boldsymbol{x})$$

$$I(\boldsymbol{x};\boldsymbol{y}) = h(\boldsymbol{y}) - h(\boldsymbol{n}|\boldsymbol{x})$$

$$I(\boldsymbol{x};\boldsymbol{y}) = h(\boldsymbol{y}) - h(\boldsymbol{n}) \tag{4.37}$$

From (4.37) given h(**n**) is constant, we can see the mutual information is maximized when h(**y**) is maximized. The Mutual information of **y** depends on covariance matrix of **y** given as:

$$\boldsymbol{R}_{yy} = E\{\,\boldsymbol{y}(k)\;(\boldsymbol{y}(k)\,)^{H}\,\} \tag{4.38}$$

Substituting (4.36) in (4.38), we get:

$$\boldsymbol{R}_{yy} = E\{(\boldsymbol{H}(k)\boldsymbol{x}(k)+\boldsymbol{n}(k)\,)\,(\boldsymbol{H}(k)\,\boldsymbol{x}(k) \;+\; \boldsymbol{n}(k)\,)^{H}\}$$

$$\boldsymbol{R}_{yy} = E\,\{(\,\boldsymbol{H}(k)\,\boldsymbol{x}(k) + \boldsymbol{n}(k)\;)\,(\;\boldsymbol{x}(k)^{\,H}\boldsymbol{H}(k)^{\,H} \;+\boldsymbol{n}(k)^{\,H}\,)\,\}$$

$$\boldsymbol{R_{yy}} = E\{ \boldsymbol{H}(k)\,\boldsymbol{x}(k)\,\boldsymbol{x}(k)^{H}\boldsymbol{H}(k)^{H} \} + E\{ \boldsymbol{H}(k)\,\boldsymbol{x}(k)\,\boldsymbol{n}(k)^{H} \} + E\{ \boldsymbol{n}(k)\,\boldsymbol{x}(k)^{H}\boldsymbol{H}(k)^{H} \} + E\{\boldsymbol{n}(k)\,\boldsymbol{n}(k)^{H}\} \qquad (4.39)$$

The processes {x(k)} and {n(k)} are assumed to be independent from each other. Since x(k) and z are uncorrelated i.e E { $\mathbf{H}$(k) $\mathbf{x}$(k) $\mathbf{n}$(k) ^{H}}=$\mathbf{0}$, E{ $\mathbf{n}$(k) $\mathbf{x}$(k) $^{H}\mathbf{H}$(k) ^{H}}= $\mathbf{0}$ and also $\mathbf{N_o}$ = E {$\mathbf{n}$(k) $\mathbf{n}$(k) ^{H} } = σ^2 $\mathbf{I}_N$. Then substituting in the above equation gives:

$$\boldsymbol{R_{yy}} = E\{(\boldsymbol{H}(k)\,\boldsymbol{x}(k)\,\boldsymbol{x}(k)^{H}\boldsymbol{H}(k)^{H} + \boldsymbol{n}(k)\,\boldsymbol{n}(k)^{H})\}$$

$$\boldsymbol{R_{yy}} = \boldsymbol{H}(k)\, E\{\boldsymbol{x}(k)\,\boldsymbol{x}(k)^{H}\}\boldsymbol{H}(k)^{H} + E\{\boldsymbol{n}(k)\,\boldsymbol{n}(k)^{H}\}$$

$$\boldsymbol{R_{yy}} = \boldsymbol{H}(k)\,\boldsymbol{R_{xx}}\boldsymbol{H}(k)^{H} + \boldsymbol{N_o} \qquad (4.40)$$

where $\mathbf{R_{xx}}$ is covariance matrix of the transmit signal, and $\mathbf{N_o}$ is the power spectral density of the additive noise. [8] As the noise components are independent complex Gaussian with variance 1/2 per dimension, the entropy of n is h($\mathbf{n}$) = $\log_2$ [det(πe $\mathbf{N_o}$)]. Entropy of $\mathbf{y}$ is maximized when R_{yy} is maximized which in turn means that $\mathbf{R_{xx}}$ has to be maximized. The differential entropy h($\mathbf{y}$) is maximized when y is ZMCSCG, which consequently requires $\mathbf{x}$ to be ZMCSCG as well. Note that, for clarity reasons, we give up the time indices (k) in all quantities.

Then, the mutual information of $\mathbf{y}$ and $\mathbf{n}$ is respectively given as:

$$h(\boldsymbol{y}) = \log_2\, [\det(\pi e\, \boldsymbol{R_{yy}})] \qquad (4.41)$$

$$h(\boldsymbol{n}) = \log_2\, [\det(\pi e\, \boldsymbol{N_o})] \qquad (4.42)$$

Then using equations he mutual information of (4.35) is expressed as:

$$I(\boldsymbol{x};\boldsymbol{y}) = \log_2\, [\det(\pi e\, \boldsymbol{R_{yy}})] - \log_2\, [\det(\pi e\, \boldsymbol{N_o})] \qquad (4.43)$$

$$I(\boldsymbol{x};\boldsymbol{y}) = \log_2 [\det(\boldsymbol{R_{yy}} / \boldsymbol{N_o})]$$

$$I(\boldsymbol{x};\boldsymbol{y}) = \log_2 [\det(\boldsymbol{I_N} + \frac{\mathbf{1}}{\boldsymbol{\sigma}^2}\, \boldsymbol{H}\boldsymbol{R}_{xx}\boldsymbol{H}^{H})] \qquad (4.44)$$

The above equation shows that $\mathbf{R_{xx}}$ is maximized when x is a ZMCSCG random vector MIMO capacity obtained by maximizing $\mathbf{R_{xx}}$. Then, the channel capacity of deterministic MIMO channel ,as a function of H and SNR= p/σ^2 ,is expressed as :

$$C_d\ (\boldsymbol{H}, p/\sigma^2) = max[log_2\, det(\boldsymbol{I_N} + \frac{1}{\sigma^2}\, \boldsymbol{H}\boldsymbol{R_{xx}}\boldsymbol{H}^H)] \qquad (4.45)$$

In this definition the channel must be normalized rather than be the actual measured channel. Therefore the problem of determining the capacity of the channel in is reduced to that of finding the input covariance $\boldsymbol{R_{xx}}$ that maximizes the RHS of (4.45), subject to the constraint tr ($\boldsymbol{R_{xx}}$) $\leq P$. A capacity achieving code has a constant rate equal to the capacity and spreads over many channel fades [28].

Then the ergodic capacity of MIMO channel is simply the average of the deterministic capacity i.e.:

$$C\,(\boldsymbol{H}, p/\sigma^2) = E\{\, C_d\ (\boldsymbol{H}, p/\sigma^2)\,\} \qquad (4.46)$$

$$C\,(\,\boldsymbol{H}, p/\sigma^2) = max[E\{log_2\, det(\boldsymbol{I_N} + \frac{1}{\sigma^2}\, \boldsymbol{H}\boldsymbol{R_{xx}}\boldsymbol{H}^H)\}] \qquad (4.47)$$

We can see that the ergodic capacity for uncorrelated channel depends only on the channel gain matrix H and the autocorrelation of the transmitted signals. In order to make a fair comparison between equal power and waterfilling power schemes, the channel matrix needs to be properly normalized.

4.8 Ergodic Capacity of Open Loop MIMO (Fast Fading)

Under the CSIR only assumption, the transmitter does not have knowledge about the communications channel, so there is no basis for transmitting signals in any sort of preferential way on different antennas. There is no reason to transmit more energy on one antenna than another; thus, the average signal power should be the same on each transmit antenna [39]. If the distribution of **H** follows ZMSW distribution (zero mean and identity covariance matrix) then allocate equal power to each transmit antenna. For Rayleigh the transmit covariance matrix can be easily found as:

$$\boldsymbol{R_{xx}} = (P/M)\, \boldsymbol{I}_M \qquad (4.48)$$

Therefore, (4.17) will be reduced to:

$$C_{FF}^{OL}(\boldsymbol{H},p/\sigma^2) = E\{log_2\, det(\boldsymbol{I_N} + \frac{P}{M\sigma^2}\, \boldsymbol{HH}^H)\} = E\{log_2 \det(\boldsymbol{I_N} + \frac{\rho_s}{M^2}\, \boldsymbol{HH}^H)\} \quad (4.49)$$

By the law of large numbers, the term $\frac{1}{M}\, \boldsymbol{HH}^H \rightarrow \boldsymbol{I}_N$ as M gets large and N is fixed. Thus the capacity in the limit of large M is :

$$C_{FF}^{OL}(M,p/\sigma^2) = E\{\, N\, log_2\ (1 + \frac{P}{\sigma^2})\,\} \quad (4.50)$$

$$C_{FF}^{OL}(M,p/\sigma^2) = N\ \ E\{\, log_2\ (1 + \frac{P}{\sigma^2})\ \} \quad (4.51)$$

Therefore the capacity only depends only on the number of receive antennas. We can use the Singular value decomposition in (4.12). Since $\Lambda = \boldsymbol{\Sigma\Sigma}^H$ for unitary matrix U, we have det($\boldsymbol{U}$) = det($\boldsymbol{U}^H$) = 1 for unitary matrix **U.** We have:

$$\boldsymbol{I}_N + \frac{P}{M\sigma^2}\, \boldsymbol{HH}^H = \boldsymbol{I}_N + \frac{P}{M\sigma^2} \boldsymbol{U}\Lambda\boldsymbol{U}^H = \boldsymbol{U}(\boldsymbol{I}_N + \frac{P}{M\sigma^2}\Lambda)\, \boldsymbol{U}^H \quad (4.52)$$

$$det(\boldsymbol{I}_N + \frac{P}{M\sigma^2}\, \boldsymbol{HH}^H) = det\ (\boldsymbol{U}(\boldsymbol{I}_N + \frac{P}{M\sigma^2}\Lambda)\, \boldsymbol{U}^H\,)$$

$$det(\boldsymbol{I}_N + \frac{P}{M\sigma^2}\, \boldsymbol{HH}^H) = det(\boldsymbol{U})\, det(\boldsymbol{I}_N + \frac{P}{M\sigma^2}\Lambda)\, det(\boldsymbol{U}^H)$$

$$det(\boldsymbol{I}_N + \frac{P}{M\sigma^2}\, \boldsymbol{HH}^H) = det(\boldsymbol{I}_N + \frac{P}{M\sigma^2}\Lambda) \quad (4.53)$$

Therefore, the channel matrix possesses r nonzero singular values $\{\lambda_i,\ i = 1... r\}$ since it is a diagonal matrix so is $\boldsymbol{I}_N + \frac{\rho_s}{M}\ \Lambda$. Each diagonal element is ($1 + \frac{\rho_s}{M}\lambda_i$). Therefore the determinant of the matrix is the product of each diagonal element i.e.:

$$\det\ (\boldsymbol{I}_N + \frac{\rho_s}{M}\Lambda)\} = \prod_{i=1}^{r}(1 + \frac{\rho_s}{M}\lambda_i^{\,2}) \quad (4.54)$$

Based on the SVD of the channel of equation (4.10), then equation (4.41) can be rewritten:

$$C_{FF}^{OL}(\boldsymbol{H},p/\sigma^2) = E\{log_2 \det(\boldsymbol{I}_N + \frac{\rho_s}{M}\boldsymbol{\Lambda})\} = \ E\{log_2 \prod_{i=1}^{r}(1 + \frac{\rho_s}{M}\lambda_i^{\,2})\} \quad (4.55)$$

$$C_{FF}^{OL}(\boldsymbol{H},p/\sigma^2) = E\{\sum_{i=1}^{r}\ log_2\,(1 + \frac{\rho_s}{M}\lambda_i^{\,2})\} = \sum_{i=1}^{r}\ E\{log_2\,(1 + \frac{\rho_s}{M}\lambda_i^{\,2})\} \quad (4.56)$$

[26] The expected value is taken with respect to the joint distribution of the singular values $\{\lambda_i\}$.If for equal values of λ_i the capacity is directly proportional to r rank of the matrices as given in (2.19). The MISO channel exhibits a performance loss of 1/M compared to the case where the instantaneous value of the CSIT is known. For the case of a MISO channel with M transmit antenna and one receive antenna. The input-output relationship of a flat SIMO channel at time k is:

$$y(k) = \mathbf{h}(k)^H \mathbf{x}(k) + \boldsymbol{n}(k) \tag{4.57}$$

Since for Rayleigh fading the covariance of the input signals $\mathbf{R_{xx}}$ = (P/M) $\boldsymbol{I}_M$ and subsisting this in the previous Section of general Equation (4.55). The ergodic capacity of a fast fading MISO i.i.d. Rayleigh channel with CSIT distribution is equal to:

$$C_{MISO}^{OL}(\boldsymbol{H}, p/\sigma^2) = E\{log_2 \, det(\boldsymbol{I}_N + \frac{\rho_s}{M} \boldsymbol{HH}^H)\} \tag{4.58}$$

Since for MISO, we have $\boldsymbol{I}_N = 1$ and $\boldsymbol{HH}^H = \sum_{i=1}^{r} |h_{1i}^2|$

Therefore the ergodic capacity of MISO is:

$$C_{MISO}^{OL}(\boldsymbol{H}, p/\sigma^2) = E\{log_2 (1 + \frac{\rho_s}{M} \sum_{i=1}^{r} (h_{1i}^2) \} \tag{4.59}$$

Note that no capacity gain is achieved even with more transmit antennas because on average the increase in $\sum_{i=1}^{r}(h_{1i}^2)$ and the increase in M tend to cancel each other.

4.9 Ergodic Capacity of Closed loop MIMO (Slow Fading)

. We can get the ergodic capacity by simply taking the mean of the deterministic under realization. Thus the random MIMO channel capacity can be given by its time average of deterministic channel capacity. With perfect CSIR and CSIT the transmitter can adapt to the channel fading and its capacity equals the average over all channel matrix realizations with optimal power allocation. With CSIT and CSIR the transmitter optimizes its transmission strategy for each fading channel realization as in the case of a static channel. The capacity is then just the average of capacities associated with each channel realization, with power optimally allocated [40].

4.9.1 Waterfilling Algorithm

Let p_i be the transmit power of eigenchannel i (the power in precoded signal $\bar{x}$ (k)). The received power, p_{ri} , is given in (4.23). Then, the capacity of each i eigenchannel, is equal to:

$$C_i^{CL} = log_2 \ (1 + \left(\frac{\lambda_i^2}{\sigma^2} \right) p_i) \qquad (4.60)$$

p_i is adjusted to maximize the capacity of the MIMO system while complying with the overall transmit power constraint: $\Sigma p_i \leq P$. In general, p_i depends on all nonzero singular values, through the power constraint given by:

$$\sum_{m=1}^{r} p_i \leq P \qquad (4.61)$$

The SU-MIMO time –invariant (TI) channel capacity is now given by a sum of the capacities of the virtual (parallel) SISO channels or the individual capacities with optimized transmit power per eigenchannel. The total time-invariant channel capacity is given as:

$$C_{TI}^{CL}(\boldsymbol{H}, p/\sigma^2) = max[\sum_{i=1}^{r} log_2 \ (1 + (\frac{{\lambda_i}^2}{\sigma^2}) p_i)] \qquad (4.62)$$

$$\gamma_i = \frac{{\lambda_i}^2}{\sigma^2} \qquad (4.63)$$

This equation is solved by using *Lagrangian method* using a *Lagrangian multiplier* γ_0 which is is the cut-off value and is determined using the power constraint such that the time-invariant (TI) channel capacity under the power constrained will be [41]:

$$C_{TI}^{CL}(\boldsymbol{H}, p/\sigma^2) = [\sum_{i=1}^{r} log_2 \ (1 + \gamma_i P_i^o)] + \gamma_0 (P - (\sum_{m=1}^{r} P_i^o)) \qquad (4.64)$$

Note that MIMO capacity only depends on γ_i's and hence the singular values of the channel matrix. Now partial differentiating $C_{MIMO}^{CL}(\mathbf{H}, p/\sigma^2)$ with respect to the optimum power P_i^o and setting it to zero to get the maximum value, we will get the optimal power allocated P_i^o to each mode for the first iteration as:

$$P_i^o = \left(\frac{1}{\gamma_0} - \frac{1}{\gamma_i} \right) = \left(\frac{\sigma^2}{{\lambda_0}^2} - \frac{\sigma^2}{{\lambda_i}^2} \right) = \sigma^2 \left(\frac{1}{{\lambda_0}^2} - \frac{1}{{\lambda_i}^2} \right) \geq 0 \qquad (4.65)$$

Each eigenvalue power must be greater than zero and their combined power is equal to the transmitted power which is equal to :

$$\sum_{i=1}^{r} P_i^o = \sum_{i=1}^{r} \left(\frac{1}{\gamma_0} - \frac{1}{\gamma_i}\right)^{+} = p \qquad (4.66)$$

For the jth iteration, depending on the total amount of available power, some q_j eigenchannels might not be allocated any power. This results in a number of active streams smaller which is equal to (r-q_j). If the power allocated to the weakest mode is negative (p_{r-j+1}<0), this mode is dropped out by setting p_{r-j+1}= 0 and the power allocation on the other modes is re-calculated with the value of j incremented by 1.

This process is iterated until the power allocated on each mode is non-negative. Then solving the above equation for $1/\gamma_{oj}$ the optimal power allocation is iteratively estimated. First set the counter j to 1 so that $1/\gamma_{o1}$= $1/\gamma_{o}$ [34]. At each iteration j, with q_j removed eigenchannels with negative values of P_i^o, the constant $1/\gamma_{oj}$ is calculated as:

$$\frac{1}{\gamma_{oj}} = \frac{P}{(r-q_j)}\left(1 + \sum_{i=1}^{r-q_j}\left(\frac{1}{\gamma_i}\right) \right) = \frac{P}{(r-q_j)}\left(1 + \sigma^2 \sum_{i=1}^{r-q_j}\left(\frac{1}{\lambda_i{}^2}\right) \right) \qquad (4.67)$$

The capacity is maximized because the algorithm finds the maximum number of non-zero eigen-channel power levels consistent with the constraint. Since the number of non-zero power levels is maximized, this, in turn, maximizes the capacity. Since *r* independently coded AWGN codewords are assigned power, the capacity of the time-invariant (static) MIMO channel depending on the optimal power P_i^o is:

$$C_{MIMO}^{CL}(\boldsymbol{H}, p/\sigma^2) = E\{\textstyle\sum_{k=1}^{r} \log_2 (1 + P_i^o \gamma_i) \} \qquad (4.68)$$

Therefore the erogdic capacity is equal to the ensemble average of the time-invariant capacity taken over long realization. Thus the ergodic capacity for closed loop MIMO is equal to:

$$C_{MIMO}^{CL}(\boldsymbol{H}, p/\sigma^2) = E\{C_{MIMO}^{CL}(\boldsymbol{H}, p/\sigma^2) \} = E\{\textstyle\sum_{k=1}^{r} \log_2 (1 + P_i^o \gamma_i) \} \qquad (4.69)$$

4.9.2 Performance of Eigenmode Transmission

Waterfilling at low and high SNR: as shown in figure 4-3, channel has four nonzero eigenvalues. We recall the optimal power allocation from (4.64).

• At high SNR (cell-centered UE), the values $1/\gamma_i$ are small compared to $1/\gamma_0$. So the power allocated to each eigenchannel is approximately constant and equal *to P / r* [14].

• At low SNR (cell-edge UE), the values $1/\gamma_i$ are large compared to $1/\gamma_0$. Only the eigenchannel with highest eigenvalue is allocated with the whole available power. The optimal waterfilling policy allocates all the power to the strongest eigenmode. The optimal strategy does not rely on multiplexing. It consists in sending a single stream through a channel with highest possible energy, which is guaranteed by proper preprocessing and postprocessing.

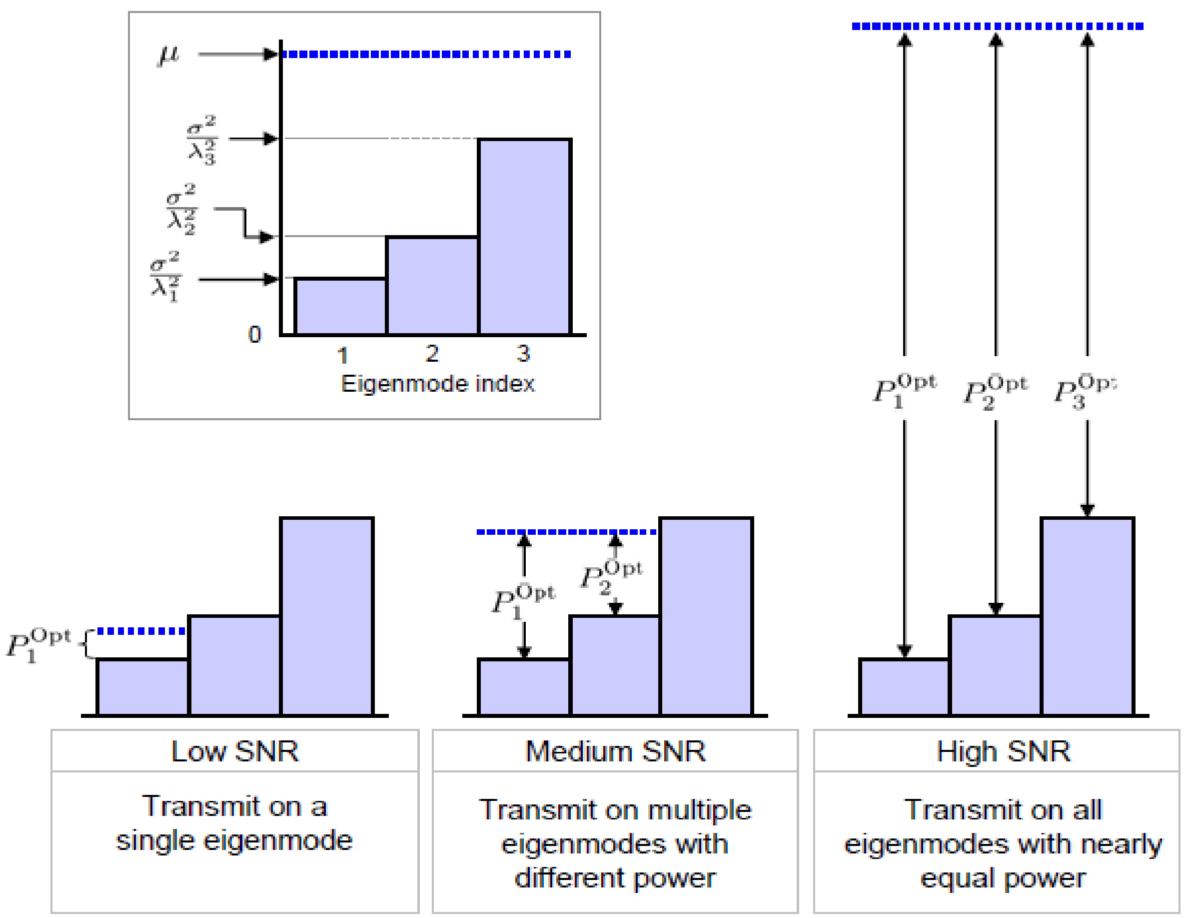

Figure 4-2 The channel has three eigenmodes, and the power allocation is shown for low, medium, and high values of SNR (P/σ^2) with (μ=.1/γ_0) [14]

4.10 Performance Gains of Different SNR Values

The MIMO gains in the low-SNR (cell-edge) regime come about through spatial diversity antenna combining, and that the gains in the high-SNR (cell-centered) regime come from spatial multiplexing.

4.10.1 Low SNR Regime (Cell-Edge UE)

i. Low SNR regime (cell-edge) for Opened loop MIMO

[14] In the low-SNR regime where P/σ^2 approaches zero. The open-loop capacity for a fixed channel **H** with rank $r \le \min(M,N)$, ${\lambda_i}^2$ are the eigenvalues of $\boldsymbol{H}\boldsymbol{H}^H$.

Using $\prod_{i=1}^{r}(1+z] \approx 1+\sum_{i=1}^{r} z$ for small value of z.

$$C_{low\,SNR}^{OL}(\boldsymbol{H}{,}p/\sigma^2) \;=\; E\{log_2 \det(\boldsymbol{I}_N + \tfrac{\rho_s}{M}\,\boldsymbol{H}\boldsymbol{H}^H)\}$$

$$C_{low\,SNR}^{OL}(\boldsymbol{H}{,}p/\sigma^2) \;=\; E\{log_2 [\prod_{i=1}^{r}(1 \,+ \tfrac{\rho_s}{M}{\lambda_i}^2\,)]\}$$

$$C_{low\,SNR}^{OL}(\boldsymbol{H}{,}p/\sigma^2) \;\approx\; E\{log_2 (1+\sum_{i=1}^{r}\tfrac{\rho_s}{M}{\lambda_i}^2)\}$$

$$C_{low\,SNR}^{OL}(\boldsymbol{H}{,}p/\sigma^2) \;=\; E\{\,log_2 (1+\tfrac{\rho_s}{M}\sum_{i=1}^{r}{\lambda_i}^2)\} \qquad (4.70)$$

Using log_2 (1 + z) ≈ $z\, log_2 e$ for small value of z. Thus we have:

$$\mathrm{E}\{tr(\boldsymbol{H}\boldsymbol{H}^{\boldsymbol{H}})\} = E\{\sum_{m=1}^{M}\sum_{n=1}^{N} |\, h_{nm}(k)|^{\,2}\} = MN$$

$$C_{low\,SNR}^{OL}(\boldsymbol{H}{,}p/\sigma^2) \;=\; E\{log_2 (1+\tfrac{\rho_s}{M}tr(\,\boldsymbol{H}\boldsymbol{H}^H))\}$$

$$C_{low\,SNR}^{OL}(\boldsymbol{H}{,}p/\sigma^2) \;\approx\; \tfrac{\rho_s}{M}\; E\{tr(\,\boldsymbol{H}\boldsymbol{H}^H)\}\, log_2 e$$

$$C_{low\,SNR}^{OL}(\boldsymbol{H}{,}p/\sigma^2) \;=\; \tfrac{\rho_s}{M}\; E\{tr(\,\boldsymbol{H}\boldsymbol{H}^H)\,\}\;\; log_2 e$$

$$C_{low\,SNR}^{OL}(\boldsymbol{H}{,}\, p/\sigma^2) \;=\; \mathrm{N}\;\; \rho_s\;\; log_2 e \qquad (4.71)$$

Therefore, in the low-SNR, multiple transmit antennas do not improve the capacity, and the capacity of any (M,N) channel with M ≥ 1 is asymptotically equivalent.

ii. **Low SNR regime (cell-edge UE) for Closed loop MIMO**

For the closed-loop capacity, waterfilling at asymptotically low SNR puts all the power P into the single best eigenmode. (With i.i.d. Rayleigh channels, the singular values will be unique with probability 1.) [15].

The average capacity is therefore and ${\lambda_{max}}^2$ is the maximum eigenvalue of $\boldsymbol{HH}^H$ which is equal to ${\lambda_{max}}^2$ = max[${\lambda_k}^2$].

In the low-SNR regime where P_k/σ^2 approaches zero so we can use the approximation of log_2 (1 + z) $\approx z\ log_2$ e.

$$C^{CL}_{low\ SNR}(\boldsymbol{H}, p/\sigma^2) = E\{\max[\sum_{k=1}^{r} log_2 (1 + \frac{P_k}{\sigma^2} {\lambda_k}^2)\ ]\} \tag{4.72}$$

$$C^{CL}_{low\ SNR}(\boldsymbol{H}, p/\sigma^2) \approx (\ E\{\max[\sum_{k=1}^{r} (\frac{P_k}{\sigma^2} {\lambda_k}^2)\ ]\}\ )\ \ log_2\, e \tag{4.73}$$

Since all power is allocated to best or maximum eigenmode P_k/σ^2=P/σ^2

$$C^{CL}_{low\ SNR}(\boldsymbol{H}, p/\sigma^2) = \frac{P}{\sigma^2} E\{{\lambda_{max}}^2\}\, log_2\, e = \rho_s E\{{\lambda_{max}}^2\}\, log_2\, e \tag{4.74}$$

Because E{${\lambda_{max}}^2$} =max(E {tr ($\boldsymbol{HH}^H$)}) ≈ max(M,N) for i.i.d. Rayleigh channels fading, from (4.17) ,So (4.67) reduces to :

$$C^{CL}_{low\ SNR}(\boldsymbol{H}, p/\sigma^2)\ = (\max(M,N))\ (\ log_2\, e\ )\ \ \rho_s \tag{4.75}$$

Therefore closed-loop MIMO capacity at low SNR benefits from combining at either the transmitter or receiver. Practically it's convenient to add more transmit antennas at eNodeB side. Keeping 1.6 meters distance between each antenna, the operator can add up to 4 antennas which is the maximum number of antennas for LTE Release 8.

4.10.2 High SNR Regime (Cell- Center UE)

i. High SNR (cell-centered UE) regime for Opened loop MIMO

For High SNR we can use the following approximation for large : log_2 (1 + z) ≈ log_2 (z)
From (4.21), the average capacity for Rayleigh channels for high SNR can be written as [15]:

$$C^{OL}_{high\,SNR}(\boldsymbol{H}, p/\sigma^2) = E\{\textstyle\sum_{k=1}^{r} log_2 (1 + \frac{\rho_s}{M}{\lambda_k}^2 \;\}$$

$$C^{OL}_{high\,SNR}(\boldsymbol{H}, p/\sigma^2) \approx E\{\textstyle\sum_{k=1}^{r} log_2 (\frac{\rho_s}{M}{\lambda_k}^2)\}$$

$$C^{OL}_{high\,SNR}(\boldsymbol{H}, p/\sigma^2) = E\{\textstyle\sum_{k=1}^{r} log_2 (\rho_s)\} + E\{\sum_{k=1}^{r}(log_2 (\frac{\lambda_k^2}{M}))\}$$

But since λ_k^2 /M is a small number $E\{\sum_{k=1}^{r}(log_2 (\frac{\lambda_k^2}{M})\}$ =0

$$C^{OL}_{high\,SNR}(\boldsymbol{H}, p/\sigma^2) = r\, log_2\ \rho_s) = min(M, N)\, log_2\ \rho_s \qquad (4.76)$$

Therefore open-loop MIMO achieves a multiplexing gain of min(M,N) at high SNR.

ii. High SNR for closed loop MIMO

For the closed-loop capacity at asymptotically high SNR, waterfilling puts equal power in each of the min(M,N) eigenmodes. Therefore with $P_k = P/r$ the average capacity is:

$$C^{CL}_{high\,SNR}(\boldsymbol{H}, p/\sigma^2) = E\{max \textstyle\sum_{k=1}^{r} log_2 (1 + \frac{P_k}{\sigma^2}{\lambda_k}^2)\;\}$$

$$C^{CL}_{high\,SNR}(\boldsymbol{H}, p/\sigma^2) = E\{max[\textstyle\sum_{k=1}^{r} log_2 (\frac{P/\sigma^2}{r}{\lambda_k}^2)\;]\}$$

$$C^{CL}_{high\,SNR}(\boldsymbol{H}, p/\sigma^2) = E\{\textstyle\sum_{k=1}^{r} max[log_2 (\frac{P/\sigma^2}{r}{\lambda_k}^2)\;]\}$$

$$C^{CL}_{high\,SNR}(\boldsymbol{H}, p/\sigma^2) = E\{\textstyle\sum_{k=1}^{r} log_2 (\frac{P/\sigma^2}{r}) + \sum_{k=1}^{r}(log_2 \lambda_k^2)\}$$

However since $\sum_{k=1}^{r}(log_2 \lambda_k^2) \approx 0$ which is a very small number we will ignore it. Therefore

$$C^{CL}_{high\,SNR}(\boldsymbol{H}, p/\sigma^2) = r\, log_2 (\frac{P/\sigma^2}{r}) = \min(M, N)\, log_2 (\frac{\rho_s}{\min(M,N)}) \qquad (4.77)$$

Where r = min(M,N). Therefore closed-loop MIMO achieves the same multiplexing gain as open-loop MIMO in (4.56) despite the advantage of CSIT.

CHAPTER 5

5 BER PERFORMANCE OF SPATIAL DIVERSITY

A channel may be affected by fading and this will impact the signal to noise ratio. In turn this will impact the error rate when the channel is in a deep fade; a reliable decoding of the transmitted signal may no longer be possible, resulting in an error. These negative effects of fading are addressed by means of diversity techniques. In a MIMO channel, multipath fading can in fact be beneficial, through increasing the *degrees of freedom* available.

Data communication requires very high reliability. Therefore operator's LTE network should have high quality of service. Errors are caused by impairments in the communication such as additive noise at the receiver or an unexpected deep fade for a wireless channel. As the channel impairments are random, so is the event of a decoding error. Hence, we define the probability of error, where the probability is taken over the channel impairments. Accordingly, spatial diversity helps to stabilize a link and improves performance by reducing error rate

This Chapter represents a bit error rate (BER) performance analysis of MIMO-OFDM system with Alamouti Space Time Block Code (STBC) and Maximal Ratio Combining (MRC) diversity scheme over Rayleigh fading channel. The analysis of Alamouti STBC is used in MIMO-OFDM system to assure transmit diversity and the receive diversity is resolved with MRC diversity technique.

We will cover the followings. Firstly, the probability of BER is derived for a SISO and them a MIMO -OFDM system employing the MRC diversity technique as receive diversity, Alamouti Coded OFDM as transmit diversity and their combinations as receiver-transmit diversity. Thirdly, analytical comparison among the SISO, MISO, SIMO and MISO-SIMO antenna configuration in MIMO-OFDM systems will be dealt. Finally, it will be shown that by increasing the number of transmit/receive antennas, the system performances increase. At the end of this thesis, we related the system capacity and the error performance of MIMO systems to the framework of the diversity-multiplexing tradeoff.

5.1 BER for QPSK Carrier Modulation

Operators uses QPSK 0.19 modulation technique for the downlink mode In case of complex-valued modulation, such as QPSK, space–time codes of rate one without any inter-symbol interference (*orthogonal space–time codes*) only exists for two antennas. Frequency-Switched Transmit Diversity (FSTD) is used for two- antenna transmission [22].

In this thesis, MIMO-OFDM is analyzed for Rayleigh fading Channel and each sub-carrier being modulated with different conventional modulation scheme of QPSK at a low symbol rate, maintaining total data rates similar to conventional single-carrier modulation schemes in the same bandwidth. Having established that diversity is not an appropriate perspective in the low-velocity regime, we henceforth focus exclusively on the high-velocity regime. This is the regime of interest for vehicular users in outdoor systems which are opened loop MIMO system without no CSIT [42].

QPSK can be regarded as a pair of orthogonal BPSK systems, i.e. the real component is one BPSK system, and the imaginary component is the second BPSK system. Because they are orthogonal, they don't interfere (to a good approximation), hence the BER curves are largely equivalent. Simulating a QPSK system is equivalent to simulating two BPSK systems in parallel. So there is no difference in bit error rate (BER). The BER is the average BER of the two parallel streams [20]. Therefore we will compute BER of BPSK instead of QPSK but in simulation we will modulate the bits with QPSK

5.2 BER Performance of SISO

In MIMO, our goal is to transmit and receive data over several independently fading channels such that the composite performance mitigates deep fades on any of the channels. In SISO (traditional system), we have just one transmitter and one receiver so we have just one channel and that means that there is no diversity. In other words, data is transmitted just one channel and if the channel damage data, received data is different from transmitted data so, communication cannot be provided normally, Generally BER can be high which is not acceptable in communication [18]. The input-output relationship of k's symbol of SIMO is:

$$y(k) = h(k)x(k) + n(k) \tag{5.1}$$

We assumed h=h(k) for block fading. The instantaneous signal-to-noise ratio is scaled by the random variable $|h|^2$. The instantaneous bit energy to noise ratio, in the presence of channel h is:

$$\rho_{SISO} = |h|^2 (\rho_s) \tag{5.2}$$

We first examine the BER for a BPSK signal as a function of the receive SNR. [42] Using results from basic digital communications, the conditional bit error rate P_{cSISO} for a given channel coefficient h can be written as:

$$P_{cSISO} = Q\left(\sqrt{\rho_{SISO}}\right) \tag{5.3}$$

$$P_{cSISO} = Q\left(\sqrt{||\mathrm{h}||^2 \rho_s}\right) \tag{5.4}$$

where the Q function is the Gaussian defined for random variable *v* and minimum value of $\sqrt{\rho_{SISO}}$ as:

$$Q(\sqrt{\rho_{SISO}}) = \frac{1}{\sqrt{2\pi}} \int_{\sqrt{\rho_{SISO}}}^{\infty} exp\left(-\frac{v^2}{2}\right) dv \tag{5.5}$$

$$P_{cSISO} = Q\left(\sqrt{|h|^2 \rho_s}\right) = \frac{1}{\sqrt{2\pi}} \int_{(h\sqrt{\rho_s})}^{\infty} exp\left(-\frac{v^2}{2}\right) dv \tag{5.6}$$

We can see that P_{cSISO} is a random variable that depends on the random variable |h|. To find the average BER, we have to average with respect to distribution of h which h follows Rayleigh distribution. [8] Averaging this conditional error rate over Rayleigh fading channel pdf which is given by f (h) = $2h\, e^{-h^2}$ from Equation (2.6)

We will get the average BER rate of SISO P_{SISO} as:

$$P_{SISO} = E\{P_{cSISO}\} \tag{5.7}$$

$$P_{SISO} = \int_0^{\infty} Q\left(\sqrt{|h|^2 \rho_s}\right) f(h) dh$$

$$P_{SISO} = \int_0^{\infty} Q\left(\sqrt{|h|^2 \rho_s}\right) * 2h\, e^{-h^2}\, dh \tag{5.8}$$

where the second equality follows since $|\mathrm{h}|^2$ is exponential with parameter 1.

As a result, the error rate is obtained through the above integration and equal to:

$$P_{SISO} = \frac{1}{2}\left(1 - \sqrt{\frac{\rho_s}{\rho_s+1}}\right) = \frac{1}{2}\left(1-\left(1+\frac{1}{\rho_s}\right)^{-\frac{1}{2}}\right) \tag{5.9}$$

For high SNR, i.e. ρ_s>>1 (cell-centered UE), we can use the Taylor expansion of one degree to simplify the above equation further. Since for small value of z, we have:

$$(1+z)^{-\frac{1}{2}} \approx 1-\frac{1}{2}z \tag{5.10}$$

$$\left(1+\frac{1}{\rho_s}\right)^{-\frac{1}{2}} \approx 1 - \frac{1}{2\rho_s} \tag{5.11}$$

Then substituting (5.19) in (5.17), we will find $P_{SISO}^{high\ SNR}$ as:

$$P_{SISO}^{high\ SNR} = \frac{1}{2}\left(1-\left(1+\frac{1}{\rho_s}\right)^{-\frac{1}{2}}\right)$$

$$P_{SISO}^{high\ SNR} \approx \frac{1}{2}\left(1-\left(1-\frac{1}{2\rho_s}\right)\right)$$

$$P_{SISO}^{high\ SNR} \approx \frac{1}{4\rho_s} \tag{5.12}$$

Thus, the BER performance is inversely proportional to SNR. Increasing the SNR by 3db will reduce the probability of error almost only by half. Strikingly, the error rate decreases only inversely with the SNR (with an asymptotic slope of one), despite the fact that the average SNR is unchanged. It has the lowest BER performance since the system isn't using redundancy.

5.3 BER Performance of Receive Diversity

In MRC, the signals received from multiple paths are weighted according to their individual signal power to noise power ratios and then summed. Here, the individual signals must be co-phased before being summed. MRC produces an output SNR equal to the sum of the individual SNRs. The signals at the output of the receivers are linearly combined in MRC to maximize the instantaneous SNR [16].

Let us first consider a one-transmitter-two-receiver (1×2) MRC model. At a given time, a signal x is sent from the transmitter. The channel between the transmit antenna and the receive antenna one is denoted by h_{11} and between the transmit antenna and the receive antenna two is denoted by h_{21}. Considering the noise and interference added at the two receivers, the resulting received signals could be written as:

$$r_1 = h_{11}\, x + n_{11} \qquad \textit{(First symbol received signal)} \qquad (5.13)$$

$$r_2 = h_{21}\, x + n_{21} \qquad \textit{(Second symbol received signal)} \qquad (5.14)$$

The term n_{11} , n_{21} are the additive white noise for the first and second receive antennas respectively. We have now two RF channels present and to be able to detect them, alternate pilots should be sent by each antenna, so the receiver can estimate the channels independently. Since from (2.3) the maximum coherence time to be T_c= 6ms for Operators's LTE which is much greater than two symbol period (2*4µs=8 µs), the channels are approximately constant over the period of two symbols.

Once the channels are estimated the original signals can be obtained by a simple combination of the received signals and the estimated channel responses. The receiver combining scheme for a two-branch MRC is as following:

$$Y = h_{11}^{*}\ (r_1) + h_{21}^{*}\ (r_2) \qquad (5.15)$$

Subsisting (5.14) and (5.15) in (5.16)

$$Y = (|h_{11}|^2 + |h_{21}|^2)\, x + h_{11}^{*}\ n_{11} + h_{21}^{*}\ n_{21} \qquad (5.16)$$

$$\bar{x} = x + (h_{11}^{*}\ n_{11} + h_{21}^{*}\ n_{21}) \,/\, (|h_{11}|^2 + |h_{21}|^2) \qquad (5.17)$$

$$\bar{x} = x + (h_{11}^{*}\ n_{11} + h_{21}^{*}\ n_{21}) \,/\, (|h_{n1}|^2) \qquad (5.18)$$

where $|h_{n1}|^2$ is the norm of the matrix which is equal to ($|h_{11}|^2 + |h_{12}|^2$)

Since the noise and the channel are uncorrelated, the noise term in this expression is complex Gaussian with mean power given by E{‖h‖² n}= ‖ h_{n1}‖² σ² . The bit energy is (| h_{n1}|²)^2 E_s; hence, the instantaneous bit energy to noise ratio, in the presence of channel h_{n1} at nth receive antenna is given by:

$$\rho_{\ ins} = \frac{|h_{n1}|^2\ E_S}{\sigma^2} \tag{5.19}$$

The total instantaneous bit energy per noise of N receive antennas is:

$$\rho_{\ insN} = \sum_{i=1}^{N} (\frac{|h_{n1}|^2\ E_S}{\sigma^2}) \tag{5.20}$$

With the N receive antenna case, the effective bit energy is :

$$\rho_{\ out} = E\ \{\rho_{\ insN}\} \tag{5.21}$$

$$\rho_{\ out} = E\{\sum_{i=1}^{N} (\frac{|h_{n1}|^2\ E_S}{\sigma^2})\} \tag{5.22}$$

$$\rho_{\ out} = (\frac{E_S}{\sigma^2})\ E\{\sum_{i=1}^{N} |\ h_{n1}|^2\} \tag{5.23}$$

$$\rho_{\ out} = \rho_s\ E\{\sum_{i=1}^{N} |\ h_{n1}|^2\} \tag{5.24}$$

[28] Since h_{n1} is a Rayleigh distributed random variable, then h_{11} , h_{21} … h_{N1} are Chi- Squared random variables, then the effective bit energy to noise ratio is the sum of N such random variables. Denoting u=$\sum_{i=1}^{N} |h_{n1}|^2$, it is well-known that u follows a χ² distribution with 2N degrees of freedom when the different channels are i.i.d. Rayleigh pdf is:

$$P(u) = \frac{u^{N-1}}{(N-1)!} e^{-u} \tag{5.25}$$

Since there are several paths, the average BER can be expressed as a function of the average channel gain over all these paths. [8] The conditional bit error rate is then given by:

$$P_{cSIMO} = \ \ Q\,(\sqrt{u\ \rho_s}\ ) \tag{5.26}$$

Then, the probability of error averaged over the Rayleigh fading channel gains which is integral of the conditional BER integrated over all possible values of u is given by:

$$P_{mrc1xN} = E\{P_{cSIMO}\} \tag{5.27}$$

$$P_{mrc1xN} = \int_0^{\infty} Q\ (\sqrt{u\ \rho_s}\ )\ )\ P(u)\ du \tag{5.28}$$

Where $Q\ (\sqrt{u\ \rho_s}\ )\ = \frac{1}{\sqrt{2\pi}} \int_{(\sqrt{u\ \rho_s})}^{\infty} exp\left(-\frac{v^2}{2}\right) dv$ as in (5.13).

Integrating equation (5.36) with respect to u and substituting u=$\sum_{i=1}^{N} |\ h_{n1}|^2$

$$P_{mrc1XN} = \frac{1}{2}\left(1 - \left(\sqrt{\frac{\rho_s}{\rho_s+1}}\ \right)\right) \sum_{n=1}^{N} (C_{n-1}^{N+n-2}\ [\frac{1}{2}\left(1 + \left(\sqrt{\frac{\rho_s}{\rho_s+1}}\ \right)\right)]^{n-1}\ ) \tag{5.29}$$

Where C is the combination of (N+n-2) taken (n-1) at a time

For two transmit antennas N=2 i.e. for 1×2 receiver diversity we will have:

$$P_{mrc1x2} = \frac{1}{4}\left(1 - \left(\sqrt{\frac{\rho_s}{\rho_s+1}}\ \right)\right)^2 * \left(2 + \left(\sqrt{\frac{\rho_s}{\rho_s+1}}\ \right)\right) \tag{5.30}$$

$$P_{mrc1x2} = \frac{1}{4}\left(\sqrt{\frac{\rho_s}{\rho_s+1}}\ \right)^3 - 3\left(\sqrt{\frac{\rho_s}{\rho_s+1}} + 2\right) \tag{5.31}$$

For high SNR ρ_s>>1 (cell-centered UE) case Using Taylor expansion of more (degrees)

$$(1 + \frac{1}{\rho_s})^{-\frac{1}{2}} \approx 1 - \frac{1}{2\rho_s} + \frac{3}{8(\rho_s)^2} \tag{5.32}$$

$$(1 + \frac{1}{\rho_s})^{-\frac{3}{2}} \approx 1 - \frac{3}{2\rho_s} + \frac{15}{8(\rho_s)^2} \tag{5.33}$$

Then substituting *(5.40)* and *(5.41)* in equation (5.39) we get:

$$P_{mrc1x2}^{high\ SNR} = \frac{3}{8(\rho_s)^2} \tag{5.34}$$

The receive diversity has lower BER than the SISO case; it decreases by about one fourth for 3dB increase in SNR value.

5.4 BER Performance of Transmit Diversity

We can produce the SFBC output symbols through a simple transformation followed by STBC using the Alamouti code. In Chapter 3, we saw that the performance of SFBC and STBC are the same. Therefore, we use STBC than SFBC for analysis purpose. Note that the symbol (*) indicates that the transmitter should change the sign of the quadrature component, in a process known as complex conjugation) .With two transmit antennas the scheme is as follows [42]:

1. Consider that we have a transmission sequence $\{x_1, x_2, x_3 \ldots . . x_n\}$
2. In normal transmission, we will be sending x_1 in the first time slot, x_2 in the second time slot, x_3 and so on.
3. Then we group the symbols into groups of two.
4. The channel h_{nm} is known at the receiver.

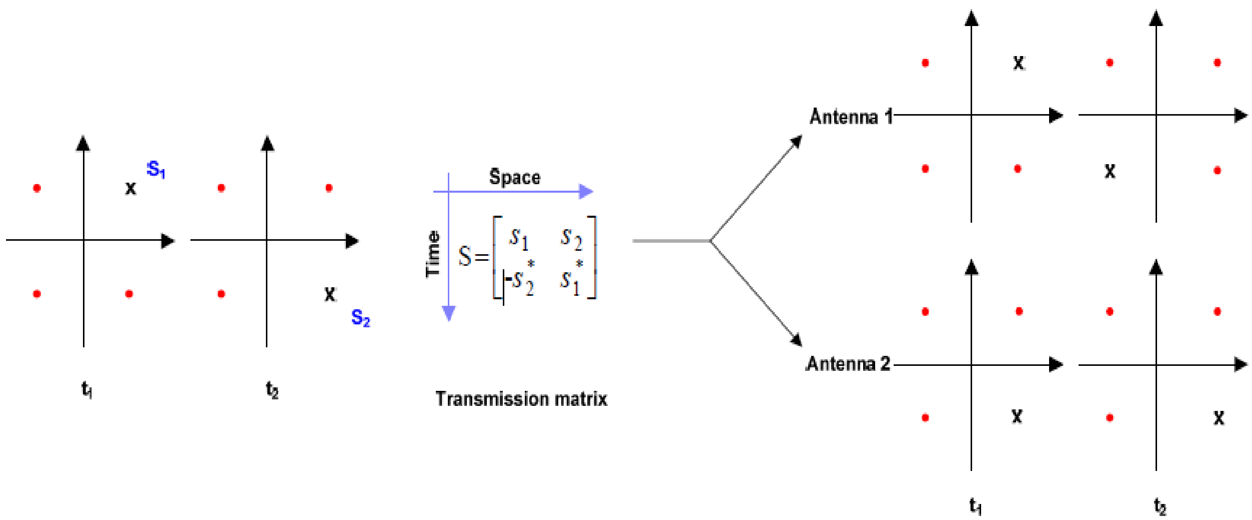

Figure 5-1 An Alamouti encoding for QPSK with transmit signal S=x [43]

Steps of transmission for Almouti STBC

i. In the first time slot, send x_1 and x_2 from the first and second antenna.
ii. In second time slot send $-x_2^*$ and x_1^* from the first and second antenna.
iii. In the third time slot send x3 and x4 from the first and second antenna.
iv. In fourth time slot send $-x_4^*$ and x_3^* from the first and second antenna and so on.

5.4.1 Analytical Analysis of Almouti Algorithm

The scheme uses two transmit antennas and one receive antenna and may be defined by the following three functions:

- the encoding and transmission sequence of information symbols at the transmitter;
- the combining scheme at the receiver;
- the decision rule for ZF .

The channel at time t may be modeled by a complex multiplicative distortion h_{11} (t) for the first transmit antenna and h_{12} (t) for the second transmit antenna . For a flat fading channel, the fading coefficients h_{nm} remain constant within a frame of length T time slots and change into new ones from frame to frame. Assuming that fading is constant across two consecutive symbols, we can write:

$$h_{11}(t) = h_{11}(t+T) = h_{11} \tag{5.35}$$

$$h_{12}(t) = h_{12}(t+T) = h_{12} \tag{5.36}$$

where T is the symbol duration. For the 2×1 Almouti STBC, in the first time slot and in the second time slot respectively of the received signals are :

$$r_1 = r_1(t) = h_{11}x_1 + h_{12}x_2 + n_{11} \tag{5.37}$$

$$r_2 = r_2(t+T) = -h_{11}x_2^* + h_{12}x_1^* + n_{12} \tag{5.38}$$

where h_{11} , h_{12} are Rayleigh channel and n_{11} , n_{12} are AWGN noise

At the receiver, MRC technique, combining coefficients being optimally chosen equal with the complex conjugated equivalent channel matrix .The combiner builds the following two combined signals as follows:

$$Y_1 = h_{11}^* r_1 + h_{12} r_2^* \tag{5.39}$$

$$Y_2 = h_{12}^* r_1 - h_{11} r_2^* \tag{5.40}$$

Substituting equation (5.45) and (5.46) in equation (5.33) and (5.34) we will get:

$$Y_1 = (|h_{11}|^2 + |h_{12}|^2)\, x_1 + h_{11}^* n_{11}{}^* + h_{12} n_{12}{}^* \qquad (5.41)$$

$$Y_2 = (|h_{11}|^2 + |h_{12}|^2)\, x_2 - h_{11} n_{12}{}^* + h_{12}^* n_{11}{}^* \qquad (5.42)$$

Let $n_1 = h_{11}^* n_{11}{}^* + h_{12} n_{12}{}^*$ and $n_2 = -h_{11} n_{12}{}^* + h_{12}^* n_{11}{}^*$

$$Y_1 = (|h_{11}|^2 + |h_{12}|^2)\, x_1 + n_1 = |h_1|^2 x_1 + n_1 \qquad (5.43)$$

$$Y_2 = (|h_{11}|^2 + |h_{12}|^2) x_2 + n_2 = |h_1|^2 x_2 + n_2 \qquad (5.44)$$

The combined symbols $\bar{x}_1$ and $\bar{x}_2$ are applied to a classical ZF decoder to obtain reliable estimates of the transmitted symbols. Even if a path is severely faded, we will recover the transmitted symbols through other propagation paths as:

$$\bar{x}_1 = x_1 + (h_{11} n_{11}{}^* + h_{12} n_{12}{}^*) \,/\, (|h_{11}|^2 + |h_{12}|^2) \qquad (5.45)$$

$$\bar{x}_2 = x_2 + (h_{11} n_{12}{}^* + h_{12} n_{11}{}^*) \,/\, (|h_{11}|^2 + |h_{12}|^2) \qquad (5.46)$$

Finally we get transmitted data with noise and channel effect. Note that, since the two columns are orthogonal, the ZF decoding is reduced to simple linear processing at the receiver.

5.4.2 BER Performance Analysis of 2 × N Alamouti Scheme

Let us derive the general 2 × N MIMO Alamouti scheme. The norm of the channel matrix for Almouti with two transmit antenna and N receive antenna is:

$$u = |h_{mn}|^2 = \sum_{m=1}^{2} \sum_{n=1}^{N} (|h_{nm}|^2) \qquad (5.47)$$

Where h_{1n} and h_{2n} (n=1…N) are the impulse response of the first transmit antenna with the receivers and the impulse response of the second antenna with the receivers respectively [8]. Then, we then need to average the conditional probability over the statistics of the channel to obtain the average bit or symbol error rate as:

$$P_{c2XN} = Q\left(\sqrt{|h_{2N}|^2 \ \rho_s}\ \right) \qquad (5.48)$$

For a Rayleigh fading channel, each of the terms in this summation are squared norms of complex Gaussian random variables with variance 1/2 in each dimension. Therefore each of these terms is chi-square distributed with two degrees of freedom with parameter 1 (i.e., exponential). Assuming that all the channel gains are, the sum of N independent and identically distributed exponential random variables is central chi-square distributed with 4N degrees of freedom [8]. Therefore, the probability density function of u is given by:

$$p(u) = (\frac{u^{2N-1}}{(2N-1)!})e^{-u} \tag{5.49}$$

Since the conditional probability is random variable, we need to average it over the statistics of the channel to obtain the average bit or symbol error rate. [8] For this case, Averaging this conditional error rate over Rayleigh fading channel statistics, the probability of bit error conditioned on the channel gains can be easily written as in :

$$P_{alm2xN} = E\{P_{c2XN}\}$$

$$P_{alm2xN} = \int_0^{\infty}\left(\frac{u^{2N-1}}{(2N-1)!}e^{-u}\right)Q\left(\sqrt{|h_{2xN}|^2 \quad \rho_s}\right)du \tag{5.50}$$

After some straightforward algebra, this integral can be simplified to:

$$P_{alm2XN} = \left(\frac{1}{2}\left(1-\sqrt{\frac{\rho_s}{\rho_s+1}}\right)\right)^{2N}\sum_{n=0}^{2N-1} C_n^{2N+n-1}\left(\frac{1}{2}\left(1+\sqrt{\frac{\rho_s}{\rho_s+2}}\right)\right)^{n} \tag{5.51}$$

where C is the combination of (2N+n-1) taken (n) at a time.

Then substituting N=1 for the above equation we can get the BER [7] for Alamouti STBC 2×1 antenna with QPSK modulation as:

$$P_{alm2x1} = P_{alm}{}^{2}\ (1+2\,(1\text{-}P_{alm}\,)) \tag{5.52}$$

Where the almouti BER is obtained from (5.46) for N=2

$$P_{alm} = \frac{1}{2}\left(1-\sqrt{\frac{\rho_s}{\rho_s+2}}\right) = \frac{1}{2}\left(1-(1+\frac{2}{\rho_s})^{-\frac{1}{2}}\right) \tag{5.53}$$

For high SNR ρ_s>>1 i.e, most of the case for cell-center UE. Using equation (5.19)

$$P_{alm} \approx \frac{1}{2}(1-(1-\frac{1}{\rho_s})) = \frac{1}{2\rho_s} \quad (5.54)$$

Then substituting (5.62) in (5.47) reduces as the followings:

$$P_{alm2x1}^{high\ SNR} = P_{alm}{}^{2}\,(3-2\,P_{a2x1}))$$

$$P_{alm}{}^{2} \approx (\frac{1}{2\rho_s})^2 \quad and \quad (3-2\,P_{alm})) \approx 3$$

$$P_{alm2x1}^{high\ SNR} = \frac{3}{4(\rho_s)^2} \quad (5.55)$$

5.4.3 Almouti 2×2 Transmit and Receive Diversity (MISO-SIMO)

This system consists of 2 Transmitter and 2 Receiver. Working principle is also similar to 2×1 Alamouti. In 2×1 Alamouti we send block codes to just one receiver but in this system we send block codes to 2 receivers. Transmit diversity can be mixed with MRC to provide a fourth order diversity MIMO scheme (2×2) [45].

$r_{11} = r_{11}\ (t+T) = h_{11}\,x_1 + h_{12}\ x_2 + n_{11}$ *(first time slot received data in Rx1)* (5.56)

$r_{12} = r_{12}\ (t+T) = -\,h_{11}\ (x_2{}^{*}) + h_{12}\ (x_1{}^{*}) + n_{12}$ *(second time slot received data in Rx1)* 5.57)

$r_{21} = r_{21}\ (t+T) = h_{21}x_1 + h_{22}\ x_2 + n_{21}$ *(first time slot received data in Rx2)* (5.58)

$r_{22} = r_{22}\ (t+T) = -h_{21}\ (x_2{}^{*}) + h_{22}\ (x_1{}^{*}) + n_{22}$ *(second time slot received data in Rx2)* (5.59)

h_{11}, h_{12} , h_{21} , h_{22} are Rayleigh channel and n_{11} , n_{12} , n_{21} , n_{22} are AWGN noise.

And also r_{11} and r_{21} are received data (for first time slot) and r_{12} and r_{22} are received data in (for second time slot) respectively.

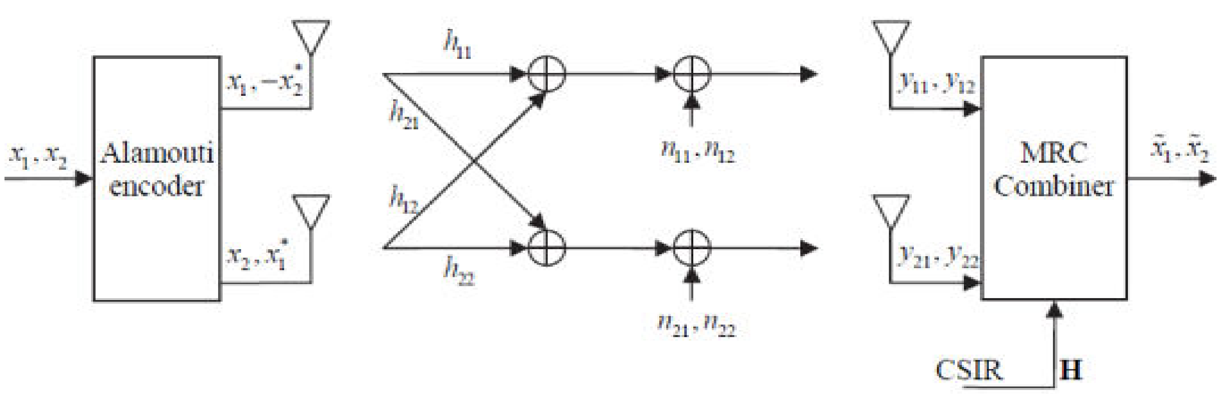

Figure 5-2 Almouti 2×2 STBC transmit and receive diversity [46]

[47] In OFDM systems, the scheme is applied on each carrier for two consecutive symbol periods since each carrier undergoes flat fading. The combiner builds the following two signals as follows:

$$y_1 = h_{11}^* r_1 + h_{12}\, r_2{}^* + h_{21}^* r_3 + h_{22}\, r_4{}^* \qquad (5.60)$$

$$y_2 = h_{12}^* r_1 - h_{11}\, r_2{}^* + h_{22}^* r_3 - h_{21}\, r_4{}^* \qquad (5.61)$$

Substituting the appropriate equations we have

$$y_1 = (/h_{11}/^2 + /h_{12}/^2 + /h_{21}/^2 + /h_{22}/^2)\, x_1 + h_{11}^* n_{11}{}^* + h_{12} n_{12}{}^* + h_{21}^* n_{21}{}^* + h_{22} n_{22}{}^* \quad (5.62)$$

$$y_1 = (/h_{11}/^2 + /h_{12}/^2 + /h_{21}/^2 + /h_{22}/^2)\, x_2 \text{ -} h_{11} n_{12}{}^* + h_{12}^* n_{11}{}^* \text{ - -} h_{21} n_{22}{}^* + h_{22}^* n_{21}{}^* \qquad (5.63)$$

$$u = /h_{mn}/^2 = (|h_{11}|^2 + |h_{12}|^2 + |h_{21}|^2 + |h_{22}|^2)$$

Thus for N=2 , (5.46) will reduce to the following:

$$P_{alm2x2} = P_{alm}^4 [1 + 4\,(1 - P_{alm}) + 10\,(1 - P_{alm})^2 + 20\,(1 - P_{alm})^3] \qquad (5.64)$$

where P_{alm} is given by (5.61).

For large signal-to-noise ratios i.e. ρ_s>>1, i.e., we can use (5.54) for approximating the value of $\mathrm{P}_{\mathrm{alm}}^4$. However we set the value of $(1 - \mathrm{P}_{\mathrm{alm}})$=1, since $\mathrm{P}_{\mathrm{alm}}$=0. Therefore, $P_{alm} = 0$ for all terms except $P_{alm}^4 = (\frac{1}{2\,\rho_o})^4$

$$P_{alm2x2}^{high\ SNR} \approx P_{alm}^4 [1 + 4(1) + 10(1)^2 + 20(1)^3]$$

$$P_{alm2x2}^{high\ SNR} = \frac{35}{16{\rho_s}^4} \qquad (5.65)$$

The combined signals in 2×2 space diversity mode are equivalent to that of four branch MRRC. Therefore, the resulting diversity order from the new two-branch transmit diversity scheme with two receivers is equal to that of the four-branch MRRC scheme. With this scaling, we can see that BER performance of 2Tx, 1Rx Alamouti STBC case has a roughly 3dB poorer performance that 1Tx, 2Rx MRC case.

5.5 Diversity-Multiplexing Trade-off

It is clear that the full benefits of diversity and multiplexing cannot be realized simultaneously. The diversity benefit assumes that the capacity is held constant and BER decreases as SNR increases as discussed before. However, multiplexing assumes that BER is held constant and capacity increases with SNR. It is in fact possible to trade one of these benefits against the other, and provide transmission schemes in which capacity increases as well as BER [48].

A scheme is said to have a spatial multiplexing gain N_m and a diversity advantage N_d . If the rate of the capacity scheme scales like $r\ log_2\ (SNR)$ as in (4.77) and the average error probability decays like $(\frac{1}{\mathrm{SNR}})^{N_d}$ as in (5.12), (5.34) and (5.75).The tradeoff has an upper bound provided by:

$$N_d \leq (M - N_m)(N - N_m) \qquad (5.66)$$

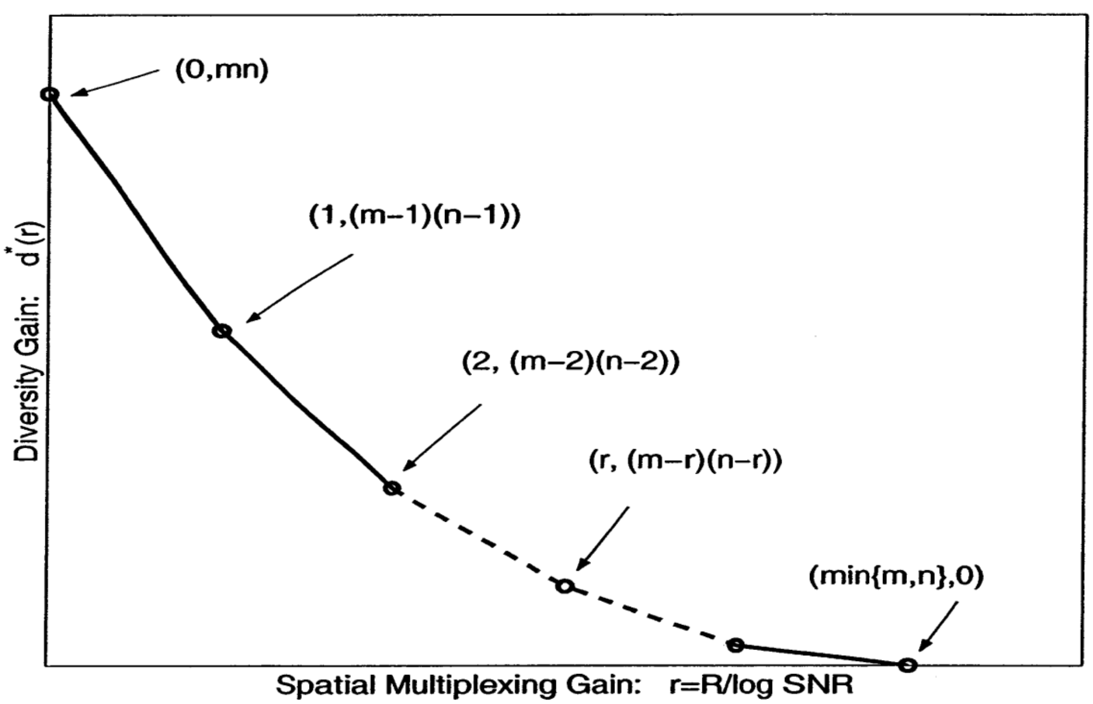

Figure 5-3 Diversity-multiplexing optimal trade-off [49]

It is as though r transmit and r receive antennas were used for multiplexing and the remaining transmit (M- r) and (N- r) receive antennas provided the diversity. The higher spatial diversity gain comes at the price of a lower spatial multiplexing gain, and vice versa.

CHAPTER 6
6 SIMULATIONS AND RESULTS

In order to design wireless communication system more easily, simulations are needed. Simulation is a practical and scientific approach to analyze a complex system. We use Matlab R2014a as simulation environment for its in-depth input analysis, flexible working environment. Our approach for this presentation and analysis is to investigate the performance of two MIMO techniques: Spatial Multiplexing (SM) and Spatial Diversity and compare the results with traditional SISO technique

This thesis work aims at evaluating the performance of LTE under varying channel conditions. Using these evaluations, further simulations will be based on performance metrics such as BER vs. SNR, ergodic capacity vs. SNR for different MIMO antenna transmission schemes. A key characteristic of MIMO is that its performance depends on a number of factors such as the SNR, the speed and location of the UE. In this Chapter simulation results, observations and interpretations on the capacity and BER performance of SU-MIMO receivers under Rayleigh fading channels are presented.

In Section 6.1 simulation parameters and assumptions are stated. In Section 6.2 detection of data sequence using different linear detection methods will be presented. Next demonstration of decoupling of SU-MIMO will be simulated. Most importantly, the ergodic capacity of SU- MIMO for different modes and different types of channel environments will be presented in Section 6.3. In its Subsections 6.4.1 and 6.4.2, we will further see the simulations for open loop and closed loop SU-MIMO system and compare them with each other. Then in each scenario, we will investigate the behavior of low and high SNR regimes for both closed and open loop MIMO systems. Thereafter in Section 6.5, we will consider the BER performance of receive diversity using MRC, transmit diversity using Almouti STBC algorithms, and their combination will be simulated and compared with each other and SISO. Then tradeoff between spatial multiplexing and diversity will follow for different antenna configuration.

6.1 Important Assumptions and Simulation Parameters

Some of the parameters used to plot for performance evaluation of SU-MIMO systems is shown in table 5.1. The MATLAB QPSK performs the algorithmic portion of our simple transceiver system to simulate the ergodic capacity and BER. This function has three variables:

- The first input is a scalar number that corresponds to SNR or E_b/N_o
- The numbers of antennas at the receiver and transmitter
- The second input is one of the stopping criteria, based on the maximum number of errors that can be observed before the simulation is stopped. We take 1000 iterations.

Table 6.1 simulation parameters

Simulation Parameters	**Values or specifications**
LTE	Release 8
Data Modulation /Demodulation	QPSK
Downlink mode	OFDM
Model used	Narrowband
Channel type	Flat- fading
Channel estimation	Perfect
Receiver decoder type	ZF, LE, LMMSE
OFDM Symbol duration	71.5 μs
Propagation channel model	Rayleigh flat fading
Noise at the receiver	zero mean complex circularly symmetric (ZMCCS)
Antenna configurations for ergodic capacity	SISO(1×1), SIMO (1×2), MISO (2×1), MIMO(2×2) , MIMO (2×4), MIMO (4×2), MIMO (4×4)
Antenna configurations for BER performance	SISO (1×1), SIMO (1×2), MISO (2×1), MIS0-SIMO (2 ×2)
Number of symbols in a frame	10^6
Number of iterations	1000
Range of SNR	-20< SNR< 20

6.2 Demonstration of MIMO Using Linear Detection Methods

This Section focuses on the linear detectors for 2×2 MIMO system which have the reasonable complexity and performance. The estimation processes featured are based on the following three algorithms: Zero Forcing (ZF), Linear Estimation (LE) and Linear Minimum Mean Square Error (LMMSE). In the plots we showed how the estimated or detected signal is resembles to the transmitted signal. The Error Vector Magnitude (EVM) is a measurement of the difference between the transmit signal waveform and its idealized counterpart. The higher the EVM, the worse the performance. In LTE, the EVM must be below 17.5% for QPSK, which our simulation results fulfill. The transmitted signal is represented in blue and estimated signal by red. In Section 2.9, we derived the analytical methods for estimating the transmitted signal.

The first simulation shows the detected signal using ZF method with EVM = 5.1% we can see that the estimation is fairly great given its less complexity. Here we used (2.28).

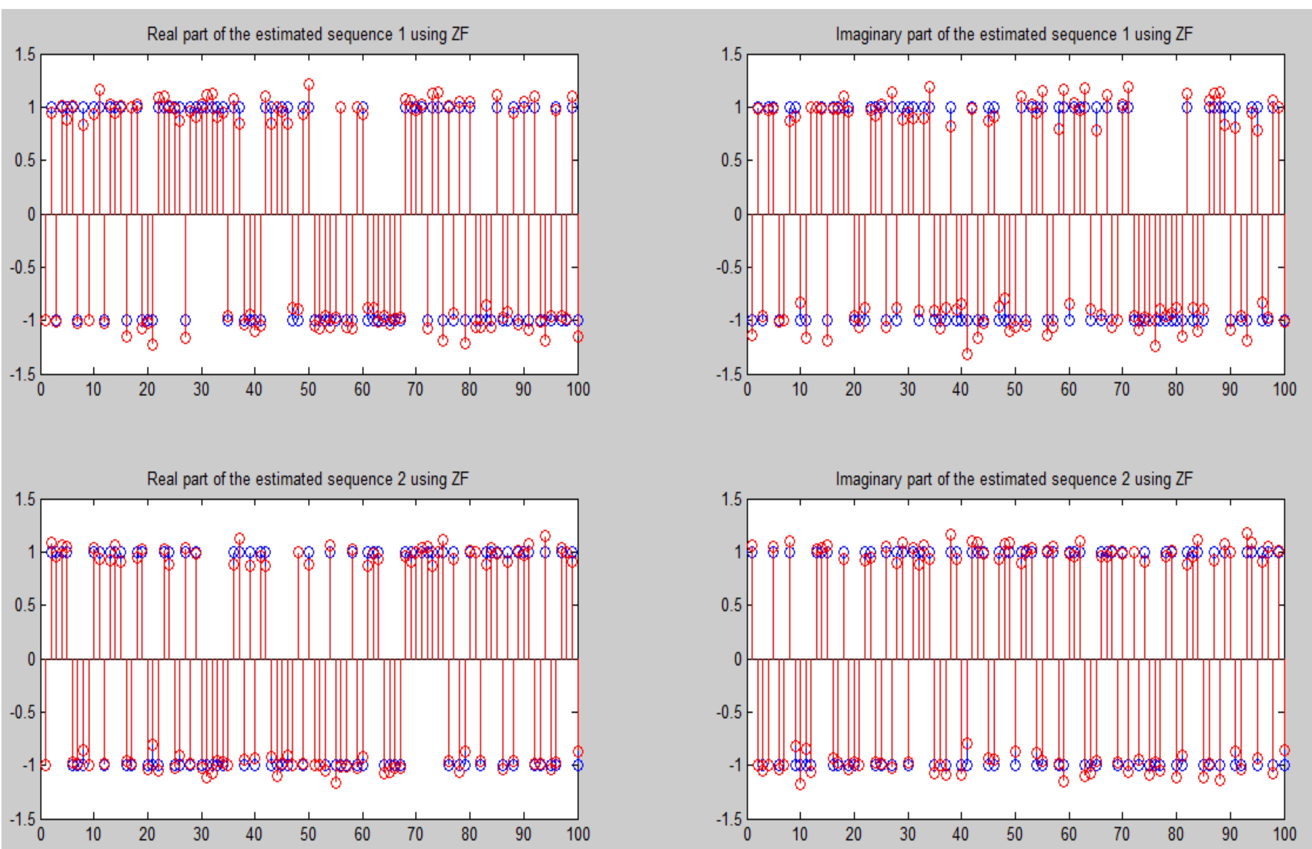

Figure 6-1 ZF estimation of the MIMO technique for the first and second received antennas

The second simulation is for least estimation (LE) algorithm with EVM=4.6% .Here we used (2.29). We can see it's more efficient than ZF algorithm.

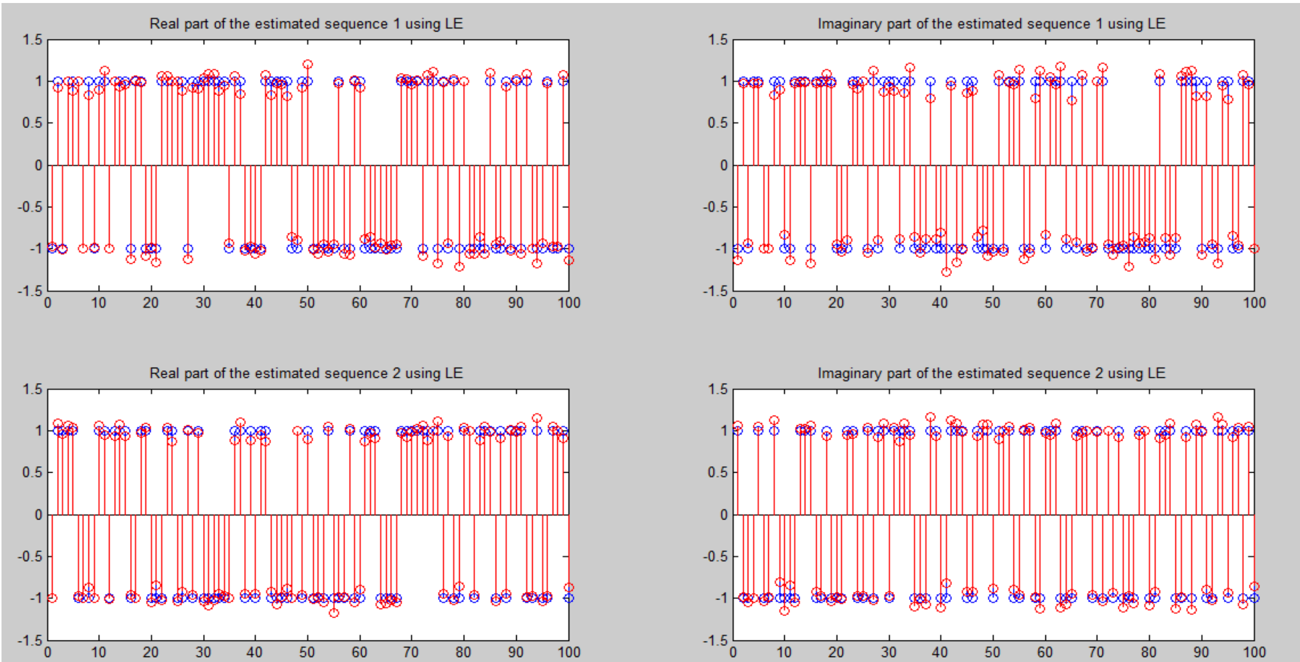

Figure 6-2 Least estimation method for the first and second received antennas

Finally a plot is made using LMMSE algorithm with EVM=3.2%. Here, we used (2.30). It has more efficiency than the rest of the linear detection methods.

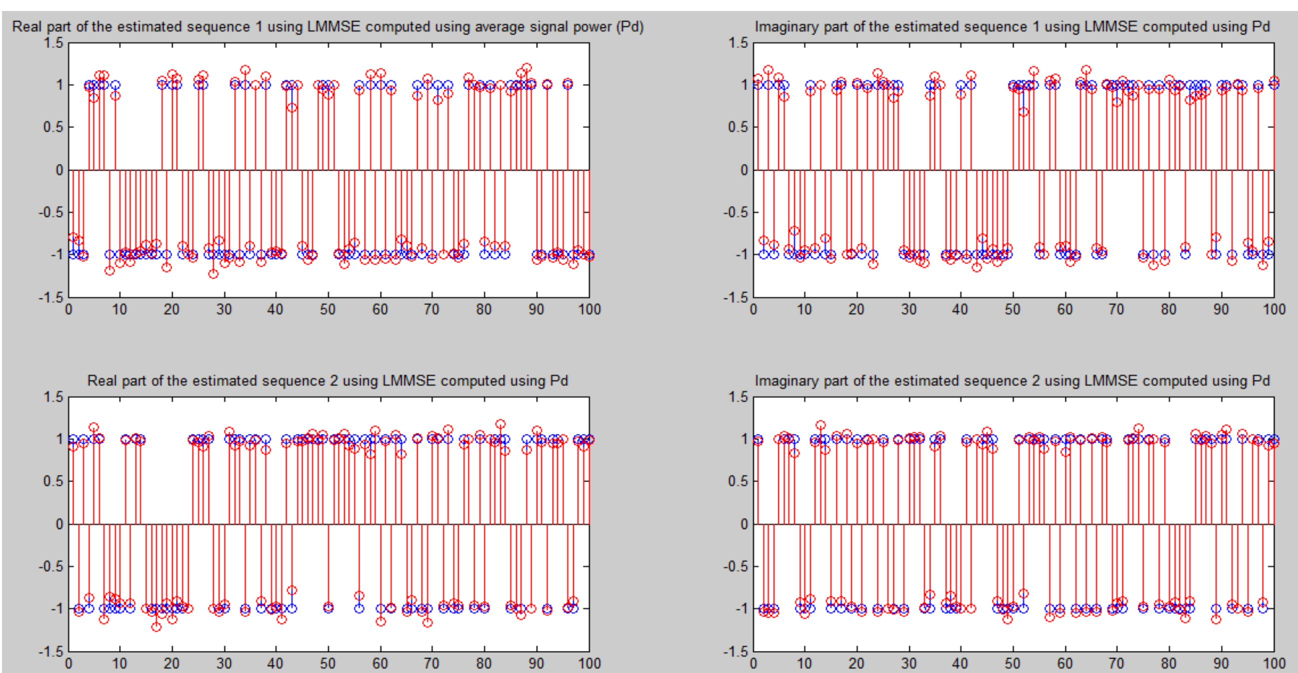

Figure 6-3 LMMSE (computed using p_d) for the first and second received antennas

6.3 Demonstration of Spatial Multiplexing Using Decoupling of SU-MIMO System

In this Section we will show how we used SVD for spatial multiplexing of 2×2 MIMO for decoupling. We will use the vector **V** as precoder and **U** as postcoder as in Chapter 4. We used SVD and MIMO detection methods as in the following steps:

1 Instead of transmitting the vector **x**, the modified vector is obtained as $\bar{\mathbf{x}} = \mathbf{V}\mathbf{x}$ and it is transmitted through the channel with channel matrix **H**.

2 The received vector in the receiver is obtained as $\tilde{\mathbf{y}} = \mathbf{\Sigma}\,\bar{\mathbf{x}} + \check{\mathbf{n}}$ as in (4.15) .

3 In the receiver Section, the detected received vector **y** as $\tilde{\mathbf{y}} = \mathbf{\Sigma}\,\bar{\mathbf{x}} + \check{\mathbf{n}}$ is pre-multiplied with

$\mathbf{y} = \mathbf{U}\mathbf{\Sigma}^{H}\tilde{\mathbf{y}}$ to obtain the estimation of x.

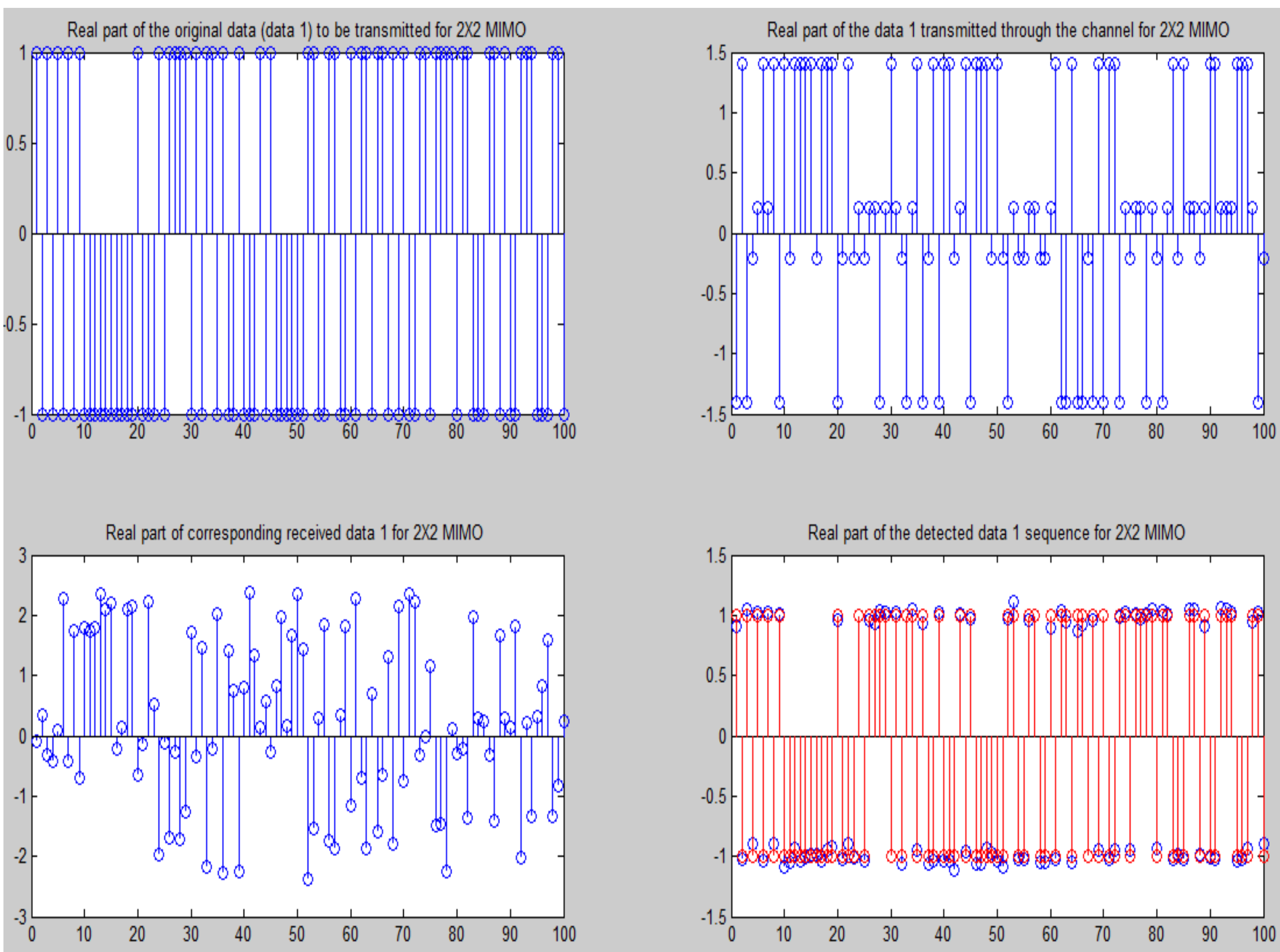

Figure 6-4 plot of real part of data 1 at the stages of after being faded, received and detected

In these two plots the real and imaginary part of transmitted signal after being Rayleigh faded and AWGN Gaussian noise added on it. Finally we will compare the real part of the transmitted signal (in blue) with the detected signal at the receiver (red).

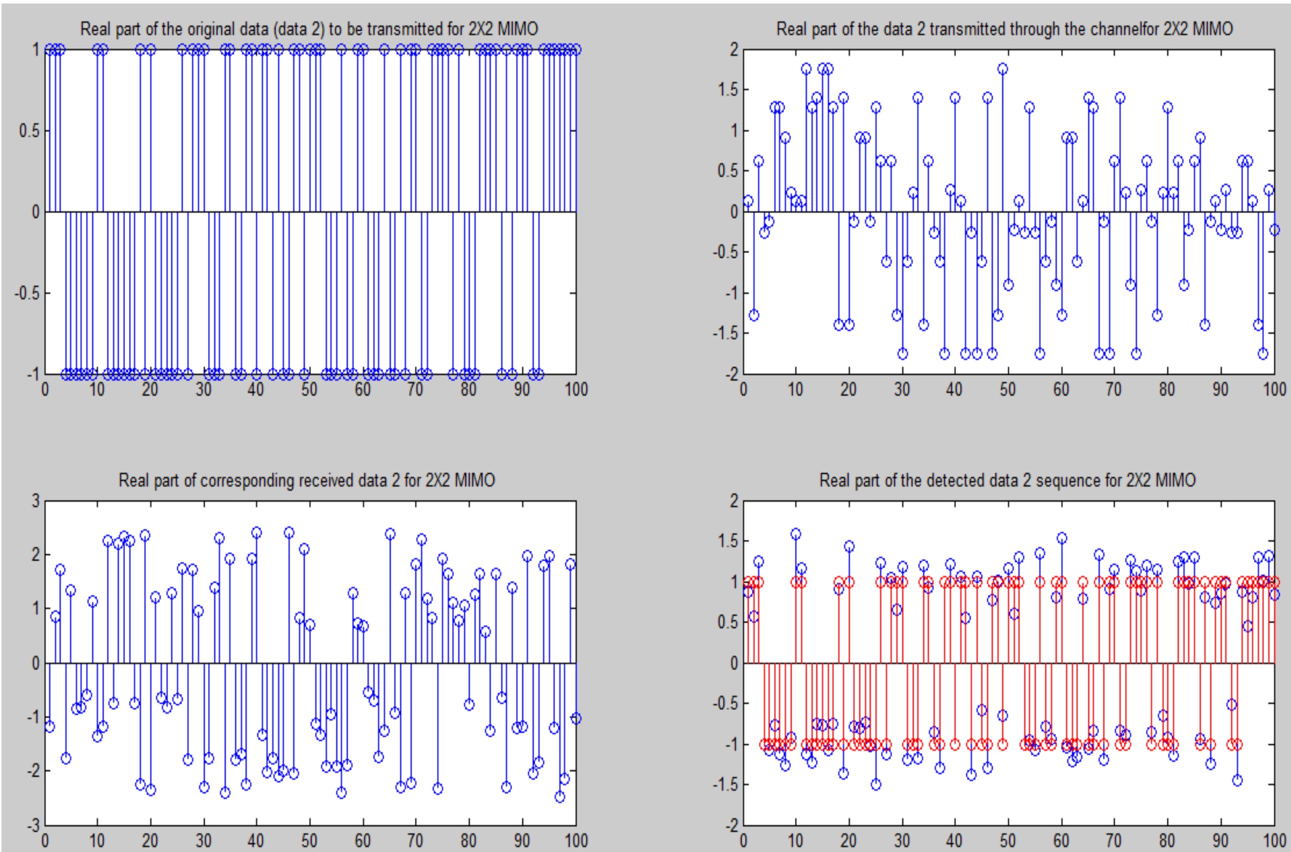

Figure 6-5 plot of imaginary part of data 2 at the stages of transmitted, received and detected

On the simulation, we can see that the transmitted signal is recovered with fair precession. Therefore the use of SVD algorithm is very essential for MIMO systems. Note that transmit precoding by the matrix V "aligns" the inputs with the eigenmodes of the channel. By aligning the inputs with the eigenmodes, simple post-multiplication of the output signal results in independent (noisy) observations of each of the inputs, i.e. a complete decoupling of the different data streams. The optimal MIMO receiver requires LMMSE detection across all receive antennas, but practical techniques of lower complexity can achieve fair performance with SVD techniques.

6.4 Ergodic Capacity of MIMO Systems

MIMO channel capacity over Rayleigh fading channel was simulated using MATLAB software for different antenna configurations, different SNR range values, and with and without CSIT. To verify the theoretical analysis presented in Chapter 4, the ergodic capacity for closed and opened loop SU-MIMO are simulated as shown in the following Subsections. We can use the general equation (4.47) and more reduced special equations.

According to the simulation scenario described in the following Sections, the simulation results will be presented and analyzed. Our approach for this presentation and analysis is to investigate the performance of three MIMO techniques: Spatial Multiplexing, Receive diversity and Transmit Diversity and compare the results with traditional SISO technique. All our simulation results are in excellent agreement with the theoretical results. We will also deal with the special scenario of low and high SNR regimes for each mode.

Generally in Chapter 4 we showed analytically that all SIMO or MISO diversity systems are "capacity additive" with respect to SISO systems, whereas MIMO reported herein are "capacity multiplicative". As been discussed in Chapter 2 and 4, closed loop MIMO modes are for slow moving UE and Opened loop MIMO modes are for fast moving UE. In this Chapter due *path loss fading* that low SNR regimes are found at the cell edge and high SNR regime are found at the cell centered. Mostly this is the case unless an *unusual shadow fading* occurs.

6.4.1 Ergodic Capacity of Open Loop (Fast fading) MIMO System

(4.41) and (4.48) express the general ergodic capacity for Open Loop SU-MIMO. First we will see the simulation for open loop MIMO channel of low SNR regime or cell-edge UE. Then simulate for open loop MIMO channel of high SNR regime or cell-centered UE. Specifically, we can also use (4.33) for opened loop SIMO (1×2) and (4.58) for opened loop MISO (2×1).

6.4.1.1 Ergodic Capacity for Low SNR Regime of Open Loop MIMO

On this simulation we can see that the ergodic capacity largely depends on the number of antennas at the receiver than the number of antennas at transmitter. We used the general equation of (4.49) for open loop MIMO system. Therefore, in the low-SNR regime (cell-edge UE), multiple transmit antennas do not improve the capacity, and the capacity of any (M,N) channel with $M \geq 1$ is asymptotically equivalent. On the plot we can see this effect in the range of ($-20 < SNR < -10$). At very low SNRs, the optimal transmission strategy benefits from diversity and combining but not from multiplexing. This result is in consistent with the more simplified linear equation (4.64) which depends only on N.

Therefore, high spectral efficiency is obtained by increasing the number of antennas at receivers for high speed UE located at cell-edge UE. Therefore operators can use two transmit antenna at eNodeB for spatial multiplexing and the other transmit antennas for space diversity. Increasing the number of receiver antennas at UE is important for this situation.

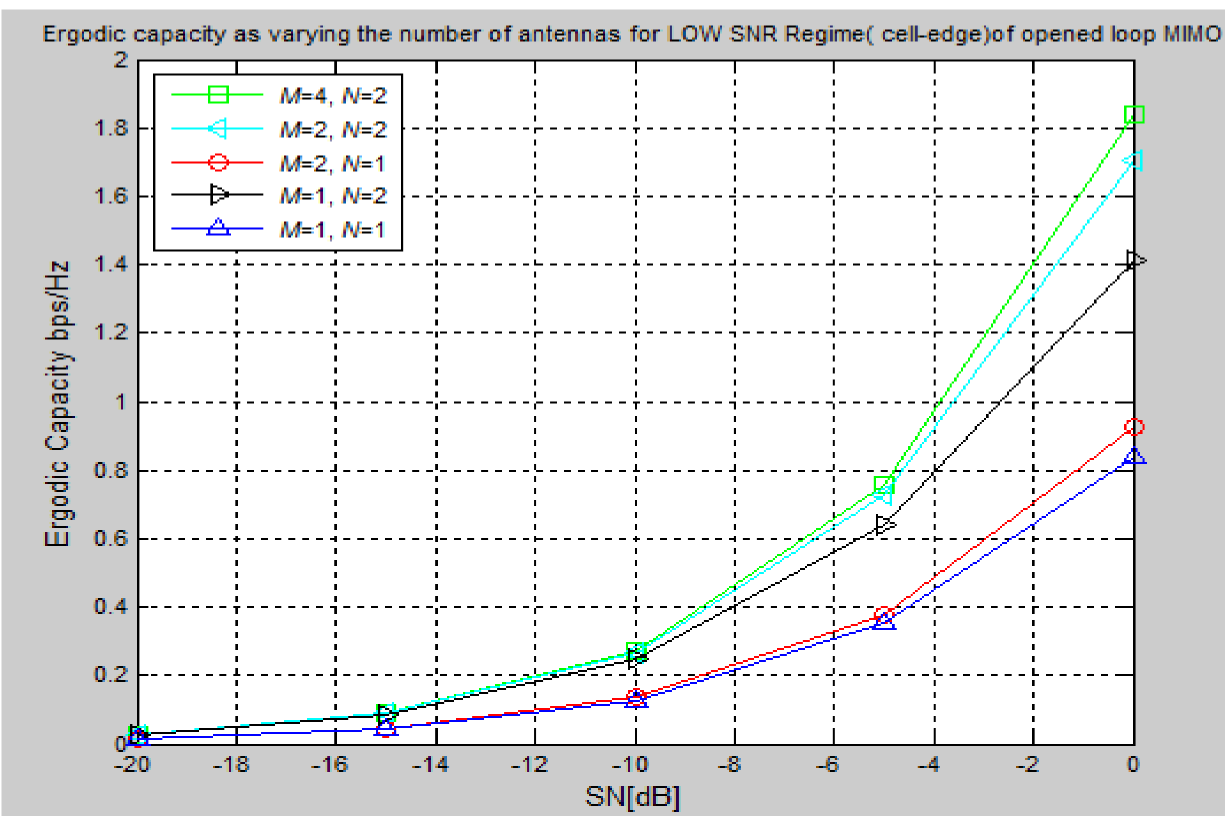

Figure 6-6 Ergodic capacity of open loop SU-MIMO of low SNR as varying number of antennas

6.4.1.2 Ergodic Capacity for High SNR Regime of Open Loop MIMO

As shown in the plot below, the ergodic capacity increases with the numbers of antennas at the transmitter and receiver. This result was formulated using the general equation of (4.49) for opened loop MIMO system. In addition; the ergodic capacity of a SIMO (1×2) channel as described in (4.33) appears to be greater than the ergodic capacity of a MISO (2×1) channel as described in equation (4.51). This is because of the transmitter power is shared equally by each transmitting antenna. This simulation result is in consistence with the linear equation of (4.76).

Therefore Operators can increase the capacity for fast moving UE which is located at cell centered UE by increasing the number of transmitters up to 4 antennas at eNodeB, which is more convenient and practical than adding more antennas at the UE receiver. Receiver with more than one antenna can use the others for spatial diversity.

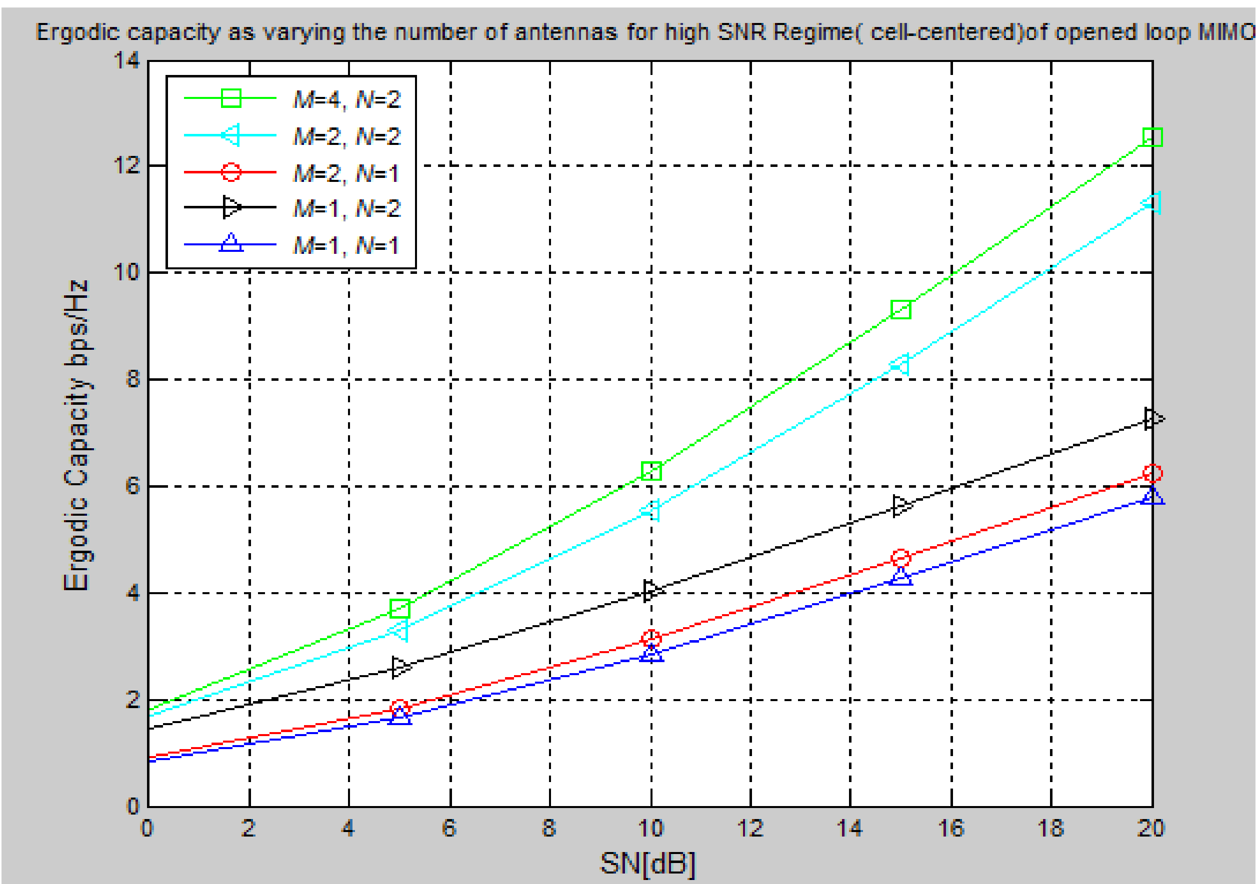

Figure 6-7 Ergodic capacity of open loop SU-MIMO vs high SNR as varying number of antenna

6.4.2 Ergodic Capacity of Closed Loop MIMO System

We will plot and implement MIMO system with waterfilling Algorithm for SVD method .Note that there is no closed loop system for MISO and SIMO system. Therefore antenna configuration of 2×1 (MISO) and 1×2 (SIMO) are not included in this simulation.

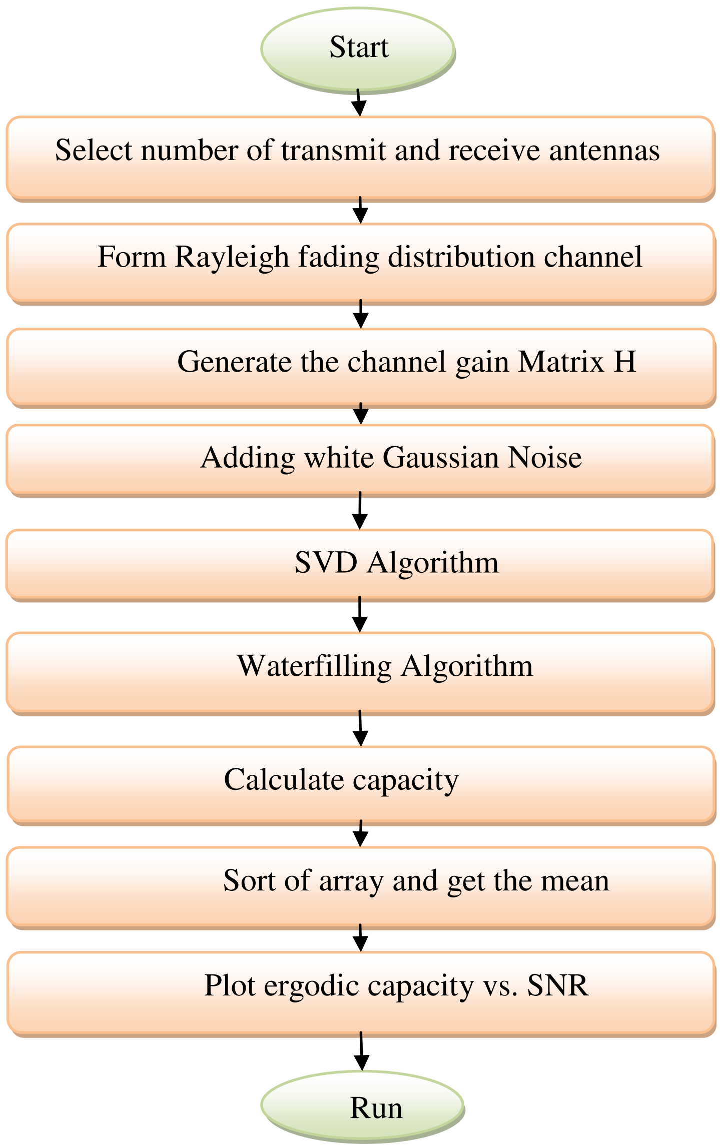

Figure 6-8 Flow chart for ergodic capacity for closed loop MIMO system

For open loop MIMO the same steps will follow the same steps except using SVD and waterfilling. This is because there is no power allocation used, the channels will equally share the total power and the ergodic capacity is given by (4.42).

6.4.3 Flow chart for Waterfilling Algorithm

Therefore the steps for flow waterfilling algorithm are as follows:

1) Use SVD and extract the eigenvalues λ_i, i=1…r.
2) Find the values of γ_i, rank the eigenvalues in ascending order.
3) Initialize loop counter j.
4) Find the values of γ_o in each iteration.
5) Find the power for each eigenvalues.
6) If all power of eigenchannels are positive, then stop iteration and calculate the capacity.
7) Otherwise assign zero values for those with negative power and continue the iteration.

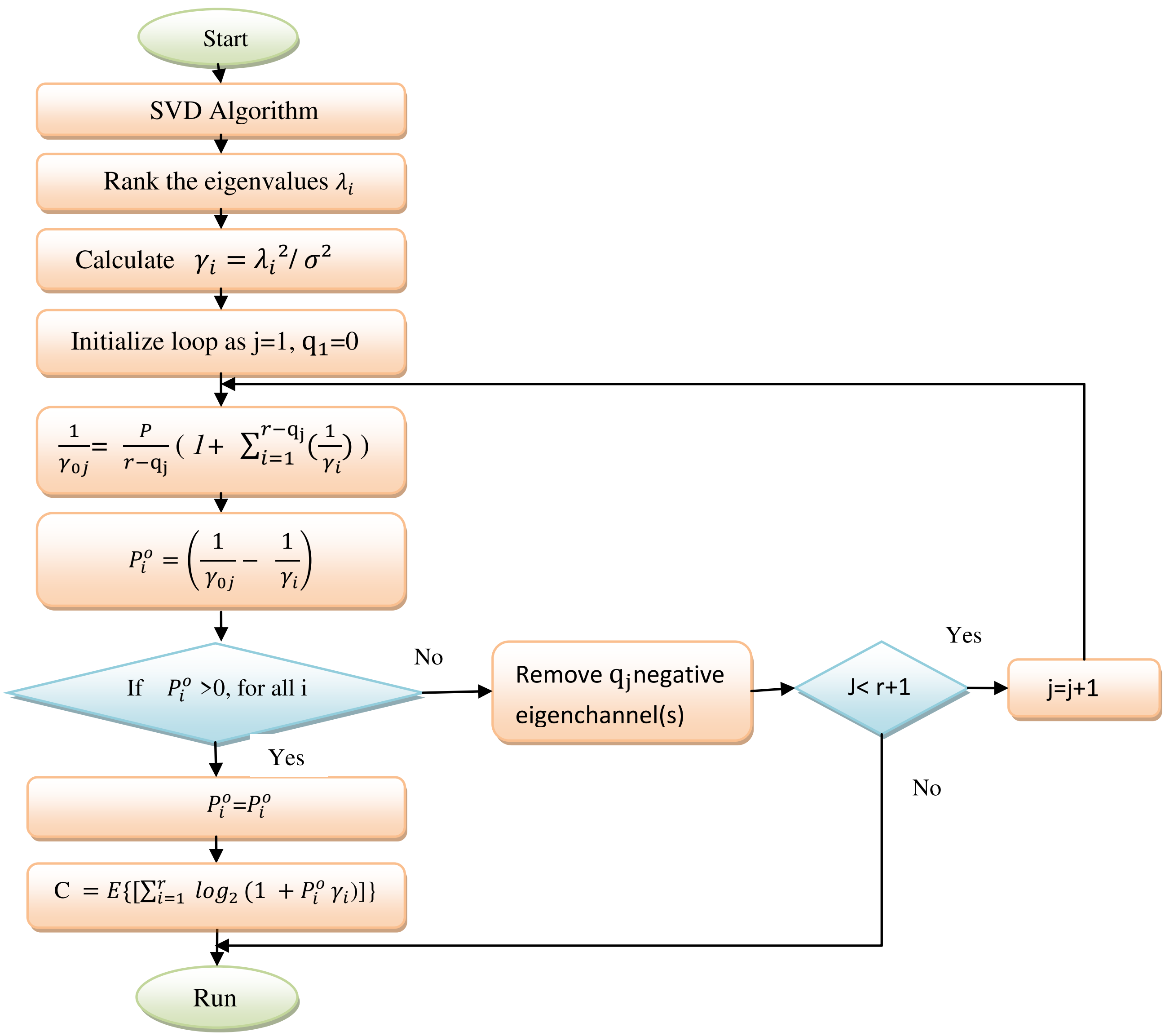

Figure 6-9 Flow chart for waterfilling algorithm of MIMO systems

6.4.3.1 Ergodic Capacity for Low SNR Regime of Closed Loop MIMO

As depicted on the simulation plot below, the capacity increases with max(M,N), that's why 2×4 and 4×2 antenna configurations have an overlapping lines. At low SNR, the water-filling algorithm of (4.69) reduces to allocating all the available power to the strongest or dominant eigenmode. The simulation result was predicted by theoretical method in (4.75).

Therefore Operators can increase the ergodic capacity by multiple of number of antennas at eNodeB to gain more capacity to slow moving UE located at cell-edge. There is no need for increasing the number of receivers more than two at UE. So the maximum ergodic capacity will be four times that of traditional SISO network if we use 4 transmitting antennas at eNodeB.

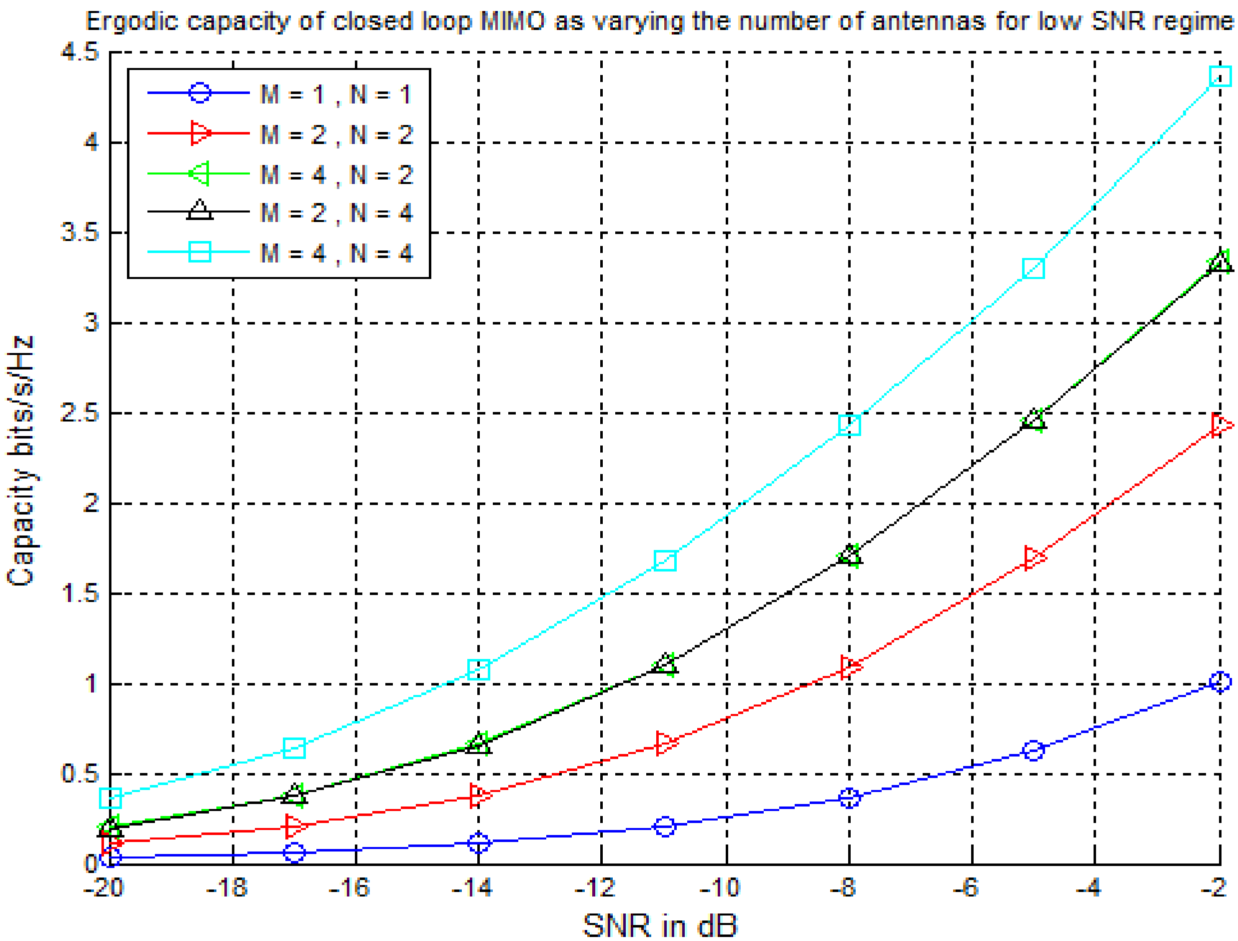

Figure 6-10 Ergodic capacity of closed loop MIMO vs low SNR as varying number of antennas

6.4.3.2 Ergodic Capacity of High SNR Regime of Closed Loop MIMO

It can be shown from the simulation plot that the ergodic capacity increases with the number of either the transmitter or the receiver i.e. min (M,N). The simulation is in consistent with the linear equation of (4.78). For the closed-loop capacity at asymptotically high SNR, waterfilling puts equal power in each of the min (M,N) eigenmodes ,the water-filling solution approaches a uniform power allocation on all non-zero eigenmodes

Therefore Operators can increase the number of transmitters at eNodeB to gain high capacity to slow moving UE which is located at cell-center. Two antennas at the receiver is enough to maintain high capacity gain. The maximum capacity is four times that of the traditional SISO system if four transmitting antennas are used at eNodeB.

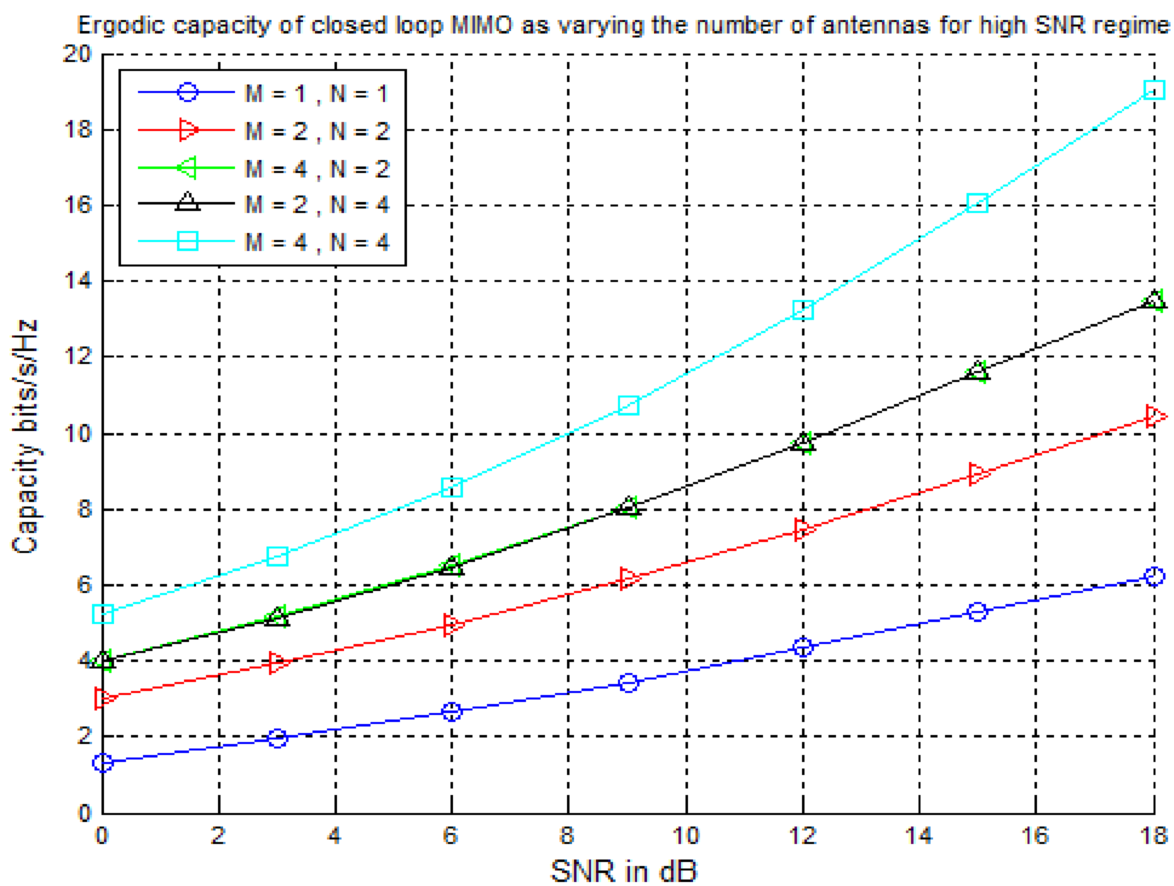

Figure 6-11 Ergodic capacity of closed SU-MIMO vs high SNR as varying number of antennas

6.4.4 Comparison of Closed Loop with Open Loop SU-MIMO

The plot below displays that the closed-loop system provides more capacity than the open-loop system. It is clear that the capacity is always higher when the channel is known than when it is unknown. From the plot, we find that the relative performance of these techniques depends on the SNR and the relative values of M and N. The gains provided by waterfilling solution are significant at low SNR and negligible at high SNR. This is because, at high SNR values, all the channels perform equally well. The reason for this difference is that under CSIR, the transmit power is assumed to be equally divided between the transmit antennas.

Therefore Operators can benefit more from closed loop MIMO system with high spectral efficiency than opened loop MIMO system. As mentioned in Section 3.3, the feedback systems partially depend on uplink data capacity at the eNodeB. Assigning more processing power for uplink can turn the open loop to closed loop MIMO system since CSIT can be available. However, as the speed of mobile terminal increases and channel conditions change more rapidly, closed loop MIMO looses much of its advantage over open loop MIMO which is simpler to implement.

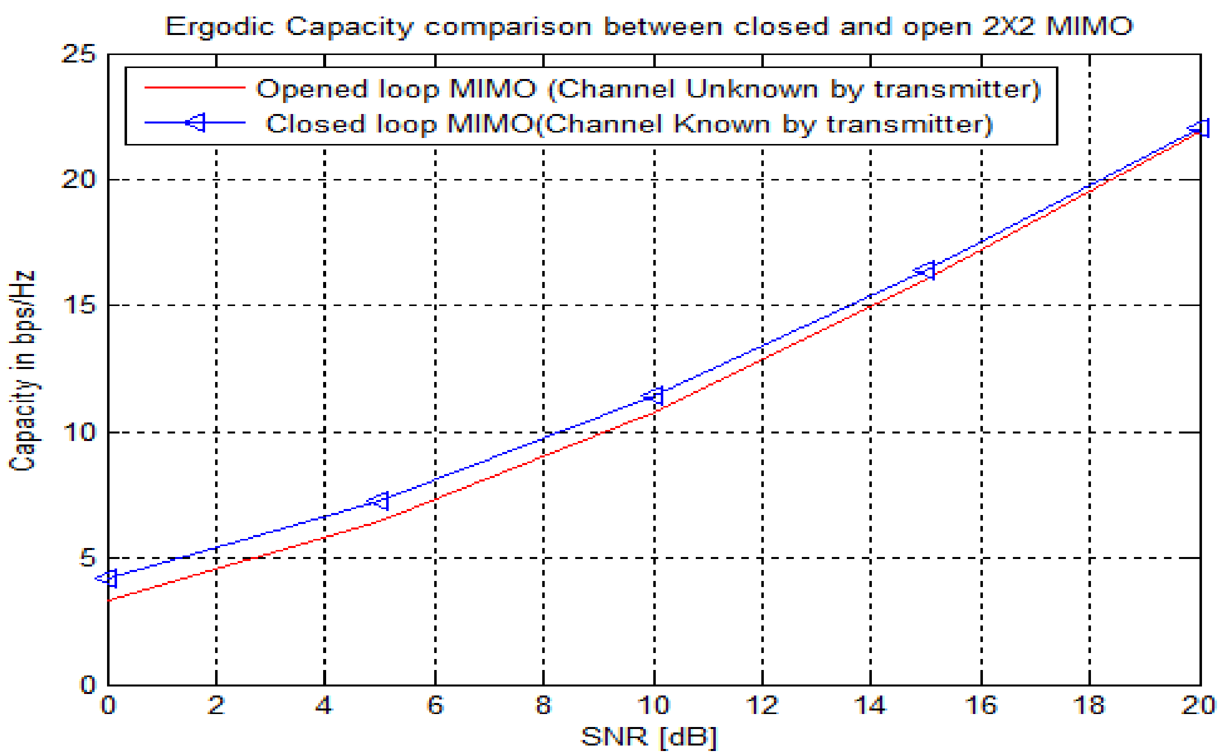

Figure 6-12 Closed loop vs opened loop SU-MIMO of 2 × 2 antenna configuration

6.5 BER Performance of Space Diversity

For each E_b/N_o value, the code runs in a while loop until either the specified maximum number of errors is observed or the maximum number of bits is processed. The code executes each system object by calling the step method. It computes BER, defined as the ratio of the observed number of errors to the number bits processed.

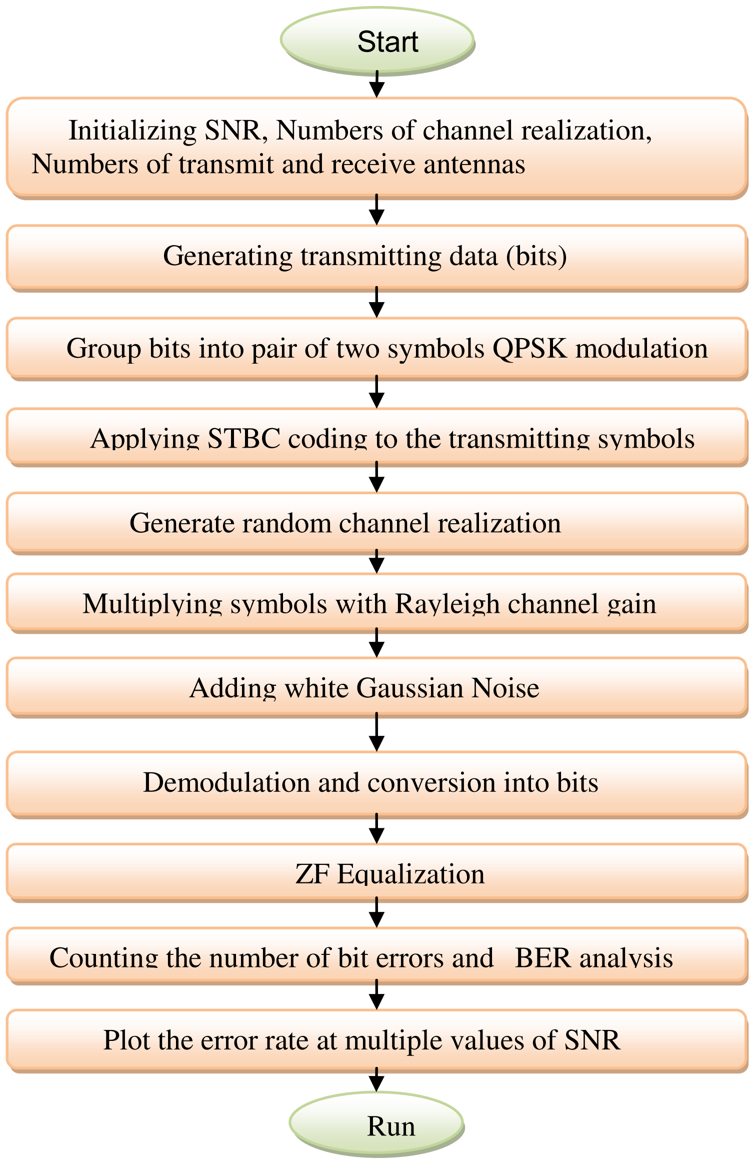

Figure 6-13 Flow chart for performance analysis STBC MIMO system

MATLAB simulations are represented to evaluate the BER with respect to SNR to analyze the MIMO-OFDM system performance applying both Alamouti STBC and MRC diversity over Rayleigh fading channel.

The evaluation results depict that the proposed MISO-SIMO (2×2) system concatenated with Alamouti STBC and MRC outperforms conventional SISO (1×1), MISO (1×2) with Alamouti STBC and SIMO (2×1) of Zero Forcing equalizer. Here, we observe that by having the extra receive antenna, the error probability decreases with SNR. The simulation results are in consistence with the theoretical analysis in (5.9), (5.31), (5.52) and (5.64).

Therefore Operators can increase BER performance and reliability of a link by using transit diversity and receive-transmit combination diversity. It's recommended that using MISO-SIMO will have a great performance gain for highly fading environment.

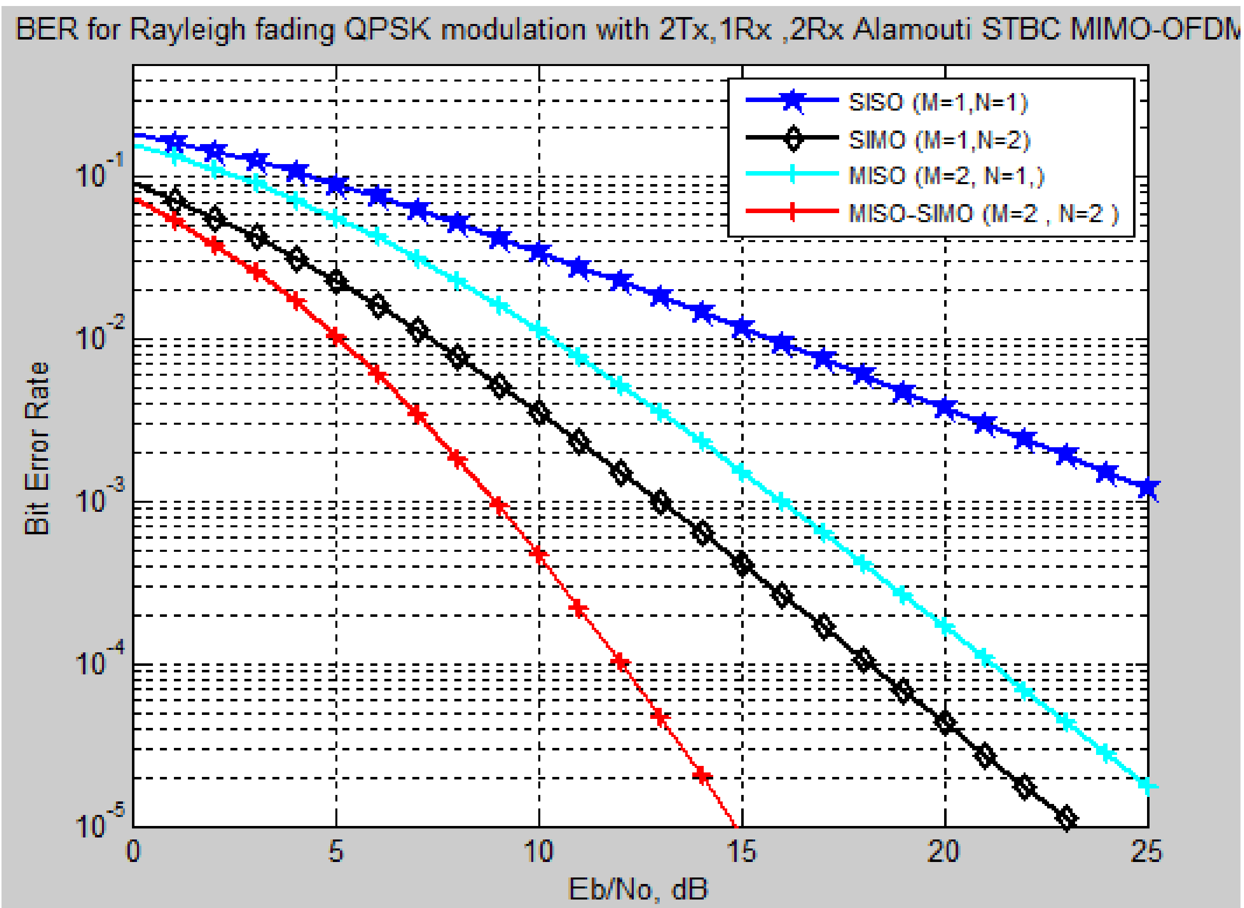

Figure 6-14 BER of receive diversity (1×2), transmit diversity of (2×1) and MISO-SIMO (2×2)

6.6 Diversity-Multiplexing Trade-off

In this plot, we showed the piecewise function for 4×4 (M=4,N=4) and 4x2 (M=4,N=2) and 2×2 (M=2,N=2) and 2x1 antenna configurations. As shown below we can use 4×4 as only spatial multiplexing at coordinate (4,0) and 4×4 as only spatial diversity at coordinate (0,16) . However we can use 3×3 as spatial multiplexing together with 1×1 spatial diversity configuration as shown at coordinate (3,1), this is more applicable for UE that needs more data rate than reliability.

We can have a combination of MIMO systems with (2×2) for spatial multiplexing and the other (2×2) for spatial diversity as shown in coordinate (2,4). In the contrary UE that demands more reliability can use 1×1 as spatial multiplexing and the other antennas as 3×3 for spatial diversity as shown at coordinate (1,9). Similarly we can used 4×2 as spatial multiplexing only and 4×2 as only spatial diversity. But in trade off we can use 3×1 as spatial multiplexing and 1×1 as spatial diversity. Similar methods can be used for 2×1 antenna configurations.

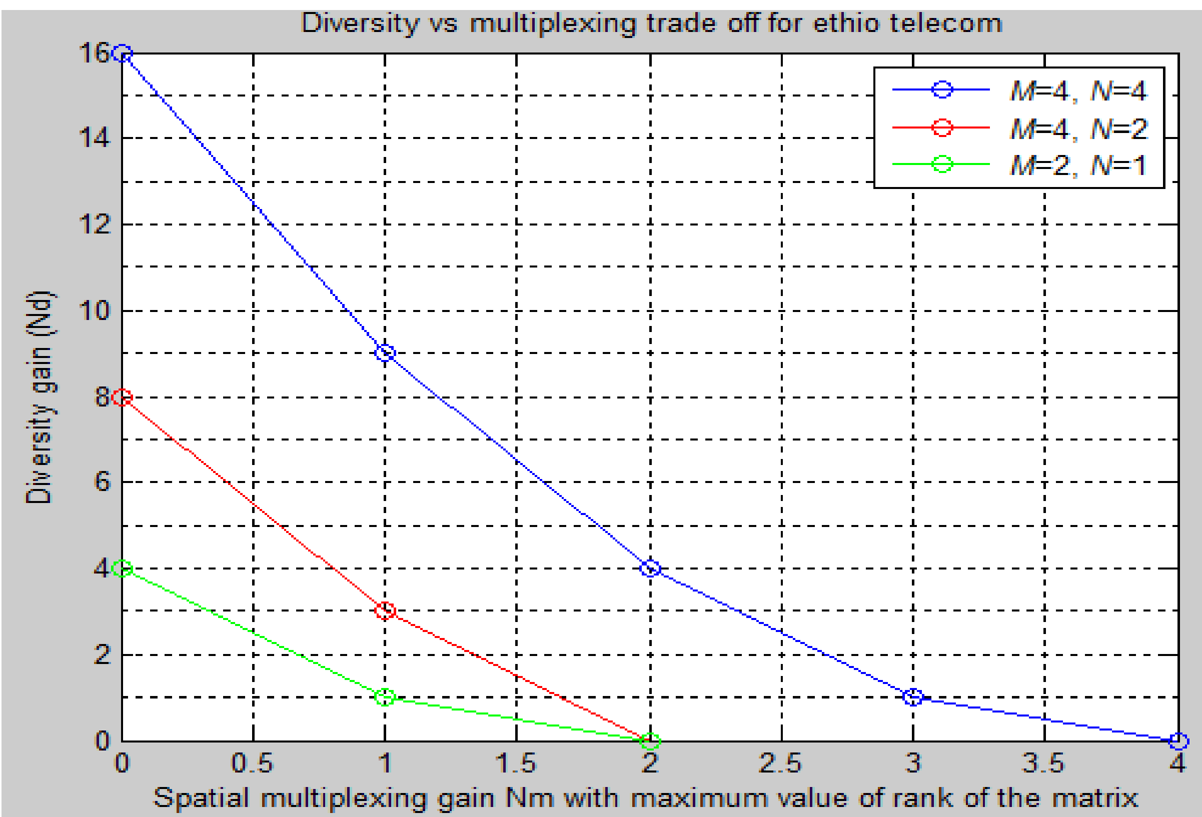

Figure 6-15 Diversity-spatial multiplexing trade –off.

CHAPTER 7

7 CONCLUSIONS AND FUTURE WORKS

This thesis focused briefly on various SU-MIMO modes for LTE Release 8 in highly scattering environment. Overall, MIMO is a must have technology to adopt the high crisis of data transmission in upcoming times. Spatial multiplexing deals for achieving very high peak rates, while transmit diversity is a valuable scheme to minimize the rate of bit error occurrence thereby improving signal quality. It's also shown that the possibility of having both gains using spatial diversity-multiplexing tradeoffs.

In this thesis work, an effective study, analysis and evaluation of the LTE downlink performance with different SU-MIMO techniques in comparison with the traditional SISO system has been carried out. All these above schemes are under the environments that need consider multipath effect and Doppler effects. These are the kind of typical channel environments in some urban environment. Besides that, we can also use MIMO systems for highly fading environment of metro railway tunnel environments.

MATLAB simulation method is used to analyze and present the results. In general, SU-MIMO under fast fading and slow fading environments scenarios were analyzed and simulated. Then special focus has been made on UEs located at cell- center and cell-edge. The simulation results show SU-MIMO brings major gain on cell edge UE and cell -centered UE in user's capacity and BER performance.

This performance evaluation also provides useful information on LTE-MIMO downlink for future planning, design and optimization for deployment. In particular, the developed techniques can be applied to fast and accurate performance evaluation of MIMO–OFDM transmission in the system level studies. System level performance studies are necessary to analyze such topics as capacity and BER performance at different location and speed of UE. Such quantitative results are required by operators for the network planning and implementation of SU-MIMO. This illustrates the deployment value and great importance of SU-MIMO to Ethio- Telecom. So the whole thesis is to show how service providers can greatly benefit by implementing SU-MIMO in LTE.

.

7.1 Recommendations for Future Work

Even though there is still a large number of open research problems in the area of MIMO wireless, both from a theoretical perspective and a hardware implementation perspective, the technology has reached a stage where it can be deployed for use in practical systems. SU-MIMO technology has opened numerous areas for future work which could be done to better understand performance of SU-MIMO. Some of the areas are as follows:

- Line-of-Sight MIMO for Microwave Links for those eNodBs without fiber optics backhaul hasn't been deployed. Line-of-sight MIMO works by making the signal streams orthogonal to each other either by spatially separating the antennas at the transmitter and receiver or by using orthogonally polarized antennas.
- Adaptive SU-MIMO Switching is a scheme to switch between multiple MIMO modes. The goal is to maximize the resources available in multiple antenna channels by using optimal schemes at all times.
- Improving or designing SU- MIMO with dual-polarized antennas so that antenna separation at UE can be more reduced than half wavelength.
- MU-MIMO for LTE-Advanced from Release 9 onwards for both downlink and uplink.
- Performance of massive MIMO (Large-Scale Antenna Systems).
- Design some pre-coding/framing mechanism which can be employed to translate a MISO or SIMO system into a mathematically equivalent SISO channel, furthermore to translate a MIMO channel into a mathematically equivalent SIMO or MISO channel.
- Optimizing a MIMO system which achieves the highest throughput and connectivity possible in a given environment by leveraging the multipath potential of the environment. It also includes configuration of antennas at the eNodeB.

References

[1] Y.S. Cho, J. Kim, W.Y. Yang, C. Kang, *MIMO-OFDM Wireless Communications with MATLAB* .1 st ed., Singapore : John Wiley & Sons, 2010.

[2] J. Furuskog, *et al*., "Field trials of LTE with 4×4 MIMO Multi-antenna reception and transmission is a key enabler of the high performance offered LTE ," *IEEE Wireless Commun.*, pp. 6–8, June 2010

[3] PCTEL Simplifying wireless, "Maximizing LTE Performance Through MIMO Optimization," White paper , 2011 .
Available: http://www.rfsolutions.pctel.com

[4] Huawei ,"Low Level Design Documentation for eUTRAN (LTE) Mobile Network in Addis Ababa," 2014 .

[5] M. Rumney, M. J. Pahls, M. Leung, *LTE and the evolution to 4G wirelesses: Design and measurement challenges.* 2nd ed., New York, USA: Agilent Technologies Publication, 2013.

[6] L. Hanzo, Y. Akhtman , L. Wang , *MIMO-OFDM for LTE, Wi-Fi and WiMAX Coherent versus Non-coherent and Cooperative Turbo-transceivers.* 1st ed., Wessen, UK: John Wiley & Sons Ltd, 2011.

[7] C.Cox, *An Introduction to LTE, LTE-Advanced, SAE and 4G Mobile Communications*. 1st ed., UK: John Wiley & Sons, 2012.

[8] C. Gessner, *et al*., "UMTS Long Term Evolution (LTE)-Technology Introduction Application Note LTE Technology Introduction," Rohde and Schwarz, 2012.

[9] H.Zarrinkoub, *Understanding LTE MATLAB® from Mathematical Modeling to Simulation and Prototyping*. Massachusetts, USA: John Wiley & Sons, Ltd, 2014.

[10] 3G Americas, "3GPP Mobile Broadband Innovation Path to 4G: Release 9, Release 10 and Beyond: HSPA+, LTE/SAE and LTE Advanced," Feb 2010. .

[11] S.Sesia, I Toufik, M.Baker, *LTE – The UMTS Long Term Evolution from Theory to Practice* . 2nd ed. , UK: John Wiley & Sons Ltd, 2011 .

[12] G. Mengistu, "Performance Evaluation of LTE Downlink with MIMO Techniques," Master thesis, Blekinge Institute of Technology, Sweden , 2010

[13] D. Girma, "Performance analysis of space time coding on MIMO and cooperative diversity system," Master thesis, School of Elect. and Comput. Eng., Addis Ababa University, Addis Ababa, 2013.

[14] H. Huang, C. Papadias, S. Venkatesan, *MIMO Communication for Cellular Networks.* 1st ed., New York, USA: Springer Science Business Media, 2012

[15] C. Oestes, B. Clerkx, *MIMO Wireless Communications From Real-World Propagation to Space-time Code Design.* 2nd ed., London ,UK: John Wiley & Sons, Ltd ,2007

[16] D. Halperin, W. Hu, A. Shethy, *802.11 With Multiple Antennas*. 2nd ed., Washington, USA: Intel Labs Seattle, 2012.

[17] C. Langton, B. Sklar, "Finding MIMO Capacity of Multiantenna Gaussian Channel," Telatar, *E.s.l.: European Transactions on Telecommunications*, Oct 2011.

[18] H. Bolcskei, D. Gesbert, C. Papadias, *Space-Time Wireless Systems From Array Processing to MIMO Communications.* 3rd ed., West Sussex,UK: Cambridge University Press 2006 .

[19] N. Costa, S. Haykin, *Multiple –Input, Multiple –Output Channel Models Theory and Practice*. New Jersey, USA : John Wiley & Sons, 2010

[20] J. G. Proakis and M. Salehi, *Digital Communications*. 5th ed., New York: McGrow-Hill, 2008.

[21] A. Ghosh, R. Ratasuk , *Essentials of LTE and LTE-A* . 1st ed., New York,US: Cambridge University Press, 2011.

[22] E. Dahlman, S. Parkvall, J.Skold, P.Beming, *3G Evolution HSPA and LTE for Mobile Broadband.* 3rd ed., California, USA: Elsevier Ltd, 2007.

[23] G. Tsoulos, *MIMO System Technology for Wireless Communications*, 2nd ed., New York, US: Taylor & Francis Group, 2006.

[24] Keysight Technologies Inc., "Concepts of Orthogonal Frequency Division Multiplexing (OFDM) and 802.11 WLAN," 2017. Available:.http://rfmw.em.keysight.com/wireless/helpfiles/89600b/webhelp/subsystems/wlan-ofdm/content/ofdm_basicprinciplesoverview.htm

[25] R. Kumar , R. Bangladesh , “BER Analysis of MIMO-OFDM System using Alamouti STBC and MRC Diversity Scheme over Rayleigh Multipath Channel, ” *Global Journal of Researches in Engineering Electrical and Electronics Engineering* Vol 13, Type: Double Blind Peer Reviewed International Research Journal Year 2013.

[26] T. Brown, E. Carvalho, P. Kyritsi , *Practical Guide to the MIMO Radio Channel with Matlab example.* West Sussex, UK: John Wiley & Sons Ltd, 2012.

[27] M. Viswanathan , “Characterizing a MIMO channel – Channel State Information (CSI) and Condition number,” 2014 .
Available : http://www.gaussianwaves.com/2014/08/characterizing-a-mimo-channel/

[28] B. Cerckx, C. Oestges, *MIMO Wireless Networks Channels, Techniques and Standards for Multi-Antenna, Multi-Cell Systems.* 2nd ed., Elsevier Ltd, 2013.

[29] Agilent Technology, *“*Agilent MIMO Channel Modeling and Emulation Test Challenges*,”* Application Note 5989-8973EN , USA: 2010 .
Available: http://rfmw.em.keysight.com/wireless/helpfiles/n5106a/5989-8973en.pdf

[30] Telesystem Innovations, “ The seven Modes of MIMO in LTE,” white Paper, 2011
Available:.http://www.tsiwireless.com/docs/whitepapers/The%20Seven%20Modes%20of%20MIMO%20in%20LTE.PDF

[31] F. Flaviis, L. Jofre, J. Romeu, A.Grau , *Multiantenna Systems for MIMO Communications* . Arizona USA: Morgan & Claypool Publishers, 2008 .

[32] H. Liu, G. Li, *OFDM-Based Broadband Wireless Networks Design and Optimization*, John Wiley & Sons, Inc., 2005.

[33] Klabs S.r.l, The ICT Knowledge factory, “ LTE MIMO Air Interface,” white paper, 2012.

[34] J. Hampton, *Introduction to MIMO Communications,* Cambridge,UK: Cambridge University Press, 2014 .

[35] M. Viswanathan, “Simulation of OFDM system in Matlab – BER Vs Eb/N0 for OFDM in AWGN channel,” Jul 2011.
Available: http://www.gaussianwaves.com/2011/07/simulation-of-ofdm-system-in-matlab-ber-vs-ebn0-for-ofdm-in-awgn-channel/

[36] N.Hajare, S.Dhotre, “BER Analysis of OFDM System Using BPSK Modulation Over Different Channel,” , *IJECT Vol. 7*, Issue 1, Jan 2012

[37] C. Oestges , B. Clerck *Introduction to multi-antenna Communications.* West Sussex, UK: John Wiley & Sons, Inc., 2005 .

[38] V. K¨uhn, *Wireless Communications over MIMO Channels Applications to CDMA and Multiple Antenna Systems*. West Sussex, UK: John Wiley & Sons Ltd, 2006

[39] A. Goldsmith, Wireless *Communications*. 2nd ed., Cambridge University Press. 2005

[40] B. Holter ,O.S. Bragstads, "On the Capacity of the MIMO Channel –Tutorial introduction:" Trondheim, Norway ,2011

[41] H. Khaleghi , *MIMO Systems , Theory and Applications* . Rijeka, Croatia : InTech , 2011

[42] G. Abbas, *et al*., "Performance Enhancement of Multi-Input Multi-Output (MIMO) System with Diversity," *International Journal of Multidisciplinary Sciences and Engineering*, Vol 3, No 5, 2013.
Available: http:// www.ijmse.org

[43] T. Duman , A. Ghrayeb, *Coding for MIMO Communication Systems . 2nd ed.,*West Sussex, England: John Wiley & Sons Ltd, 2007.

[44] E. Hassan, *Carrier Communication Systems with Example sin MATLAB® A New Perspective*. New York, USA: Taylor & Francis Group, an Informa business, 2016.

[45] Siavash M., "A Simple Transmit Diversity Technique for Wireless Communications Alamouti ",*IEEE Journal on select areas in Communications*, VOL. 16, NO. 8, Oct 1998.

[46] L. Korowajczuk , *LTE, WIMAX and WLAN Network Design Optimization and Performance Analysis CelPlan Technologies,* 1st ed., Reston, VA, USA: John Wiley & Sons, Ltd, 2011.

[47] S. Gupta, *et al*., "Comparison of BER Performance & Capacity Analysis of MIMO System with STBC & MRC to improve Link Performance in Fading Environment," *International Journal of Scientific Engineering and Applied Science (IJSEAS) – Vol2*, Issue-5, May 2016.
Available: http:// www.ijseas.com

[48] A. Sibile, C. Ostages, A. Zabella, *MIMO from Theory to Implementation*. 2nd ed., California, USA: Elsevier Inc, 2011.

[49] L. Zheng, *et al*., "Diversity and Multiplexing: A Fundamental Tradeoff in Multiple-Antenna Channels," *IEEE Transactions on Information on information theory*, VOL. 49, NO. 5, May 2003.